Red Misfits in the Sloan Digital Sky Survey

Red Misfits in the Sloan Digital Sky Survey: Properties of Star-Forming Red Galaxies

By
Fraser A.F. Evans, B.Sc.

A Thesis
Submitted to the School of Graduate Studies
in Partial Fulfilment of the Requirements
for the Degree
Master of Science

McMaster University

MASTER OF SCIENCE (2017) McMaster University

(Physics and Astronomy) Hamilton, Ontario

TITLE: Red Misfits in the Sloan Digital Sky Survey: Properties of Star-Forming Red Galaxies

AUTHOR: Fraser Evans, B.Sc. (McMaster University)

SUPERVISORS: Laura Parker

NUMBER OF PAGES: xii, 149

Abstract

Galaxies in the Universe are primarily blue and star-forming or red and passively evolving. Here we study an outlier population of red, star-forming galaxies in the local Universe which we call Red Misfits. These galaxies are classified based on inclination-corrected optical colours and specific star formation rates derived from the Sloan Digital Sky Survey Data Release 7. We find that $\sim$11 per cent of galaxies at all stellar masses are classified as red in colour yet actively star-forming. Using the wealth of information provided by the SDSS and related products we explore a number of properties of these galaxies and demonstrate that Red Misfits are a distinct population of galaxies in the Universe and not simply blue star-forming galaxies whose colours are reddened by intrinsic dust extinction. Red Misfit galaxies exhibit intermediate, bulge-dominated disk morphologies, intermediate stellar ages, slightly enhanced dust extinction and gas-phase metallicities, and an enhanced likelihood of hosting an active galactic nucleus. The proportion of Red Misfits in galaxy groups remains constant irrespective of group halo mass or projected distance to the group centre. We conclude that Red Misfits are a transition population being gradually quenched on their way to the red sequence and that this quenching is dominated by internal mechanisms rather than environmentally-driven processes.

Acknowledgements

Thank you to my friends and classmates who made this entire experience more fun than it had any right to be. I would not be where I am today without your support and motivation and my seven years here would not have flown by so quickly.

Thanks as well to Dr. Madusha Gunawardhana and all my LEAPS colleagues, who gave me an unforgettable and valuable experience in Leiden and who gave me the fire I needed late in the game.

Special thanks to Benjamin Davis-Purcell, who has stuck with me throughout this entire experience and who never hesitated to lift me up when I was feeling down. I'm sorry I ultimately opted for the name 'Red Misfits' over your more obscene suggestions.

Most of all, I would like to thank my supervisor Dr. Laura Parker. Your infectious love for science and your enthusiastic guidance made this all worth doing. I wouldn't change a thing.

Finally, thank you to my family, whose love and support followed me no matter how far I wandered and who learned quickly that "How's the paper going?" is a question that is rarely received well.

Table of Contents

List of Figures

List of Tables

Co-Authorship

Chapter 2 of this thesis has been submitted to the refereed journal *Monthly Notices of the Royal Astronomical Society* (MNRAS). This work was co-authored with my supervisor Dr. Laura Parker. The third co-author, Ian Roberts, generated the sample of isolated field galaxies used in the work. I hereby grant an irrevocable, non-exclusive license to McMaster University and Library Archives Canada to reproduce the material as part of this thesis.

Chapter 1

Introduction

Galaxies are the building blocks of structure in the Universe. It is by observing the positions and properties of galaxies and comparing these to simulations that we gradually come to understand the state of the Universe today, how it was in the distant past and what the future holds for it. The last two decades have yielded a number of revolutionary galaxy surveys such as the Two-degree-Field Galaxy Redshift Survey (2dFGRS; Colless et al., 2001), the Sloan Digital Sky Survey (SDSS; York et al., 2000), the Two Micron All Sky Survey (2MASS; Skrutskie et al., 2006) and the Cosmic Evolution Survey (COSMOS; Scoville et al., 2007), pushing galaxy surveys to wider angles, deeper magnitudes and higher redshifts. Using the enormous samples these surveys provide, we can study intimately the properties of galaxies in our Universe and expose the mechanisms by which they evolve through cosmic time.

1.1 Galaxy Properties

Galaxies can be described by a range of physical properties. It is through careful study of these properties and how they interrelate that we elucidate the physical mechanisms driving galaxy evolution in the Universe. Although not a comprehensive list, this section will detail the galaxy properties most relevant to this thesis and how they can be measured. Correlations between

these properties lead to a number of interesting populations, some of which will be discussed in Section 1.2.

1.1.1 Colour

Colour is a popular galaxy property to measure on account of the relative ease with which it can be measured. The colour of a galaxy is typically defined as the magnitude difference between two photometric bands. Because blue, hot, massive stars are short-lived compared to red, cooler stars, optical colours are often used to probe the star formation rate of a galaxy or its mean stellar age. Colours both in the optical and elsewhere in the spectrum can also be used to characterize other galaxy properties such as dust extinction, stellar metallicity and AGN contribution. The *u'g'r'i'z'* system (Fukugita et al., 1996; Smith et al., 2002) used by the SDSS has become the most common photometric system given the unprecedented sample size provided by SDSS. Several Multiple photometric systems exist, e.g. the JHK_s system used by 2MASS or the [3.6μm,4.5μm,5.8μm,8.0μm] system of *Spitzer IRAC* (Werner et al., 2004).

By combining data at many wavelengths we can construct spectral energy distributions (SEDs) for galaxies, which can be matched to stellar population models in order to estimate properties such as stellar mass, star formation rate, or redshift (e.g. Tinsley, 1972; Searle et al., 1973; Charlot & Bruzual, 1991; Kennicutt et al., 2009). The uncertainties in these properties are much smaller when using spectroscopy (dispersing a galaxy's light and measuring its intensity as a function of wavelength) over photometry (measuring the intensity of a galaxy across a series of wavelength bands). However, photometry can measure many more sources than spectroscopy with greater sensitivity in a given timeframe, making it the more practical option for many science goals. Interesting objects in photometric observations are often selected for spectroscopic follow-up.

As with any property, there are important caveats to consider when measuring colours. Firstly, as most galaxies are observed at non-negligible redshifts, the redshifting of emission into and out of filters will alter a galaxy's measured colour. Galaxy colours are often therefore k-corrected, i.e. corrected to what they *would be* in the rest frame of the galaxy or at a chosen redshift. Additionally, dust clouds in the Milky Way along the line of sight will preferentially extinguish bluer light over redder light, artificially reddening observed colours. Dust extinction maps (e.g. Schlegel et al., 1998) can be used to correct for this effect. Similarly, the light from highly-inclined or dusty galaxies can be significantly reddened by their own intrinsic dust. These effects are harder to characterize and so are not often corrected for. In Section 2.7 I present an effective method to correct for inclination-induced reddening.

Several works have found that galaxy colours follow a bimodal distribution across a variety of environments and redshifts. (e.g. Strateva et al., 2001; Baldry et al., 2004; Balogh et al., 2004b). In Fig. 1.1 I show the distribution of g-r vs. M_r colour-magnitude for a large sample of low-z, $M_{stellar}>10^{9.5}M_{\odot}$ galaxies in the SDSS (see Section 2.2 for more information about our sample selection). There exists a tightly-clustered population of galaxies at redder (larger) colours and a broad mode at bluer (smaller) colours. The distribution at fixed M_r is well-fit by a double-Gaussian; the red points show the location of the red peak of the colour distribution in bins of M_r, and the shaded region the average width of the peak. Together, these define the 'red sequence' of galaxies while the more dispersed blue mode is called the 'blue cloud'. Further discussion of these populations as well as the important 'green valley' region where the distributions overlap can be found in Section 1.2.

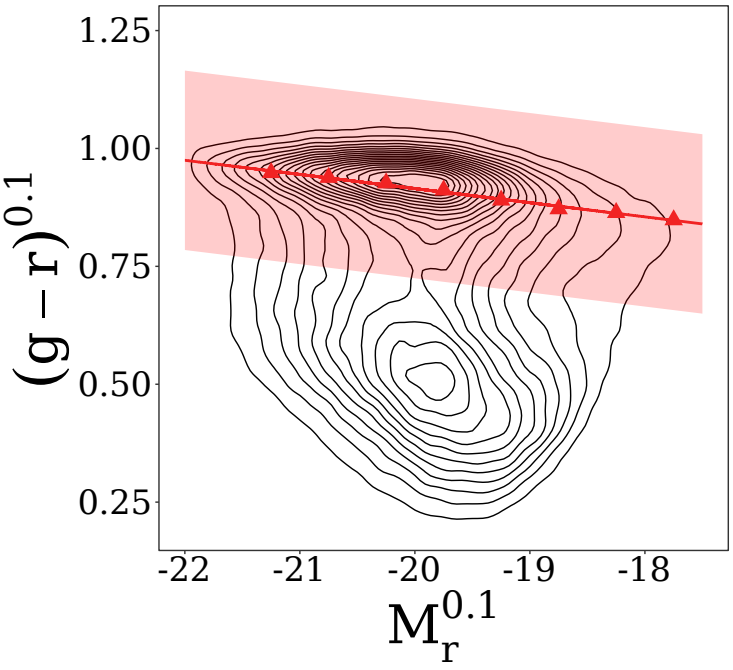

Figure 1.1 Distribution of ∼300,000 low-z SDSS galaxies on a colour-magnitude diagram. All magnitudes are k-corrected to z=0.1, as denoted by superscript. Red points show the locations of the red peaks of double Gaussian fits to the $(g\text{-}r)^{0.1}$ distribution in bins of $M_r^{0.1}$. Shaded region is average 1σ dispersion of the red mode. Red line is linear fit to points.

1.1.2 Star Formation Rate

Accurately determining galaxy star formation rates (SFRs, in $M_{\odot}$/yr) and how they depend on redshift, environment and other internal galaxy properties is critical for understanding galaxy evolution. Although in many cases it remains a difficult property to measure precisely, there exist a wide range of star formation rate diagnostics across a range of wavelengths which are suitable for different science goals. Here I will detail the most common SFR diagnostics and the ones most relevant to this thesis. See Kennicutt (1998) and Kennicutt & Evans (2012) for more comprehensive overviews of SFR measures.

Since emission from young stars peaks in the UV, the UV continuum is a common probe of recent SFR. This measure of SFR has been used extensively in recent years due to the wealth of high quality UV data from the GALEX mission (Martin et al., 2005). Given that the largest contribution to the UV continuum of galaxies is from short-lived, massive young stars, the UV emission is useful for probing the star formation rate over the last 10-200 Myr (e.g. Hao et al., 2011). The most significant issue in UV-derived SFRs is how susceptible UV light is to dust attenuation, $\sim$30-50 per cent of the UV light is suspected to be absorbed and re-processed by dust (Dole et al., 2006; Kennicutt et al., 2009). For this reason, the IR continuum has also emerged as a useful SFR diagnostic (e.g. Kennicutt, 1998), especially when focusing on dust-obscured star formation. Using *both* the UV and IR continuum can therefore capture both the starlight absorbed *and* not absorbed by dust, provided both UV and IR measurements are available, which is increasingly becoming the case given the large samples provided by missions/surveys such as *GALEX*, *WISE* (Wright et al., 2010) and *Spitzer IRAC+MIPS* (Werner et al., 2004). Whereas UV or optical SFR measurements used alone can have statistical uncertainties of factors of two or more (e.g. Brinchmann et al., 2004; Salim et al., 2007), these composite indicators (e.g. Kennicutt et al., 2009) do much better.

Along with the continuum, the luminosities or equivalent widths of certain emission lines or photometric bands from ionized gas can be used to trace SFR. Hα remains the line of choice for most low-z SFR measurements, though others are commonly used such as [OII] for intermediate z, Lyα for high z, or 15μm or 24μm emission for dust-obscured star formation (e.g. Koyama et al., 2008; Saintonge et al., 2008; Brand et al., 2009). Note that dust reprocessing can also affect these measurements.

In the absence of strong continuum emission or emission lines, the so-called 4000 angstrom break can be used as a SFR diagnostic (Balogh et al., 1999). Absorption lines from ionized metals in old stellar atmospheres populate a narrow wavelength range near 4000 Å, causing this to be the strongest discontinuity in the optical spectrum of a galaxy. The presence of multiply-ionized metals in young, hot stars decreases stellar opacity and weakens the strength of this break (Hamilton, 1985). The strength of the break in a galaxy's spectrum at 4000 Å is therefore sensitive to recent star formation.

Galaxies can be broadly separated into two populations based on their star formation rates (e.g. Balogh et al., 2004a; Wetzel et al., 2012). Fig. 1.2 shows distributions of *specific* star formation rates (sSFR; SFR/$M_{stellar}$) for ∼300,000 low-z SDSS galaxies binned by stellar mass. I normalize the star formation rate by $M_{stellar}$ since it has been shown that star formation rate and stellar mass are correlated for star-forming galaxies (e.g. Noeske et al., 2007b; Elbaz et al., 2007; Daddi et al., 2007). No matter the stellar mass, the sSFR distributions are bimodal, with an actively star-forming peak and a quiescent peak, but a relative dearth of galaxies near $\sim 10^{-11}$ $M_\odot$/yr. The fraction of galaxies in each mode changes with stellar mass; however, this break exists in the same location at all stellar masses and over a variety of environments (Wetzel et al., 2012). The types of galaxies that populate the active peak and the quiescent peak will be discussed in Section 1.2.

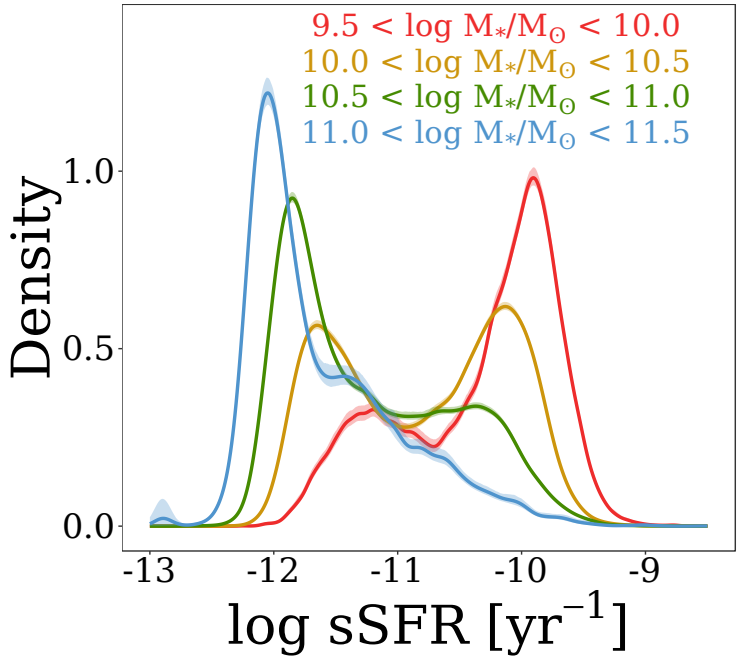

Figure 1.2 Specific star formation rate (sSFR) distribution of ∼300,000 low-z SDSS galaxies binned by stellar mass. Shaded regions are 99% confidence intervals from 1000 bootstrap resamplings.

1.1.3 Stellar Mass

Understanding and constraining the galaxy mass function is crucial in building up a framework for galaxy evolution and mass assembly (see Baugh, 2006, for a review of hierarchical galaxy evolution). Additionally, the fact that most galaxy properties depend more strongly on stellar mass than on any other property (e.g. Kauffmann et al., 2003a; Noeske et al., 2007b; van den Bosch et al., 2008; Peng et al., 2010; Woo et al., 2013, see also Section 1.2.) places even more importance on accurate stellar mass estimates when studying galaxy evolution. Stellar mass is notoriously difficult to measure and involves assumptions about the stellar initial mass function (IMF) and the mass-to-light ratio (M/L) of the galaxy. Typical methods involve using stellar population synthesis (SPS) models (e.g. Fioc & Rocca-Volmerange, 1997; Bruzual & Charlot, 2003) which include libraries of different star formation histories and stellar metallicities. Codes using these models are used to fit NIR-optical spectra or photometry (e.g. Brinchmann & Ellis, 2000; Bell et al., 2003; Zibetti et al., 2009) or spectral features such as the 4000 Å break or the $H\delta_A$ spectral index (Worthey & Ottaviani, 1997). The combination of stellar templates that best fit the spectra or photometry can be used to estimate the stellar mass. Having NIR measurements is particularly useful, as M/L ratios in the NIR vary much less among different galaxies as compared to M/L in the optical (Bell & de Jong, 2001) since, as mentioned above, NIR light is much less susceptible to dust attenuation. Current techniques can estimate stellar mass with a statistical uncertainty of $\sim$0.1-0.15 dex (see the comparison paper of Mobasher et al., 2015).

1.1.4 Morphology

It is relatively straightforward to assign a numerical value to many galaxy properties. However, it is much more difficult to quantify galaxy morphology.

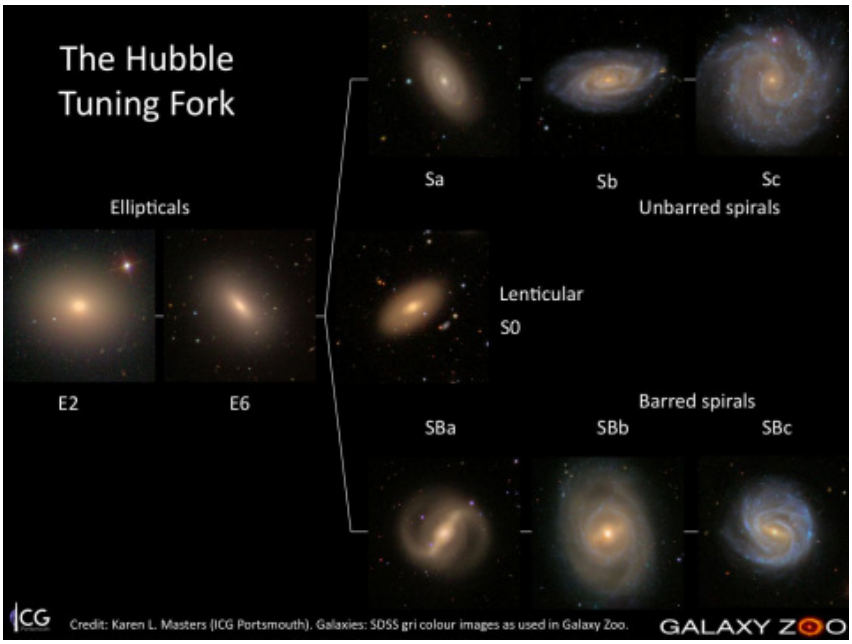

Figure 1.3 The Hubble Sequence. Early-type (elliptical) galaxies shown on the left, late-type (barred and unbarred spirals) shown on the right.

The first standardized system to classify galaxies by their morphology is the Hubble Sequence (Hubble, 1926, 1936), shown in Fig. 1.3. Hubble broadly categorized galaxies ('extragalactic nebulae', at the time) into three categories: ellipticals (E), spirals (S/SB) and irregulars (Irr). Ellipticals are further broken down by their ellipticity in projection, $e = 1 - \frac{b}{a}$, where a and b are the semi-major and semi-minor axes of the ellipse, respectively. Ellipticals are denoted by this ellipticity multiplied by ten and rounded, i.e. an E0 galaxy would look nearly circular on the sky, while an E7 galaxy would be a highly-elliptical, cigar-shaped galaxy. Observationally ellipticals do not appear flatter than an E7 class. Spirals are divided into two parallel tracks depending on the presence or absence of a stellar bar. These tracks are further subdivided into three classes each based on the woundedness of their spiral arms and bulge prominence, which go hand in hand. Sa (or SBa if a bar is seen) galaxies display tightly wound spiral arms and a prominent, bright central bulge. Sc (SBc) show only

loosely bound spiral arms and a faint bulge if any. Sb (SBb) galaxies are intermediate between the two. The bridge between early-type and late-type on the sequence in Fig. 1.3 is the S0 (or lenticular) class, described by a prominent bulge and a defined disk, but lacking any spiral arms.

By-eye visual classification by experts (e.g. Hubble, 1926; Sandage, 1961; Nair & Abraham, 2010; Baillard et al., 2011) into Hubble types was historically the principle method by which morphology was measured. The time-consuming nature of this method, has made it intractable for the most part in the modern age of massive surveys such as the SDSS. However, creative modern methods can bypass the challenges of visual classification through crowdsourced science (Galaxy Zoo[1], Lintott et al., 2008, 2011) or through machine learning (Huertas-Company et al., 2011). Galaxy Zoo and its successors will be discussed in greater detail in Section 3.3.

When full morphological classifications of galaxies are not available, or when the morphologies of a large sample of galaxies need to be compared in a quantitative way, some aspects of the light profiles of galaxies can be used as useful morphological proxies. Although there are more sophisticated quantitative tools or proxies available, in this thesis I use a single Sérsic fit (Sérsic, 1963, 1968) as the main measure of morphology. The Sérsic index, often denoted n or n_s is a fitting parameter in the radial surface brightness profile of a galaxy:

$$\ln \mathrm{I}_r = \ln \mathrm{I}_e - k(r/r_e)^{1/n_s} \ , \tag{1.1}$$

where r_e is the effective radius of the profile, I_e is the intensity at the effective radius and k and n_s are free parameters. n_s=4 gives the classic de Vaucouleurs profile (de Vaucouleurs, 1948) describing elliptical galaxies. An n_s=1 purely exponential profile is generally a good fit to pure, bulgeless spiral galaxies. In

[1] https://www.galaxyzoo.org/

practice, galaxies can be best fit by Sérsic indices in the range $1 \lesssim n_s \lesssim 10$, although the upper and lower bounds chosen by fitting schemes can change.

1.1.5 AGN Contribution

It has become increasingly clear that the supermassive black holes (SMBHs) lurking at the centres of all large galaxies have a profound effect on the growth and evolution of their host galaxy, particularly the bulge (e.g. Richstone et al., 1998; Ferrarese & Merritt, 2000; Kauffmann et al., 2003a). The energetic, multi-wavelength emission from Active Galactic Nuclei (AGN) – gas accretion onto an SMBH (Lynden-Bell, 1969; Soltan, 1982) – heats and displaces surrounding gas, see Fig. 1.4. AGN feedback is invoked in many modern models for galaxy growth and evolution (e.g. Granato et al., 2004; Springel et al., 2005; Hopkins et al., 2006; Bower et al., 2006; Sijacki et al., 2015). Though AGN feedback quenches star formation in the long term, the link between *ongoing* AGN emission and star formation is still debated, with various studies finding that AGN hosts experience enhanced star formation (e.g. Silverman et al., 2009; Rosario et al., 2015), suppressed star formation (e.g. Salim et al., 2007; Gürkan et al., 2015; Ellison et al., 2016) or normal star formation (Harrison et al., 2012; Lanzuisi et al., 2015). Regardless, the presence (or lack thereof) of an AGN is a valuable piece of information about a galaxy.

The broad-spectrum emission of AGN, from the X-ray all the way to the radio, provides a wide array of available diagnostics to detect them, including 1.4GHz luminosity (e.g. Best et al., 2005; Kauffmann et al., 2008), infrared colours (e.g. Lacy et al., 2004; Stern et al., 2005; Stern et al., 2012), optical emission line diagnostics (e.g. Baldwin et al., 1981; Kauffmann et al., 2003a; Schawinski et al., 2007) and X-ray $\sim$0.5keV - $\sim$10keV luminosity (e.g. Silverman et al., 2009; Hickox et al., 2009; Rosario et al., 2015). This wide range of AGN identification tools is double-edged; on the one hand, having diagnos-

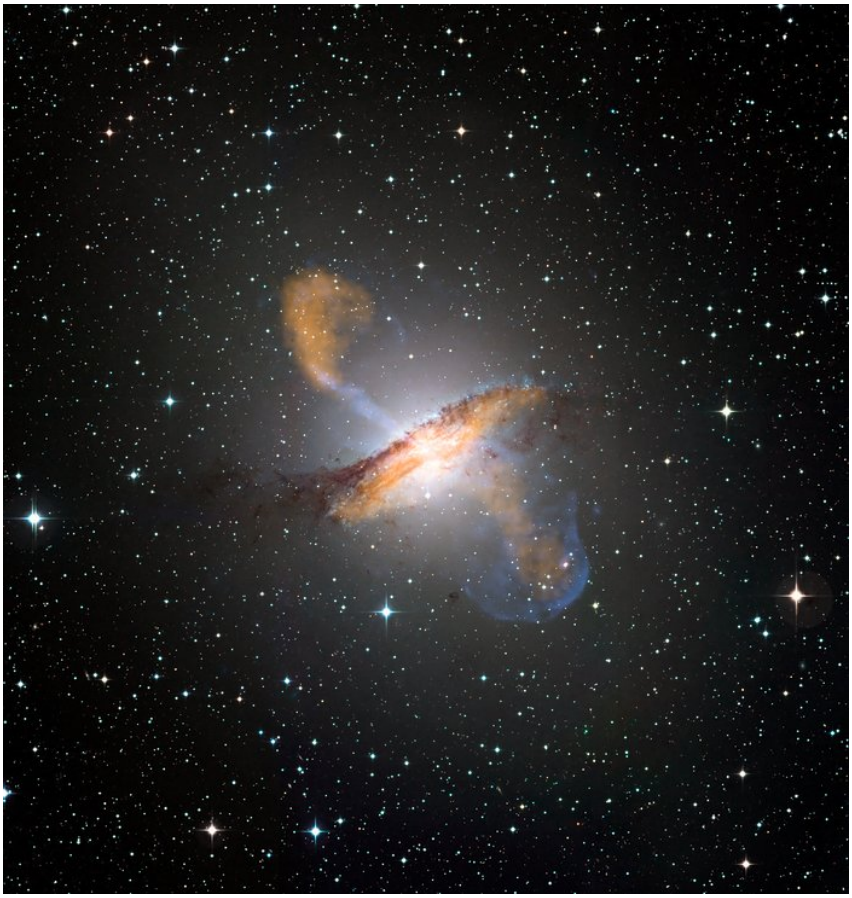

Figure 1.4 Composite image of nearby active galaxy Centaurus A. Jets and lobes are clearly seen emanating away from the disk of the galaxy. 870μm emission shown in orange. X-ray emission shown in blue. Optical emission shown in true colour. Image credit: ESO/WFI (Optical); MPIfR/ESO/APEX/A. Weiss et al. (870μm); NASA/CXC/CfA/R. Kraft et al. (X-ray)

tics across a broad wavelength range means that AGN can be detected with a wide range of instruments and in a wide range of surveys. On the other, the properties of AGN-hosting galaxies and the AGN themselves depend on which diagnostic is used to select the AGN (e.g. Hickox et al., 2009) which makes comparisons among studies difficult and can lead to seemingly contradictory results. In this work I select AGN with a diagnostic using optical emission lines, a more in-depth discussion of which is can be found in Sections 2.3.5 and 3.2. See Fabian (2012) and Alexander & Hickox (2012) for a review of AGN physics and AGN diagnostics, respectively.

1.1.6 Environment

Galaxies in the Universe reside in a range of environments and in many cases a galaxy's local environments has a profound effect on its evolution. Here I briefly outline several metrics used in the literature and in this thesis to characterize galaxy environment. For a more comprehensive overview of environmental measures, see Haas et al. (2012) and Carollo et al. (2013). One common and relatively simple environment diagnostic is the nth nearest neighbour density, i.e. $\Sigma_n = \frac{n}{\pi d_n^2}$, the surface density of galaxies within d_n, the projected distance from a galaxy to its nth nearest neighbour (or equivalently the density of galaxies within a sphere of radius d_n if precision redshifts are known). Several works use the nth nearest neighbour density (or slight variations) with different choices of n to characterize environment (e.g. Balogh et al., 2004a; Baldry et al., 2006; Masters et al., 2010; Li et al., 2011). This is often transformed to a local galaxy overdensity, the fractional offset from the mean nearest neighbour density, $\delta_n = (\Sigma_n - \overline{\Sigma_n})/\overline{\Sigma_n}$, to more clearly investigate how underdense or overdense environments affect galaxies (e.g. Peng et al., 2010, 2012; Woo et al., 2013; Knobel et al., 2015).

When group or cluster membership can be established (e.g. Yang et al., 2005, 2007), other environmental measures become available. The dark matter halo mass of the group or cluster, typically calculated using the line-of-sight velocities of member galaxies or using a weighted group luminosity (e.g. Eke et al., 2004a,b; Yang et al., 2005, 2007), has been shown to correlate well with local overdensity (Haas et al., 2012; Carollo et al., 2013). Similarly, the projected distance of a galaxy to the centre of its host group or cluster correlates with local overdensity as well (e.g. Peng et al., 2012; Woo et al., 2013). A more detailed discussion of how M_{halo} and group-centric distance are calculated for my purposes is presented in Section 2.2. The group centre is most often defined by the location of the 'central', the brightest, most massive galaxy in the group, while all remaining galaxies in the group are deemed satellites. This 'central galaxy paradigm' (van den Bosch et al., 2005) – the assumption that the brightest group galaxy resides at the centre of the group's dark matter halo – is an important assumption for many works including this thesis. In unrelaxed or high-M_{halo} groups, however, its validity can be questionable (van den Bosch et al., 2005; Skibba et al., 2011).

Several galaxy properties have been found to depend on environment, including morphology (e.g. Dressler, 1980; Postman & Geller, 1984; van der Wel, 2008; Wilman & Erwin, 2012), star formation rate (e.g. Hashimoto et al., 1998; McGee et al., 2011; Wijesinghe et al., 2012; Wetzel et al., 2012; Grootes et al., 2017), colour (e.g. Baldry et al., 2006; Blanton & Berlind, 2007; Bamford et al., 2009; Skibba, 2009; Wilman et al., 2010) and AGN fraction (e.g. Kauffmann et al., 2004; Montero-Dorta et al., 2009; Pimbblet et al., 2013) (although several works (e.g. Miller et al., 2003; von der Linden et al., 2010) find no AGN dependence). See Fig. 1.5 for an example. This figure, taken from Knobel et al. (2015), shows how the quenched fraction of satellites (i.e. the fraction of satellites that are no longer star-forming) in the SDSS DR7 group sample of Yang et al. (2012) depends on both on the stellar mass of the satellite and its en-

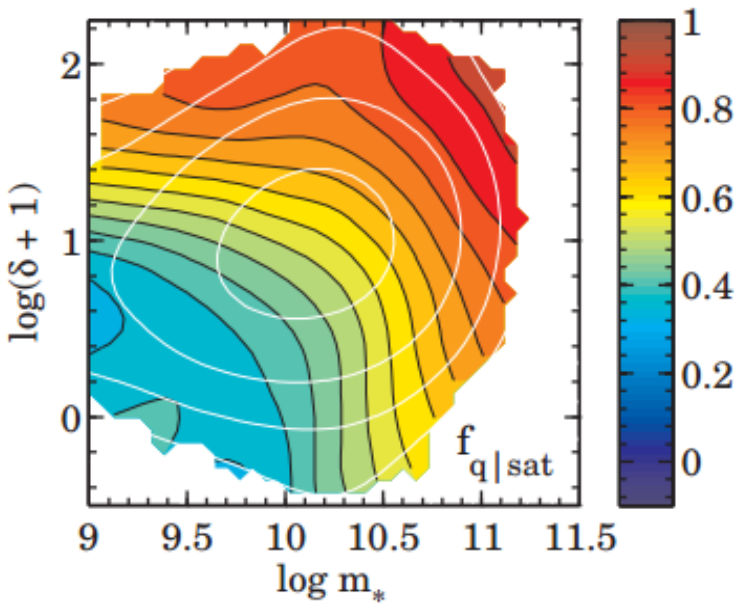

Figure 1.5 Colour scale shows quenched fraction of Yang et al. (2012) group sample satellites as a function of local overdensity (see text for definition) and stellar mass. Black lines show contours of constant f_q, white contours indicate number density of objects in logarithmic scale. Credit: Knobel et al. (2015).

vironment (characterized by local overdensity) with a varying dependence in different regions of parameter space.

1.2 Property Correlations & Galaxy Taxonomy

In the previous sections I provided a list of integrated properties one can use to characterize a galaxy and how these properties are measured. This list was not close to exhaustive. In addition to having multiple ways to assess each property, other properties include, but are not limited to: gas-phase and stellar metallicity, luminosity (across a range of wavebands), disk inclination, dust extinction, gas and dust mass, rotational velocity/velocity dispersion and redshift. There is therefore a very wide and highly-dimensional parameter space of properties within which galaxies reside. Observationally, however, we find that many galaxy properties are correlated, and there is a deep body of literature describing these correspondences and establishing causal links between properties. In this section I describe not only the two broad galaxy populations generated by these correlations but also some well-studied populations of galaxies which defy the typical correspondence between properties.

In Fig. 1.6 I show a correlation plot matrix among all the pairs of properties: stellar mass, $z = 0.1$ k-corrected $g - r$ colour, specific star formation rate ($\mathrm{SFR}/\mathrm{M}_{stellar}$) and morphology (as measured using the Sérsic index) for $\sim$300,000 low-z SDSS galaxies. 1-D density distributions are shown along diagonal and 2-D distributions among different property pairs are shown below the diagonal. Spearman rank coefficients (Spearman, 1904) are shown above the diagonal for corresponding pairs. Here a number of interesting relationships betweens properties supported by the literature are seen:

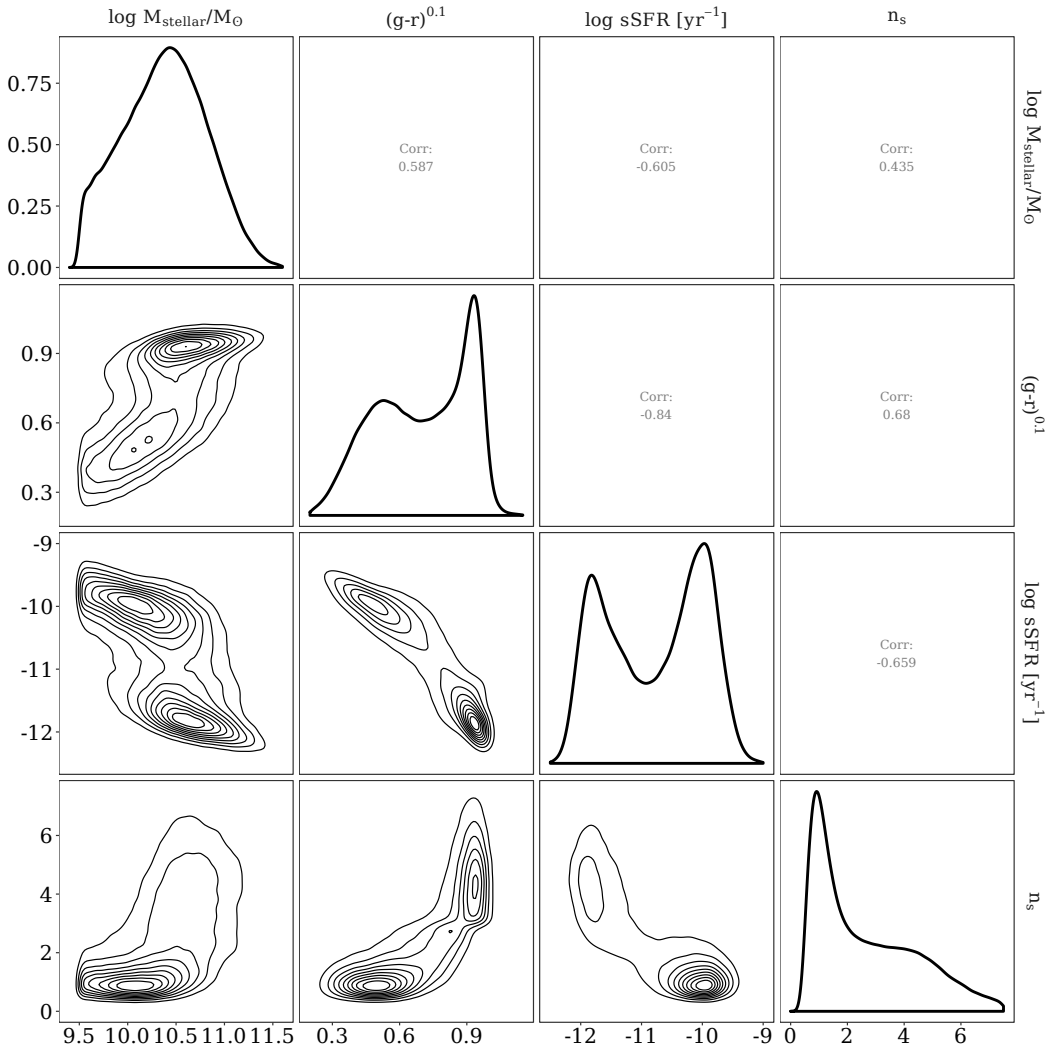

Figure 1.6 Plot matrix showing correlations between stellar mass, $z = 0.1$ k-corrected $g - r$ colour, specific star formation rate ($SFR/M_{stellar}$) and Sérsic index in a sample of ∼300,000 low-redshift SDSS galaxies. 1D Gaussian-smoothed density distributions shown along diagonal. 2D distribution for galaxy property pairs shown below the diagonal. Spearman rank coefficient for corresponding property pair shown above diagonal.

- The fraction of red galaxies increases with stellar mass and the average colour of galaxies reddens with stellar mass (see also e.g. Baldry et al., 2006; van den Bosch et al., 2008; Bamford et al., 2009).

- Similarly, both the fraction of passive galaxies and the average sSFR of galaxies decline with increasing stellar mass (see also e.g. Noeske et al., 2007a; Elbaz et al., 2007; McGee et al., 2011; Wetzel et al., 2012).

- Early-type (high n_s) galaxies become more common at high stellar mass (see also e.g. Kauffmann et al., 2003b; van der Wel, 2008; Calvi et al., 2012).

- There is a strong negative correlation between optical colour and sSFR (see also e.g. Weinmann et al., 2006; Mahajan & Raychaudhury, 2009).

- Redder galaxies have more early-type morphologies (see also e.g. de Vaucouleurs, 1961; Larson et al., 1980; Strateva et al., 2001; Krywult et al., 2017).

- Galaxies with higher sSFRs have more late-type morphologies (see also e.g. Kauffmann et al., 2003b; Bell et al., 2012; Woo et al., 2015; Snyder et al., 2015).

These correlations, coupled with the bimodality in colour and sSFR, yield two main populations of galaxies in the universe:

- **Blue** galaxies exhibit **late-type** morphologies and are **active** in their star formation. They are biased towards **low** stellar masses.

- **Red** galaxies exhibit **early-type** morphologies and **suppressed** specific star formation rates. They are biased towards **high** stellar masses.

These two broad populations are often referred to as the *red sequence* and *blue cloud*, due to the tight linear feature red galaxies form when plotted on a colour-magnitude diagram (Visvanathan & Sandage, 1977) and the more widespread region that blue galaxies inhabit by comparison (see Fig. 1.1). Because the red sequence and blue cloud are defined solely by the colour-magnitude diagram with no regard for sSFR or morphology, I shy away from this terminology and instead refer to them as *Red Passives* and *Blue Actives* when defining them based on inclination-corrected optical colour and sSFR in section 2.2.

I point out that the tight correlations between properties and the clear bimodality in galaxy populations apparent in Fig. 1.6 applies only in the specific case of low-to-intermediate-z, massive galaxies. The galaxies shown in Fig. 1.6 are all low redshift (z<0.1) and relatively massive ($M_{stellar}$>$10^{9.5}M_{\odot}$) galaxies. In the dwarf galaxy regime ($\sim$$10^{7}M_{\odot}$– $\sim$$10^{9}M_{\odot}$), dwarf early-types are more often fit with $n_s = 1$ exponential profiles (Faber & Lin, 1983), are more likely evolutionarily linked to low-mass spirals and irregulars rather than massive ellipticals (Moore et al., 1998; Kormendy et al., 2009) and can exhibit complex, bursty star formation histories (e.g. Mateo, 1998; Tolstoy et al., 2009, and references therein). Along with being harder to measure, at high redshift galaxy morphologies become more clumpy and irregular (Glazebrook et al., 1995; Abraham et al., 1996; Elmegreen et al., 2005). Consequently determining how other properties scale with morphology becomes non-trivial. For the remainder of this thesis it should be assumed that when I discuss galaxy populations I am referring only to low-redshift, reasonably massive galaxies.

It is important to remember that correlation does not necessarily imply causation. Morphology and colour are positively correlated in Fig. 1.6, and yet both correlate with stellar mass. Is there still a relationship between morphology and colour at fixed stellar mass? To establish causal relationships between galaxy properties and understand the mechanisms affecting galaxy evolution,

one has to study correlations in the full, highly-dimensional parameter space, keeping all but one parameter fixed (see Section 15.5 of Mo et al., 2010).

This issue becomes even more pronounced when trying to discern the effect of environment. Fig. 1.7 shows the same plot matrix as Fig. 1.6, except now two environmental metrics have been added; group halo mass and projected group-centric distance (normalized by r_{200}). Distributions are shown for galaxies in the Yang et al. (2007) group catalog derived from SDSS Data Release 7 (DR7; Abazajian et al., 2009). See Section 2.2 for a more detailed discussion of this group sample and the calculation of M_{halo} and r/r_{200}. Notice from the colour and sSFR 1D distributions (panels [2,2] and [3,3] respectively) that this sample is biased towards more red and quiescent galaxies. In addition to showing the same trends seen in Fig. 1.6, a number of environmental trends can be seen as well:

- A *slight* indication that the mean stellar mass of galaxies increases towards more dense (high M_{halo}, low r/r_{200}) environments (consistent with Roberts et al., 2014; Balogh et al., 2014; Joshi et al., 2016).
- There is a dearth of blue galaxies in high-density environments (see also e.g. Cooper et al., 2006; Blanton & Berlind, 2007; van den Bosch et al., 2008; Bamford et al., 2009)
- There is also a dearth of highly-starforming galaxies in high-density environments (see also e.g Gómez et al., 2003; Pasquali et al., 2009; Kimm et al., 2009; Wetzel et al., 2012)
- Late-type galaxies become rare in high-density environments (see also e.g. Dressler, 1980; Postman & Geller, 1984; Wilman & Erwin, 2012)

I can then add an addendum to my statement about the broad red and blue populations, again avoiding any bold claims about causality between properties:

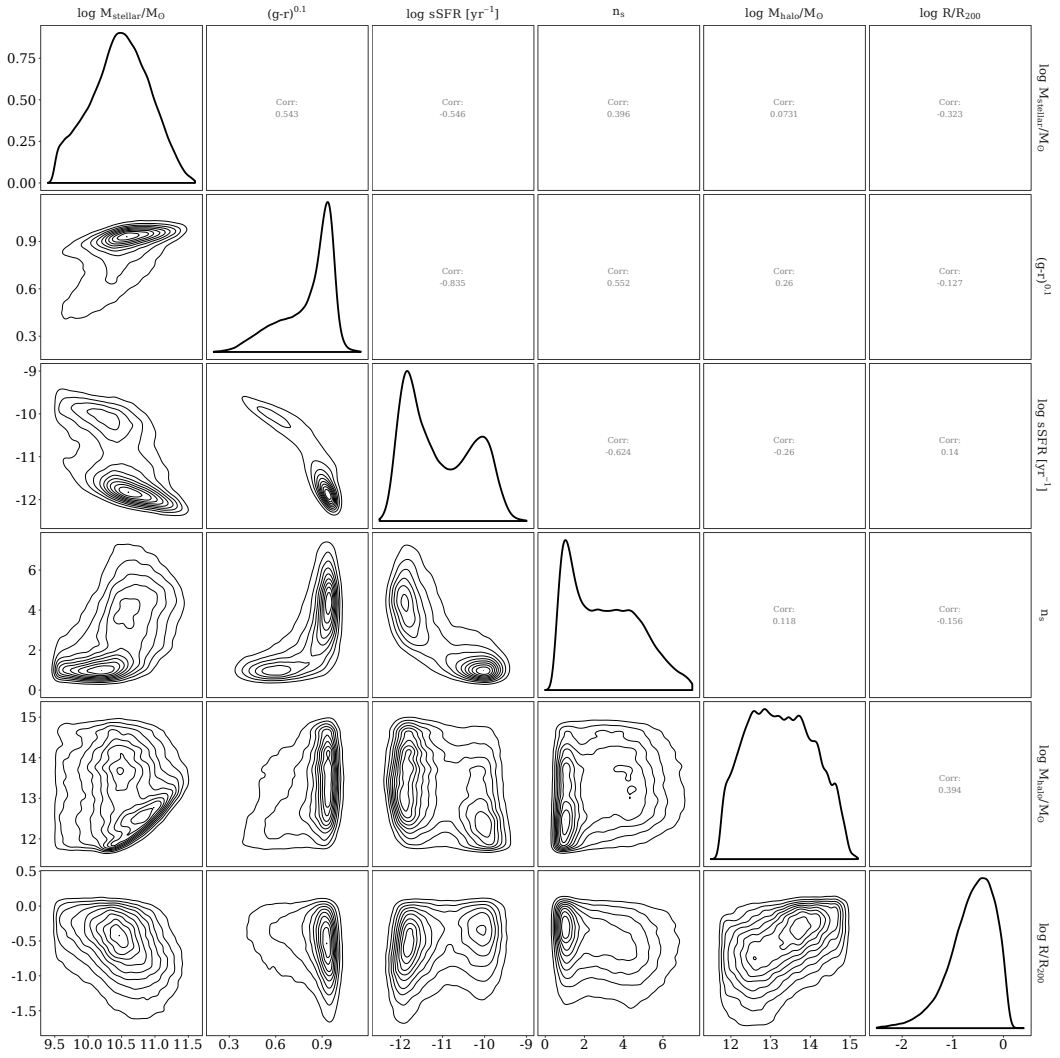

Figure 1.7 Plot matrix showing correlations between stellar mass, $g-r$ colour, specific star formation rate, Sérsic index, group halo mass and normalized projected group-centric distance in a sample of ∼100,000 low-redshift SDSS group and cluster galaxies. 1D Gaussian-smoothed density distributions shown along diagonal. 2D distribution for galaxy property pairs shown below the diagonal. Spearman rank coefficient for corresponding property pair shown above diagonal.

- The blue, star-forming, late-type galaxies are preferentially found in low-density environments such as the isolated field or on the outskirts of low-M_{halo} groups.

- The red, quiescent, early-type galaxies are preferentially found in high density environments such as near the centres of groups and clusters.

1.2.1 Outlier Populations and Red Misfits

One method of studying galaxy evolution is to disentangle all the interrelationships between galaxy properties in an effort to discern which mechanisms are affecting galaxy evolution. Another another option is to study outlier populations, i.e. galaxies for which one or multiple correspondences seen between galaxy properties break down. These galaxies may be following an interesting evolutionary pathway or they may be in the midst of transforming from blue, late-type and star-forming to red, early-type and quiescent, a process known as quenching (see Section 2.1 for a discussion of quenching mechanisms). Some of these outlier populations include: the so-called 'red spirals' – late-type quiescent red galaxies that break the correspondence between colour and morphology (e.g. van den Bergh, 1976; Poggianti et al., 1999; Goto et al., 2003; Bundy et al., 2010; Masters et al., 2010; Tojeiro et al., 2013, and references therein), early-type blue galaxies – which again break colour-morphology correspondence but in the opposite direction (e.g. Schawinski et al., 2009; Kannappan et al., 2009; Huertas-Company et al., 2010; Tojeiro et al., 2013), the similar population of quiescent blue galaxies (e.g. Mahajan & Raychaudhury, 2009), the 'green valley' – galaxies which inhabit the sparsely-populated region between the red sequence and the blue cloud (e.g. Bell et al., 2004; Faber et al., 2007; Wyder et al., 2007; Mendez et al., 2011; Gonçalves et al., 2012; Schawinski et al., 2014, and references therein), green pea galaxies – Galaxy

Zoo-identified galaxies are visually green and having very clumpy morphologies (e.g. Cardamone et al., 2009; Izotov et al., 2011; Amorín et al., 2012; Jaskot & Oey, 2013), or simply all galaxies with interesting morphologies such as S0's (for a review see van den Bergh, 2009) or irregular galaxies. I will return to the most relevant of these populations (the red spirals, the green valley and S0's) in Section 2.4.3 and discuss them in greater detail.

In this study, I focus on an outlier population of galaxies which I have coined 'Red Misfits'. These galaxies are red in optical colour but actively forming stars, i.e. they defy the strong sSFR-colour correspondence seen in panel [3,2] of Fig. 1.6 and Fig. 1.7. I study whether and how the properties of Red Misfits (their stellar masses, morphologies, dust extinctions, gas-phase metallicities, stellar ages, AGN abundance and preferred environments) differ from the 'Blue Actives' and 'Red Passives', the two broad populations seen in this parameter space.

1.3 Outline of this Thesis

The goal of this thesis is to take full advantage of the SDSS and related data products to study the properties of Red Misfits. In particular, I want to determine whether Red Misfits truly represent a physically distinct population in the Universe or if they can simply be explained by scatter from the Blue Active and Red Passive populations. If they are a unique population, the evolutionary histories and properties of Red Misfits may help constrain quenching mechanisms and timescales. If they can be entirely explained by scatter from the Blue Active and Red Passive populations, this study can help assess the uncertainties involved in measuring colour and star formation rate which are important for interpreting many other SDSS results.

In Chapter 2 I present the results of my investigation into Red Misfits. I outline the full sample of galaxies I generate by matching several SDSS DR7-derived catalogues. I define Red Misfits as red and starforming by the bimodal distributions of specific star formation rates and inclination-corrected g-r colours among SDSS galaxies; while the majority of the galaxies in my sample will be either optically blue and actively star-forming *or* optically red and quiescent, the small but significant population of Red Misfits will be on the star-forming end of the sSFR distribution and the red end of the colour distribution. I show through their intermediate morphologies, enhanced AGN fraction and remarkable indifference towards environment that Red Misfits are a population distinct from Blue Actives and Red Passives and that their evolution is likely dominated by internal processes rather than environmental ones. I compare them to the red spiral population, green valley galaxies and S0's and find that while they share some similarities with these populations, these populations cannot account entirely for Red Misfits. A cornerstone of this study is my use of inclination-corrected colours when defining Red Misfits to reduce contamination from intrinsically blue but highly inclined star-forming galaxies. The Appendix of Chapter 2 is devoted to outlining my colour correction methodology and testing its effectiveness. Chapter 2 represents a paper recently submitted to *Monthly Notices of the Royal Astronomical Society*, with Section 2.7 originally an appendix to the paper text in Chapter 2. In Chapter 3 I present results from further investigations into Red Misfit properties, omitted from the submitted paper for brevity and clarity. In this chapter I delve more deeply into the purported enhanced AGN fraction of Red Misfits, employ the morphological classifications of Galaxy Zoo (Lintott et al., 2008) to confirm the intermediate morphologies of Red Misfits and ensure the enhanced AGN fraction and significant star formation rates of Red Misfits are not a result of them being found in close galaxy pairs. In Chapter 4 I summarize my re-

sults and compare them to studies of similar populations of red, star-forming galaxies and discuss future work.

Bibliography

Abazajian, K. N., Adelman-McCarthy, J. K., Agüeros, M. A., Allam, S. S., Prieto, C. A., An, D., Anderson, K. S. J., Anderson, S. F., Annis, J., Bahcall, N. A., Bailer-Jones, C. A. L., Barentine, J. C., Bassett, B. A., Becker, A. C., Beers, T. C., Bell, E. F., Belokurov, V., Berlind, A. A., Berman, E. F., Bernardi, M., Bickerton, S. J., Bizyaev, D., Blakeslee, J. P., Blanton, M. R., Bochanski, J. J., Boroski, W. N., Brewington, H. J., Brinchmann, J., Brinkmann, J., Brunner, R. J., Budavári, T., Carey, L. N., Carliles, S., Carr, M. A., Castander, F. J., Cinabro, D., Connolly, A. J., Csabai, I., Cunha, C. E., Czarapata, P. C., Davenport, J. R. A., de Haas, E., Dilday, B., Doi, M., Eisenstein, D. J., Evans, M. L., Evans, N. W., Fan, X., Friedman, S. D., Frieman, J. A., Fukugita, M., Gänsicke, B. T., Gates, E., Gillespie, B., Gilmore, G., Gonzalez, B., Gonzalez, C. F., Grebel, E. K., Gunn, J. E., Györy, Z., Hall, P. B., Harding, P., Harris, F. H., Harvanek, M., Hawley, S. L., Hayes, J. J. E., Heckman, T. M., Hendry, J. S., Hennessy, G. S., Hindsley, R. B., Hoblitt, J., Hogan, C. J., Hogg, D. W., Holtzman, J. A., Hyde, J. B., ichi Ichikawa, S., Ichikawa, T., Im, M., Ivezić, Ž., Jester, S., Jiang, L., Johnson, J. A., Jorgensen, A. M., Jurić, M., Kent, S. M., Kessler, R., Kleinman, S. J., Knapp, G. R., Konishi, K., Kron, R. G., Krzesinski, J., Kuropatkin, N., Lampeitl, H., Lebedeva, S., Lee, M. G., Lee, Y. S., Leger, R. F., Lépine, S., Li, N., Lima, M., Lin, H., Long, D. C., Loomis, C. P., Loveday, J., Lupton, R. H., Magnier, E., Malanushenko, O., Malanushenko, V., Mandelbaum, R., Margon, B., Marriner, J. P., Martínez-Delgado, D., Matsubara, T., McGehee, P. M., McKay, T. A., Meiksin, A., Morrison, H. L., Mullally, F., Munn, J. A., Murphy, T., Nash, T., Nebot, A., Neilsen, E. H., Newberg, H. J., Newman, P. R., Nichol, R. C., Nicinski, T., Nieto-Santisteban, M., Nitta,

A., Okamura, S., Oravetz, D. J., Ostriker, J. P., Owen, R., Padmanabhan, N., Pan, K., Park, C., Pauls, G., Peoples, J., Percival, W. J., Pier, J. R., Pope, A. C., Pourbaix, D., Price, P. A., Purger, N., Quinn, T., Raddick, M. J., Fiorentin, P. R., Richards, G. T., Richmond, M. W., Riess, A. G., Rix, H.-W., Rockosi, C. M., Sako, M., Schlegel, D. J., Schneider, D. P., Scholz, R.-D., Schreiber, M. R., Schwope, A. D., Seljak, U., Sesar, B., Sheldon, E., Shimasaku, K., Sibley, V. C., Simmons, A. E., Sivarani, T., Smith, J. A., Smith, M. C., Smolčić, V., Snedden, S. A., Stebbins, A., Steinmetz, M., Stoughton, C., Strauss, M. A., SubbaRao, M., Suto, Y., Szalay, A. S., Szapudi, I., Szkody, P., Tanaka, M., Tegmark, M., Teodoro, L. F. A., Thakar, A. R., Tremonti, C. A., Tucker, D. L., Uomoto, A., Berk, D. E. V., Vandenberg, J., Vidrih, S., Vogeley, M. S., Voges, W., Vogt, N. P., Wadadekar, Y., Watters, S., Weinberg, D. H., West, A. A., White, S. D. M., Wilhite, B. C., Wonders, A. C., Yanny, B., Yocum, D. R., York, D. G., Zehavi, I., Zibetti, S., & Zucker, D. B. 2009, ApJS, 182, 543

Abraham, R. G., Tanvir, N. R., Santiago, B. X., Ellis, R. S., Glazebrook, K., & van den Bergh, S. 1996, MNRAS, 279, L47

Alexander, D. M. & Hickox, R. C. 2012, New A Rev., 56, 93

Amorín, R., Pérez-Montero, E., Vílchez, J. M., & Papaderos, P. 2012, ApJ, 749, 185

Baillard, A., Bertin, E., de Lapparent, V., Fouqué, P., Arnouts, S., Mellier, Y., Pelló, R., Leborgne, J.-F., Prugniel, P., Makarov, D., Makarova, L., McCracken, H. J., Bijaoui, A., & Tasca, L. 2011, A&A, 532, A74

Baldry, I. K., Balogh, M. L., Bower, R. G., Glazebrook, K., Nichol, R. C., Bamford, S. P., & Budavari, T. 2006, MNRAS, 373, 469

Baldry, I. K., Glazebrook, K., Brinkmann, J., Ivezić, Ž., Lupton, R. H., Nichol, R. C., & Szalay, A. S. 2004, ApJ, 600, 681

Baldwin, J. A., Phillips, M. M., & Terlevich, R. 1981, PASP, 93, 5

Balogh, M., Eke, V., Miller, C., Lewis, I., Bower, R., Couch, W., Nichol, R., Bland-Hawthorn, J., Baldry, I. K., Baugh, C., Bridges, T., Cannon, R., Cole, S., Colless, M., Collins, C., Cross, N., Dalton, G., Propris, R. D., Driver, S. P., Efstathiou, G., Ellis, R. S., Frenk, C. S., Glazebrook, K., Gomez, P., Gray, A., Hawkins, E., Jackson, C., Lahav, O., Lumsden, S., Maddox, S., Madgwick, D., Norberg, P., Peacock, J. A., Percival, W., Peterson, B. A., Sutherland, W., & Taylor, K. 2004a, MNRAS, 348, 1355

Balogh, M. L., Baldry, I. K., Nichol, R., Miller, C., Bower, R., & Glazebrook, K. 2004b, ApJ, 615, L101

Balogh, M. L., McGee, S. L., Mok, A., Wilman, D. J., Finoguenov, A., Bower, R. G., Mulchaey, J. S., Parker, L. C., & Tanaka, M. 2014, MNRAS, 443, 2679

Balogh, M. L., Morris, S. L., Yee, H. K. C., Carlberg, R. G., & Ellingson, E. 1999, ApJ, 527, 54

Bamford, S. P., Nichol, R. C., Baldry, I. K., Land, K., Lintott, C. J., Schawinski, K., Slosar, A., Szalay, A. S., Thomas, D., Torki, M., Andreescu, D., Edmondson, E. M., Miller, C. J., Murray, P., Raddick, M. J., & Vandenberg, J. 2009, MNRAS, 393, 1324

Baugh, C. M. 2006, Reports on Progress in Physics, 69, 3101

Bell, E. F. & de Jong, R. S. 2001, ApJ, 550, 212

Bell, E. F., McIntosh, D. H., Katz, N., & Weinberg, M. D. 2003, ApJS, 149, 289

Bell, E. F., van der Wel, A., Papovich, C., Kocevski, D., Lotz, J., McIntosh, D. H., Kartaltepe, J., Faber, S. M., Ferguson, H., Koekemoer, A., Grogin, N., Wuyts, S., Cheung, E., Conselice, C. J., Dekel, A., Dunlop, J. S., Giavalisco, M., Herrington, J., Koo, D. C., McGrath, E. J., de Mello, D., Rix, H.-W., Robaina, A. R., & Williams, C. C. 2012, ApJ, 753, 167

Bell, E. F., Wolf, C., Meisenheimer, K., Rix, H.-W., Borch, A., Dye, S., Kleinheinrich, M., Wisotzki, L., & McIntosh, D. H. 2004, ApJ, 608, 752

Best, P. N., Kauffmann, G., Heckman, T. M., Brinchmann, J., Charlot, S., IveziÄĞ, Å., & White, S. D. M. 2005, Monthly Notices of the Royal Astronomical Society, 362, 25

Blanton, M. R. & Berlind, A. A. 2007, ApJ, 664, 791

Bower, R. G., Benson, A. J., Malbon, R., Helly, J. C., Frenk, C. S., Baugh, C. M., Cole, S., & Lacey, C. G. 2006, MNRAS, 370, 645

Brand, K., Moustakas, J., Armus, L., Assef, R. J., Brown, M. J. I., Cool, R. R., Desai, V., Dey, A., Floc'h, E. L., Jannuzi, B. T., Kochanek, C. S., Melbourne, J., Papovich, C. J., & Soifer, B. T. 2009, ApJ, 693, 340

Brinchmann, J., Charlot, S., White, S. D. M., Tremonti, C., Kauffmann, G., Heckman, T., & Brinkmann, J. 2004, MNRAS, 351, 1151

Brinchmann, J. & Ellis, R. S. 2000, ApJ, 536, L77

Bruzual, G. & Charlot, S. 2003, MNRAS, 344, 1000

Bundy, K., Scarlata, C., Carollo, C. M., Ellis, R. S., Drory, N., Hopkins, P., Salvato, M., Leauthaud, A., Koekemoer, A. M., Murray, N., Ilbert, O., Oesch, P., Ma, C.-P., Capak, P., Pozzetti, L., & Scoville, N. 2010, ApJ, 719, 1969

Calvi, R., Poggianti, B. M., Fasano, G., & Vulcani, B. 2012, MNRAS, 419, L14

Cardamone, C., Schawinski, K., Sarzi, M., Bamford, S. P., Bennert, N., Urry, C. M., Lintott, C., Keel, W. C., Parejko, J., Nichol, R. C., Thomas, D., Andreescu, D., Murray, P., Raddick, M. J., Slosar, A., Szalay, A., & Vandenberg, J. 2009, MNRAS, 399, 1191

Carollo, C. M., Cibinel, A., Lilly, S. J., Miniati, F., Norberg, P., Silverman, J. D., van Gorkom, J., Cameron, E., Finoguenov, A., Peng, Y., Pipino, A., & Rudick, C. S. 2013, ApJ, 776, 71

Charlot, S. & Bruzual, A. G. 1991, ApJ, 367, 126

Colless, M., Dalton, G., Maddox, S., Sutherland, W., Norberg, P., Cole, S., Bland-Hawthorn, J., Bridges, T., Cannon, R., Collins, C., Couch, W., Cross, N., Deeley, K., De Propris, R., Driver, S. P., Efstathiou, G., Ellis, R. S., Frenk, C. S., Glazebrook, K., Jackson, C., Lahav, O., Lewis, I., Lumsden, S., Madgwick, D., Peacock, J. A., Peterson, B. A., Price, I., Seaborne, M., & Taylor, K. 2001, MNRAS, 328, 1039

Cooper, M. C., Newman, J. A., Croton, D. J., Weiner, B. J., Willmer, C. N. A., Gerke, B. F., Madgwick, D. S., Faber, S. M., Davis, M., Coil, A. L., Finkbeiner, D. P., Guhathakurta, P., & Koo, D. C. 2006, MNRAS, 370, 198

Daddi, E., Dickinson, M., Morrison, G., Chary, R., Cimatti, A., Elbaz, D., Frayer, D., Renzini, A., Pope, A., Alexander, D. M., Bauer, F. E., Giavalisco, M., Huynh, M., Kurk, J., & Mignoli, M. 2007, ApJ, 670, 156

de Vaucouleurs, G. 1948, Annales d'Astrophysique, 11, 247

—. 1961, ApJS, 5, 233

Dole, H., Lagache, G., Puget, J.-L., Caputi, K. I., Fernández-Conde, N., Le Floc'h, E., Papovich, C., Pérez-González, P. G., Rieke, G. H., & Blaylock, M. 2006, A&A, 451, 417

Dressler, A. 1980, ApJ, 236, 351

Eke, V. R., Baugh, C. M., Cole, S., Frenk, C. S., Norberg, P., Peacock, J. A., Baldry, I. K., Bland-Hawthorn, J., Bridges, T., Cannon, R., Colless, M., Collins, C., Couch, W., Dalton, G., de Propris, R., Driver, S. P., Efstathiou, G., Ellis, R. S., Glazebrook, K., Jackson, C., Lahav, O., Lewis, I., Lumsden, S., Maddox, S., Madgwick, D., Peterson, B. A., Sutherland, W., & Taylor, K. 2004a, MNRAS, 348, 866

Eke, V. R., Frenk, C. S., Baugh, C. M., Cole, S., Norberg, P., Peacock, J. A., Baldry, I. K., Bland-Hawthorn, J., Bridges, T., Cannon, R., Colless, M., Collins, C., Couch, W., Dalton, G., de Propris, R., Driver, S. P., Efstathiou, G., Ellis, R. S., Glazebrook, K., Jackson, C. A., Lahav, O., Lewis, I., Lumsden, S., Maddox, S. J., Madgwick, D., Peterson, B. A., Sutherland, W., & Taylor, K. 2004b, MNRAS, 355, 769

Elbaz, D., Daddi, E., Le Borgne, D., Dickinson, M., Alexander, D. M., Chary, R.-R., Starck, J.-L., Brandt, W. N., Kitzbichler, M., MacDonald, E., Nonino, M., Popesso, P., Stern, D., & Vanzella, E. 2007, A&A, 468, 33

Ellison, S. L., Teimoorinia, H., Rosario, D. J., & Mendel, J. T. 2016, MNRAS, 458, L34

Elmegreen, D. M., Elmegreen, B. G., & Ferguson, T. E. 2005, ApJ, 623, L71

Faber, S. M. & Lin, D. N. C. 1983, ApJ, 266, L17

Faber, S. M., Willmer, C. N. A., Wolf, C., Koo, D. C., Weiner, B. J., Newman, J. A., Im, M., Coil, A. L., Conroy, C., Cooper, M. C., Davis, M., Finkbeiner, D. P., Gerke, B. F., Gebhardt, K., Groth, E. J., Guhathakurta, P., Harker, J., Kaiser, N., Kassin, S., Kleinheinrich, M., Konidaris, N. P., Kron, R. G., Lin, L., Luppino, G., Madgwick, D. S., Meisenheimer, K., Noeske, K. G.,

Phillips, A. C., Sarajedini, V. L., Schiavon, R. P., Simard, L., Szalay, A. S., Vogt, N. P., & Yan, R. 2007, ApJ, 665, 265

Fabian, A. C. 2012, ARA&A, 50, 455

Ferrarese, L. & Merritt, D. 2000, ApJ, 539, L9

Fioc, M. & Rocca-Volmerange, B. 1997, A&A, 326, 950

Fukugita, M., Ichikawa, T., Gunn, J. E., Doi, M., Shimasaku, K., & Schneider, D. P. 1996, AJ, 111, 1748

Glazebrook, K., Ellis, R., Santiago, B., & Griffiths, R. 1995, MNRAS, 275, L19

Gómez, P. L., Nichol, R. C., Miller, C. J., Balogh, M. L., Goto, T., Zabludoff, A. I., Romer, A. K., Bernardi, M., Sheth, R., Hopkins, A. M., Castander, F. J., Connolly, A. J., Schneider, D. P., Brinkmann, J., Lamb, D. Q., SubbaRao, M., & York, D. G. 2003, ApJ, 584, 210

Gonçalves, T. S., Martin, D. C., Menéndez-Delmestre, K., Wyder, T. K., & Koekemoer, A. 2012, ApJ, 759, 67

Goto, T., Okamura, S., Sekiguchi, M., Bernardi, M., Brinkmann, J., Gómez, P. L., Harvanek, M., Kleinman, S. J., Krzesinski, J., Long, D., Loveday, J., Miller, C. J., Neilsen, E. H., Newman, P. R., Nitta, A., Sheth, R. K., Snedden, S. A., & Yamauchi, C. 2003, PASJ, 55, 757

Granato, G. L., Zotti, G. D., Silva, L., Bressan, A., & Danese, L. 2004, ApJ, 600, 580

Grootes, M. W., Tuffs, R. J., Popescu, C. C., Norberg, P., Robotham, A. S. G., Liske, J., Andrae, E., Baldry, I. K., Gunawardhana, M., Kelvin, L. S., Madore, B. F., Seibert, M., Taylor, E. N., Alpaslan, M., Brown, M. J. I., Cluver, M. E., Driver, S. P., Bland-Hawthorn, J., Holwerda, B. W., Hopkins, A. M., Lopez-Sanchez, A. R., Loveday, J., & Rushton, M. 2017, AJ, 153, 111

Gürkan, G., Hardcastle, M. J., Jarvis, M. J., Smith, D. J. B., Bourne, N., Dunne, L., Maddox, S., Ivison, R. J., & Fritz, J. 2015, MNRAS, 452, 3776

Haas, M. R., Schaye, J., & Jeeson-Daniel, A. 2012, MNRAS, 419, 2133

Hamilton, D. 1985, ApJ, 297, 371

Hao, C.-N., Kennicutt, R. C., Johnson, B. D., Calzetti, D., Dale, D. A., & Moustakas, J. 2011, ApJ, 741, 124

Harrison, C. M., Alexander, D. M., Mullaney, J. R., Altieri, B., Coia, D., Charmandaris, V., Daddi, E., Dannerbauer, H., Dasyra, K., Del Moro, A., Dickinson, M., Hickox, R. C., Ivison, R. J., Kartaltepe, J., Le Floc'h, E., Leiton, R., Magnelli, B., Popesso, P., Rovilos, E., Rosario, D., & Swinbank, A. M. 2012, ApJ, 760, L15

Hashimoto, Y., Augustus Oemler, J., Lin, H., & Tucker, D. L. 1998, ApJ, 499, 589

Hickox, R. C., Jones, C., Forman, W. R., Murray, S. S., Kochanek, C. S., Eisenstein, D., Jannuzi, B. T., Dey, A., Brown, M. J. I., Stern, D., Eisenhardt, P. R., Gorjian, V., Brodwin, M., Narayan, R., Cool, R. J., Kenter, A., Caldwell, N., & Anderson, M. E. 2009, ApJ, 696, 891

Hopkins, P. F., Hernquist, L., Cox, T. J., Di Matteo, T., Robertson, B., & Springel, V. 2006, ApJS, 163, 1

Hubble, E. P. 1926, ApJ, 64

—. 1936, Realm of the Nebulae

Huertas-Company, M., Aguerri, J. A. L., Bernardi, M., Mei, S., & Sánchez Almeida, J. 2011, A&A, 525, A157

Huertas-Company, M., Aguerri, J. A. L., Tresse, L., Bolzonella, M., Koekemoer, A. M., & Maier, C. 2010, A&A, 515, A3

Izotov, Y. I., Guseva, N. G., & Thuan, T. X. 2011, ApJ, 728, 161

Jaskot, A. E. & Oey, M. S. 2013, ApJ, 766, 91

Joshi, G. D., Parker, L. C., & Wadsley, J. 2016, MNRAS, 462, 761

Kannappan, S. J., Guie, J. M., & Baker, A. J. 2009, ApJ, 138, 579

Kauffmann, G., Heckman, T. M., & Best, P. N. 2008, MNRAS, 384, 953

Kauffmann, G., Heckman, T. M., Tremonti, C., Brinchmann, J., Charlot, S., White, S. D. M., Ridgway, S. E., Brinkmann, J., Fukugita, M., Hall, P. B., Ivezić, Ž., Richards, G. T., & Schneider, D. P. 2003a, MNRAS, 346, 1055

Kauffmann, G., Heckman, T. M., White, S. D. M., Charlot, S., Tremonti, C., Peng, E. W., Seibert, M., Brinkmann, J., Nichol, R. C., SubbaRao, M., & York, D. 2003b, MNRAS, 341, 54

Kauffmann, G., White, S. D. M., Heckman, T. M., Ménard, B., Brinchmann, J., Charlot, S., Tremonti, C., & Brinkmann, J. 2004, MNRAS, 353, 713

Kennicutt, R. C. & Evans, N. J. 2012, ARA&A, 50, 531

Kennicutt, Jr., R. C. 1998, ARA&A, 36, 189

Kennicutt, Jr., R. C., Hao, C.-N., Calzetti, D., Moustakas, J., Dale, D. A., Bendo, G., Engelbracht, C. W., Johnson, B. D., & Lee, J. C. 2009, ApJ, 703, 1672

Kimm, T., Somerville, R. S., Yi, S. K., van den Bosch, F. C., Salim, S., Fontanot, F., Monaco, P., Mo, H., Pasquali, A., Rich, R. M., & Yang, X. 2009, MNRAS, 394, 1131

Knobel, C., Lilly, S. J., Woo, J., & Kovač, K. 2015, ApJ, 800, 24

Kormendy, J., Fisher, D. B., Cornell, M. E., & Bender, R. 2009, ApJS, 182, 216

Koyama, Y., Kodama, T., Shimasaku, K., Okamura, S., Tanaka, M., Lee, H. M., Im, M., Matsuhara, H., Takagi, T., Wada, T., & Oyabu, S. 2008, MNRAS, 391, 1758

Krywult, J., Tasca, L. A. M., Pollo, A., Vergani, D., Bolzonella, M., Davidzon, I., Iovino, A., Gargiulo, A., Haines, C. P., Scodeggio, M., Guzzo, L., Zamorani, G., Garilli, B., Granett, B. R., de la Torre, S., Abbas, U., Adami, C., Bottini, D., Cappi, A., Cucciati, O., Franzetti, P., Fritz, A., Le Brun, V., Le Fèvre, O., Maccagni, D., Małek, K., Marulli, F., Polletta, M., Tojeiro, R., Zanichelli, A., Arnouts, S., Bel, J., Branchini, E., Coupon, J., De Lucia, G., Ilbert, O., McCracken, H. J., Moscardini, L., & Takeuchi, T. T. 2017, A&A, 598, A120

Lacy, M., Storrie-Lombardi, L. J., Sajina, A., Appleton, P. N., Armus, L., Chapman, S. C., Choi, P. I., Fadda, D., Fang, F., Frayer, D. T., Heinrichsen, I., Helou, G., Im, M., Marleau, F. R., Masci, F., Shupe, D. L., Soifer, B. T., Surace, J., Teplitz, H. I., Wilson, G., & Yan, L. 2004, ApJS, 154, 166

Lanzuisi, G., Ranalli, P., Georgantopoulos, I., Georgakakis, A., Delvecchio, I., Akylas, T., Berta, S., Bongiorno, A., Brusa, M., Cappelluti, N., Civano, F., Comastri, A., Gilli, R., Gruppioni, C., Hasinger, G., Iwasawa, K., Koekemoer, A., Lusso, E., Marchesi, S., Mainieri, V., Merloni, A., Mignoli, M., Piconcelli, E., Pozzi, F., Rosario, D. J., Salvato, M., Silverman, J., Trakhtenbrot, B., Vignali, C., & Zamorani, G. 2015, A&A, 573, A137

Larson, R. B., Tinsley, B. M., & Caldwell, C. N. 1980, ApJ, 237, 692

Li, I. H., Glazebrook, K., Gilbank, D., Balogh, M., Bower, R., Baldry, I., Davies, G., Hau, G., & McCarthy, P. 2011, MNRAS, 411, 1869

Lintott, C., Schawinski, K., Bamford, S., Slosar, A., Land, K., Thomas, D., Edmondson, E., Masters, K., Nichol, R. C., Raddick, M. J., Szalay, A., Andreescu, D., Murray, P., & Vandenberg, J. 2011, MNRAS, 410, 166

Lintott, C. J., Schawinski, K., Slosar, A., Land, K., Bamford, S., Thomas, D., Raddick, M. J., Nichol, R. C., Szalay, A., Andreescu, D., Murray, P., & Vandenberg, J. 2008, MNRAS, 389, 1179

Lynden-Bell, D. 1969, Nature, 223, 690

Mahajan, S. & Raychaudhury, S. 2009, MNRAS, 400, 687

Martin, D. C., Fanson, J., Schiminovich, D., Morrissey, P., Friedman, P. G., Barlow, T. A., Conrow, T., Grange, R., Jelinsky, P. N., Milliard, B., Siegmund, O. H. W., Bianchi, L., Byun, Y.-I., Donas, J., Forster, K., Heckman, T. M., Lee, Y.-W., Madore, B. F., Malina, R. F., Neff, S. G., Rich, R. M., Small, T., Surber, F., Szalay, A. S., Welsh, B., & Wyder, T. K. 2005, ApJ, 619, L1

Masters, K. L., Mosleh, M., Romer, A. K., Nichol, R. C., Bamford, S. P., Schawinski, K., Lintott, C. J., Andreescu, D., Campbell, H. C., Crowcroft, B., Doyle, I., Edmondson, E. M., Murray, P., Raddick, M. J., Slosar, A., Szalay, A. S., & Vandenberg, J. 2010, MNRAS, 405, 783

Mateo, M. L. 1998, ARA&A, 36, 435

McGee, S. L., Balogh, M. L., Wilman, D. J., Bower, R. G., Mulchaey, J. S., Parker, L. C., & Oemler, A. 2011, MNRAS, 413, 996

Mendez, A. J., Coil, A. L., Lotz, J., Salim, S., Moustakas, J., & Simard, L. 2011, ApJ, 736, 110

Miller, C. J., Nichol, R. C., Gómez, P. L., Hopkins, A. M., & Bernardi, M. 2003, ApJ, 597, 142

Mo, H., van den Bosch, F. C., & White, S. 2010, Galaxy Formation and Evolution

Mobasher, B., Dahlen, T., Ferguson, H. C., Acquaviva, V., Barro, G., Finkelstein, S. L., Fontana, A., Gruetzbauch, R., Johnson, S., Lu, Y., Papovich, C. J., Pforr, J., Salvato, M., Somerville, R. S., Wiklind, T., Wuyts, S., Ashby, M. L. N., Bell, E., Conselice, C. J., Dickinson, M. E., Faber, S. M., Fazio, G., Finlator, K., Galametz, A., Gawiser, E., Giavalisco, M., Grazian, A., Grogin, N. A., Guo, Y., Hathi, N., Kocevski, D., Koekemoer, A. M., Koo, D. C., Newman, J. A., Reddy, N., Santini, P., & Wechsler, R. H. 2015, ApJ, 808, 101

Montero-Dorta, A. D., Croton, D. J., Yan, R., Cooper, M. C., Newman, J. A., Georgakakis, A., Prada, F., Davis, M., Nandra, K., & Coil, A. 2009, MNRAS, 392, 125

Moore, B., Lake, G., & Katz, N. 1998, ApJ, 495, 139

Nair, P. B. & Abraham, R. G. 2010, ApJS, 186, 427

Noeske, K. G., Faber, S. M., Weiner, B. J., Koo, D. C., Primack, J. R., Dekel, A., Papovich, C., Conselice, C. J., Le Floc'h, E., Rieke, G. H., Coil, A. L., Lotz, J. M., Somerville, R. S., & Bundy, K. 2007a, ApJ, 660, L47

Noeske, K. G., Weiner, B. J., Faber, S. M., Papovich, C., Koo, D. C., Somerville, R. S., Bundy, K., Conselice, C. J., Newman, J. A., Schiminovich, D., Le Floc'h, E., Coil, A. L., Rieke, G. H., Lotz, J. M., Primack, J. R., Barmby, P., Cooper, M. C., Davis, M., Ellis, R. S., Fazio, G. G., Guhathakurta, P., Huang, J., Kassin, S. A., Martin, D. C., Phillips, A. C.,

Rich, R. M., Small, T. A., Willmer, C. N. A., & Wilson, G. 2007b, ApJ, 660, L43

Pasquali, A., van den Bosch, F. C., Mo, H. J., Yang, X., & Somerville, R. 2009, MNRAS, 394, 38

Peng, Y., Lilly, S. J., Kovač, K., Bolzonella, M., Pozzetti, L., Renzini, A., Zamorani, G., Ilbert, O., Knobel, C., Iovino, A., Maier, C., Cucciati, O., Tasca, L., Carollo, C. M., Silverman, J., Kampczyk, P., de Ravel, L., Sanders, D., Scoville, N., Contini, T., Mainieri, V., Scodeggio, M., Kneib, J.-P., Fèvre, O. L., Bardelli, S., Bongiorno, A., Caputi, K., Coppa, G., de la Torre, S., Franzetti, P., Garilli, B., Lamareille, F., Borgne, J.-F. L., Brun, V. L., Mignoli, M., Montero, E. P., Pello, R., Ricciardelli, E., Tanaka, M., Tresse, L., Vergani, D., Welikala, N., Zucca, E., Oesch, P., Abbas, U., Barnes, L., Bordoloi, R., Bottini, D., Cappi, A., Cassata, P., Cimatti, A., Fumana, M., Hasinger, G., Koekemoer, A., Leauthaud, A., Maccagni, D., Marinoni, C., McCracken, H., Memeo, P., Meneux, B., Nair, P., Porciani, C., Presotto, V., & Scaramella, R. 2010, ApJ, 721, 193

Peng, Y., Lilly, S. J., Renzini, A., & Carollo, M. 2012, ApJ, 757, 4

Pimbblet, K. A., Shabala, S. S., Haines, C. P., Fraser-McKelvie, A., & Floyd, D. J. E. 2013, MNRAS, 429, 1827

Poggianti, B. M., Smail, I., Dressler, A., Couch, W. J., Barger, A. J., Butcher, H., Ellis, R. S., & Oemler, Jr., A. 1999, ApJ, 518, 576

Postman, M. & Geller, M. J. 1984, ApJ, 281, 95

Richstone, D., Ajhar, E. A., Bender, R., Bower, G., Dressler, A., Faber, S. M., Filippenko, A. V., Gebhardt, K., Green, R., Ho, L. C., Kormendy, J., Lauer, T. R., Magorrian, J., & Tremaine, S. 1998, Nature, 395, A14

Roberts, I. D., Parker, L. C., Joshi, G. D., & Evans, F. A. 2014, MNRAS: Letters, 448, L1

Rosario, D. J., McIntosh, D. H., van der Wel, A., Kartaltepe, J., Lang, P., Santini, P., Wuyts, S., Lutz, D., Rafelski, M., Villforth, C., Alexander, D. M., Bauer, F. E., Bell, E. F., Berta, S., Brandt, W. N., Conselice, C. J., Dekel, A., Faber, S. M., Ferguson, H. C., Genzel, R., Grogin, N. A., Kocevski, D. D., Koekemoer, A. M., Koo, D. C., Lotz, J. M., Magnelli, B., Maiolino, R., Mozena, M., Mullaney, J. R., Papovich, C. J., Popesso, P., Tacconi, L. J., Trump, J. R., Avadhuta, S., Bassett, R., Bell, A., Bernyk, M., Bournaud, F., Cassata, P., Cheung, E., Croton, D., Donley, J., DeGroot, L., Guedes, J., Hathi, N., Herrington, J., Hilton, M., Lai, K., Lani, C., Martig, M., McGrath, E., Mutch, S., Mortlock, A., McPartland, C., O'Leary, E., Peth, M., Pillepich, A., Poole, G., Snyder, D., Straughn, A., Telford, O., Tonini, C., & Wandro, P. 2015, A&A, 573, A85

Saintonge, A., Tran, K.-V. H., & Holden, B. P. 2008, ApJ, 685, L113

Salim, S., Rich, R. M., Charlot, S., Brinchmann, J., Johnson, B. D., Schiminovich, D., Seibert, M., Mallery, R., Heckman, T. M., Forster, K., Friedman, P. G., Martin, D. C., Morrissey, P., Neff, S. G., Small, T., Wyder, T. K., Bianchi, L., Donas, J., Lee, Y.-W., Madore, B. F., Milliard, B., Szalay, A. S., Welsh, B. Y., & Yi, S. K. 2007, ApJS, 173, 267

Sandage, A. 1961, The Hubble Atlas of Galaxies

Schawinski, K., Lintott, C., Thomas, D., Sarzi, M., Andreescu, D., Bamford, S. P., Kaviraj, S., Khochfar, S., Land, K., Murray, P., Nichol, R. C., Raddick, M. J., Slosar, A., Szalay, A., Vandenberg, J., & Yi, S. K. 2009, MNRAS, 396, 818

Schawinski, K., Thomas, D., Sarzi, M., Maraston, C., Kaviraj, S., Joo, S.-J., Yi, S. K., & Silk, J. 2007, MNRAS, 382, 1415

Schawinski, K., Urry, C. M., Simmons, B. D., Fortson, L., Kaviraj, S., Keel, W. C., Lintott, C. J., Masters, K. L., Nichol, R. C., Sarzi, M., Skibba, R., Treister, E., Willett, K. W., Wong, O. I., & Yi, S. K. 2014, MNRAS, 440, 889

Schlegel, D. J., Finkbeiner, D. P., & Davis, M. 1998, ApJ, 500, 525

Scoville, N., Aussel, H., Brusa, M., Capak, P., Carollo, C. M., Elvis, M., Giavalisco, M., Guzzo, L., Hasinger, G., Impey, C., Kneib, J.-P., LeFevre, O., Lilly, S. J., Mobasher, B., Renzini, A., Rich, R. M., Sanders, D. B., Schinnerer, E., Schminovich, D., Shopbell, P., Taniguchi, Y., & Tyson, N. D. 2007, ApJS, 172, 1

Searle, L., Sargent, W. L. W., & Bagnuolo, W. G. 1973, ApJ, 179, 427

Sérsic, J. L. 1963, Boletin de la Asociacion Argentina de Astronomia La Plata Argentina, 6, 41

—. 1968, Atlas de Galaxias Australes

Sijacki, D., Vogelsberger, M., Genel, S., Springel, V., Torrey, P., Snyder, G. F., Nelson, D., & Hernquist, L. 2015, MNRAS, 452, 575

Silverman, J. D., Lamareille, F., Maier, C., Lilly, S. J., Mainieri, V., Brusa, M., Cappelluti, N., Hasinger, G., Zamorani, G., Scodeggio, M., Bolzonella, M., Contini, T., Carollo, C. M., Jahnke, K., Kneib, J.-P., Le Fèvre, O., Merloni, A., Bardelli, S., Bongiorno, A., Brunner, H., Caputi, K., Civano, F., Comastri, A., Coppa, G., Cucciati, O., de la Torre, S., de Ravel, L., Elvis, M., Finoguenov, A., Fiore, F., Franzetti, P., Garilli, B., Gilli, R., Iovino, A., Kampczyk, P., Knobel, C., Kovač, K., Le Borgne, J.-F., Le Brun, V., Mignoli, M., Pello, R., Peng, Y., Perez Montero, E., Ricciardelli, E., Tanaka, M., Tasca, L., Tresse, L., Vergani, D., Vignali, C., Zucca, E., Bottini, D.,

Cappi, A., Cassata, P., Fumana, M., Griffiths, R., Kartaltepe, J., Koekemoer, A., Marinoni, C., McCracken, H. J., Memeo, P., Meneux, B., Oesch, P., Porciani, C., & Salvato, M. 2009, ApJ, 696, 396

Skibba, R. A. 2009, MNRAS, 392, 1467

Skibba, R. A., van den Bosch, F. C., Yang, X., More, S., Mo, H., & Fontanot, F. 2011, MNRAS, 410, 417

Skrutskie, M. F., Cutri, R. M., Stiening, R., Weinberg, M. D., Schneider, S., Carpenter, J. M., Beichman, C., Capps, R., Chester, T., Elias, J., Huchra, J., Liebert, J., Lonsdale, C., Monet, D. G., Price, S., Seitzer, P., Jarrett, T., Kirkpatrick, J. D., Gizis, J. E., Howard, E., Evans, T., Fowler, J., Fullmer, L., Hurt, R., Light, R., Kopan, E. L., Marsh, K. A., McCallon, H. L., Tam, R., Van Dyk, S., & Wheelock, S. 2006, AJ, 131, 1163

Smith, J. A., Tucker, D. L., Kent, S., Richmond, M. W., Fukugita, M., Ichikawa, T., Ichikawa, S.-i., Jorgensen, A. M., Uomoto, A., Gunn, J. E., Hamabe, M., Watanabe, M., Tolea, A., Henden, A., Annis, J., Pier, J. R., McKay, T. A., Brinkmann, J., Chen, B., Holtzman, J., Shimasaku, K., & York, D. G. 2002, AJ, 123, 2121

Snyder, G. F., Torrey, P., Lotz, J. M., Genel, S., McBride, C. K., Vogelsberger, M., Pillepich, A., Nelson, D., Sales, L. V., Sijacki, D., Hernquist, L., & Springel, V. 2015, MNRAS, 454, 1886

Soltan, A. 1982, MNRAS, 200, 115

Spearman, C. 1904, The American Journal of Psychology, 15, 201

Springel, V., Di Matteo, T., & Hernquist, L. 2005, MNRAS, 361, 776

Stern, D., Assef, R. J., Benford, D. J., Blain, A., Cutri, R., Dey, A., Eisenhardt, P., Griffith, R. L., Jarrett, T. H., Lake, S., Masci, F., Petty, S., Stanford, S. A., Tsai, C.-W., Wright, E. L., Yan, L., Harrison, F., & Madsen, K. 2012, ApJ, 753, 30

Stern, D., Eisenhardt, P., Gorjian, V., Kochanek, C. S., Caldwell, N., Eisenstein, D., Brodwin, M., Brown, M. J. I., Cool, R., Dey, A., Green, P., Jannuzi, B. T., Murray, S. S., Pahre, M. A., & Willner, S. P. 2005, The Astrophysical Journal, 631, 163

Strateva, I., Ivezić, Ž., Knapp, G. R., Narayanan, V. K., Strauss, M. A., Gunn, J. E., Lupton, R. H., Schlegel, D., Bahcall, N. A., Brinkmann, J., Brunner, R. J., Budavári, T., Csabai, I., Castander, F. J., Doi, M., Fukugita, M., Győry, Z., Hamabe, M., Hennessy, G., Ichikawa, T., Kunszt, P. Z., Lamb, D. Q., McKay, T. A., Okamura, S., Racusin, J., Sekiguchi, M., Schneider, D. P., Shimasaku, K., & York, D. 2001, AJ, 122, 1861

Tinsley, B. M. 1972, A&A, 20, 383

Tojeiro, R., Masters, K. L., Richards, J., Percival, W. J., Bamford, S. P., Maraston, C., Nichol, R. C., Skibba, R., & Thomas, D. 2013, MNRAS, 432, 359

Tolstoy, E., Hill, V., & Tosi, M. 2009, ARA&A, 47, 371

van den Bergh, S. 1976, ApJ, 206, 883

—. 2009, ApJ, 702, 1502

van den Bosch, F. C., Pasquali, A., Yang, X., Mo, H. J., Weinmann, S., McIntosh, D. H., & Aquino, D. 2008, ArXiv e-prints

van den Bosch, F. C., Weinmann, S. M., Yang, X., Mo, H. J., Li, C., & Jing, Y. P. 2005, MNRAS, 361, 1203

van der Wel, A. 2008, ApJ, 675, L13

Visvanathan, N. & Sandage, A. 1977, ApJ, 216, 214

von der Linden, A., Wild, V., Kauffmann, G., White, S. D. M., & Weinmann, S. 2010, MNRAS, 404, 1231

Weinmann, S. M., van den Bosch, F. C., Yang, X., & Mo, H. J. 2006, MNRAS, 366, 2

Werner, M. W., Roellig, T. L., Low, F. J., Rieke, G. H., Rieke, M., Hoffmann, W. F., Young, E., Houck, J. R., Brandl, B., Fazio, G. G., Hora, J. L., Gehrz, R. D., Helou, G., Soifer, B. T., Stauffer, J., Keene, J., Eisenhardt, P., Gallagher, D., Gautier, T. N., Irace, W., Lawrence, C. R., Simmons, L., Van Cleve, J. E., Jura, M., Wright, E. L., & Cruikshank, D. P. 2004, ApJS, 154, 1

Wetzel, A. R., Tinker, J. L., & Conroy, C. 2012, MNRAS, 424, 232

Wijesinghe, D. B., Hopkins, A. M., Brough, S., Taylor, E. N., Norberg, P., Bauer, A., Brown, M. J. I., Cameron, E., Conselice, C. J., Croom, S., Driver, S., Grootes, M. W., Jones, D. H., Kelvin, L., Loveday, J., Pimbblet, K. A., Popescu, C. C., Prescott, M., Sharp, R., Baldry, I., Sadler, E. M., Liske, J., Robotham, A. S. G., Bamford, S., Bland-Hawthorn, J., Gunawardhana, M., Meyer, M., Parkinson, H., Drinkwater, M. J., Peacock, J., & Tuffs, R. 2012, MNRAS, 423, 3679

Wilman, D. J. & Erwin, P. 2012, ApJ, 746, 160

Wilman, D. J., Zibetti, S., & Budavári, T. 2010, MNRAS, 406, 1701

Woo, J., Dekel, A., Faber, S. M., & Koo, D. C. 2015, MNRAS, 448, 237

Woo, J., Dekel, A., Faber, S. M., Noeske, K., Koo, D. C., Gerke, B. F., Cooper, M. C., Salim, S., Dutton, A. A., Newman, J., Weiner, B. J., Bundy, K., Willmer, C. N. A., Davis, M., & Yan, R. 2013, MNRAS, 428, 3306

Worthey, G. & Ottaviani, D. L. 1997, ApJS, 111, 377

Wright, E. L., Eisenhardt, P. R. M., Mainzer, A. K., Ressler, M. E., Cutri, R. M., Jarrett, T., Kirkpatrick, J. D., Padgett, D., McMillan, R. S., Skrutskie, M., Stanford, S. A., Cohen, M., Walker, R. G., Mather, J. C., Leisawitz, D., Gautier, III, T. N., McLean, I., Benford, D., Lonsdale, C. J., Blain, A., Mendez, B., Irace, W. R., Duval, V., Liu, F., Royer, D., Heinrichsen, I., Howard, J., Shannon, M., Kendall, M., Walsh, A. L., Larsen, M., Cardon, J. G., Schick, S., Schwalm, M., Abid, M., Fabinsky, B., Naes, L., & Tsai, C.-W. 2010, AJ, 140, 1868

Wyder, T. K., Martin, D. C., Schiminovich, D., Seibert, M., Budavári, T., Treyer, M. A., Barlow, T. A., Forster, K., Friedman, P. G., Morrissey, P., Neff, S. G., Small, T., Bianchi, L., Donas, J., Heckman, T. M., Lee, Y.-W., Madore, B. F., Milliard, B., Rich, R. M., Szalay, A. S., Welsh, B. Y., & Yi, S. K. 2007, ApJS, 173, 293

Yang, X., Mo, H. J., van den Bosch, F. C., & Jing, Y. P. 2005, MNRAS, 356, 1293

Yang, X., Mo, H. J., van den Bosch, F. C., Pasquali, A., Li, C., & Barden, M. 2007, ApJ, 671, 153

Yang, X., Mo, H. J., van den Bosch, F. C., Zhang, Y., & Han, J. 2012, ApJ, 752, 41

York, D. G., Adelman, J., John E. Anderson, J., Anderson, S. F., Annis, J., Bahcall, N. A., Bakken, J. A., Barkhouser, R., Bastian, S., Berman, E.,

Boroski, W. N., Bracker, S., Briegel, C., Briggs, J. W., Brinkmann, J., Brunner, R., Burles, S., Carey, L., Carr, M. A., Castander, F. J., Chen, B., Colestock, P. L., Connolly, A. J., Crocker, J. H., Csabai, I., Czarapata, P. C., Davis, J. E., Doi, M., Dombeck, T., Eisenstein, D., Ellman, N., Elms, B. R., Evans, M. L., Fan, X., Federwitz, G. R., Fiscelli, L., Friedman, S., Frieman, J. A., Fukugita, M., Gillespie, B., Gunn, J. E., Gurbani, V. K., de Haas, E., Haldeman, M., Harris, F. H., Hayes, J., Heckman, T. M., Hennessy, G. S., Hindsley, R. B., Holm, S., Holmgren, D. J., hao Huang, C., Hull, C., Husby, D., Ichikawa, S.-I., Ichikawa, T., Ivezić, Ž., Kent, S., Kim, R. S. J., Kinney, E., Klaene, M., Kleinman, A. N., Kleinman, S., Knapp, G. R., Korienek, J., Kron, R. G., Kunszt, P. Z., Lamb, D. Q., Lee, B., Leger, R. F., Limmongkol, S., Lindenmeyer, C., Long, D. C., Loomis, C., Loveday, J., Lucinio, R., Lupton, R. H., MacKinnon, B., Mannery, E. J., Mantsch, P. M., Margon, B., McGehee, P., McKay, T. A., Meiksin, A., Merelli, A., Monet, D. G., Munn, J. A., Narayanan, V. K., Nash, T., Neilsen, E., Neswold, R., Newberg, H. J., Nichol, R. C., Nicinski, T., Nonino, M., Okada, N., Okamura, S., Ostriker, J. P., Owen, R., Pauls, A. G., Peoples, J., Peterson, R. L., Petravick, D., Pier, J. R., Pope, A., Pordes, R., Prosapio, A., Rechenmacher, R., Quinn, T. R., Richards, G. T., Richmond, M. W., Rivetta, C. H., Rockosi, C. M., Ruthmansdorfer, K., Sandford, D., Schlegel, D. J., Schneider, D. P., Sekiguchi, M., Sergey, G., Shimasaku, K., Siegmund, W. A., Smee, S., Smith, J. A., Snedden, S., Stone, R., Stoughton, C., Strauss, M. A., Stubbs, C., SubbaRao, M., Szalay, A. S., Szapudi, I., Szokoly, G. P., Thakar, A. R., Tremonti, C., Tucker, D. L., Uomoto, A., Berk, D. V., Vogeley, M. S., Waddell, P., i Wang, S., Watanabe, M., Weinberg, D. H., Yanny, B., & Yasuda, N. 2000, The Astronomical Journal, 120, 1579

Zibetti, S., Charlot, S., & Rix, H.-W. 2009, MNRAS, 400, 1181

Chapter 2

Red Misfits in the SDSS

This chapter represents the scientific work, *"Red Misfits in the Sloan Digital Sky Survey: Properties of Star-Forming Red Galaxies"* submitted to the refereed journal *Monthly Notices of the Royal Astronomical Society* by the following authors:

Fraser A. Evans, Laura C. Parker, Ian D. Roberts

Department of Physics & Astronomy, McMaster University

1280 Main Street West, Hamilton, ON, L8S 4L8, Canada

Abstract

We study Red Misfits, a population of red, star-forming galaxies in the local Universe. We classify galaxies based on inclination-corrected optical colours and specific star formation rates derived from the Sloan Digital Sky Survey Data Release 7. Although the majority of blue galaxies are star-forming and most red galaxies exhibit little to no ongoing star formation, a small but significant population of galaxies ($\sim$11 per cent at all stellar masses) are classified as red in colour yet actively star-forming. We explore a number of properties of these galaxies and demonstrate that Red Misfits are a distinct population and not simply dusty star-forming galaxies or early type galaxies with a sprinkling of star formation. Most significantly, the proportion of Red Misfits is nearly independent of environment and this population exhibits both intermediate morphologies and an enhanced likelihood of hosting an AGN. We conclude that Red Misfits are a transition population, gradually quenching on their way to the red sequence and this quenching is dominated by internal secular processes rather than environmentally-driven processes.

2.1 Introduction

Large-scale galaxy redshift surveys such as the Sloan Digital Sky Survey (SDSS; York et al., 2000) have demonstrated that the distributions of colour and star formation rate (SFR) for galaxies in the local Universe are bimodal (e.g. Strateva et al., 2001; Blanton et al., 2003; Kauffmann et al., 2003b; Baldry et al., 2004; Balogh et al., 2004a,b). Galaxies are almost all red with elliptical morphologies and little-to-no ongoing star formation, or blue and late-type with substantial ongoing star formation. The origin and maintenance of this bimodality is an important open question in galaxy formation and evolution.

Exploring how colour, morphology and star formation rate correlate with other galaxy properties can provide some hints. The strong correlation between these properties and stellar mass (e.g. Kauffmann et al., 2003c; Noeske et al., 2007b,a; Wetzel et al., 2012) suggests that a galaxy's stellar mass is the main parameter upon which its other properties depend (e.g. Peng et al., 2010; Woo et al., 2013).

In addition, it has long been known that galaxy properties differ across environments: galaxy demographics in rich environments such as the cores of galaxy clusters are dominated by red, early-type galaxies with negligible star formation, while blue, star-forming, late-type galaxies are most commonly found in the low density field (e.g. Oemler, 1974; Dressler, 1980; Lewis et al., 2002; Gómez et al., 2003; Balogh et al., 2004b). These correlations could simply be due to more massive galaxies residing in denser environments (Hogg et al., 2003); however, recent studies show that these trends persist even at fixed stellar mass (Kauffmann et al., 2004; Blanton et al., 2005a; Skibba, 2009; McGee et al., 2011). Not limited to the local Universe, this environmental dependence has been observed out to at least $z \approx 1$ (Cooper et al., 2007; Peng et al., 2010). Together, these results motivate a complex picture of galaxy evolution wherein secular (internal) mechanisms scaling with stellar mass and

mechanisms scaling with environment work in tandem to transform blue, star-forming galaxies to red and quiescent ones (e.g. van den Bosch et al., 2008; Peng et al., 2010, 2012; Woo et al., 2013). This evolutionary picture is supported by the fact that the total amount of stellar mass in red sequence galaxies has doubled since z=1 (e.g. Bell et al., 2004; Faber et al., 2007).

The exact balance of environmental and secular mechanisms that dominate this transition is unclear and many mechanisms likely play a role. A number of secular galaxy transformation processes scale with stellar mass, including Active Galactic Nuclei (AGN) feedback, disc instabilities and stellar feedback. Radiative and mechanical feedback from AGN can displace cold gas from the disc and heat central gas, suppressing gas cooling and subsequent star formation (e.g. Bower et al., 2006; Croton et al., 2006). Recent semi-analytic models and hydrodynamic simulations (e.g. Springel et al., 2005; Hopkins et al., 2006; Dubois et al., 2014; Sijacki et al., 2015) argue that AGN feedback prescriptions are required to suppress star formation. Bar features in galaxies can efficiently drive gas into nuclear regions, inducing central star formation thereby reducing gas consumption timescales (e.g. Knapen et al., 1995; Sheth et al., 2005; Cheung et al., 2013) and spurring (pseudo)bulge growth (Kormendy & Kennicutt, 2004; Athanassoula, 2005). Morphological quenching, wherein the growth of a stellar bulge stabilizes the gas disc against fragmentation (Martig et al., 2009) can further inhibit star formation. Finally, outflows driven by supernova feedback can eject cold gas from the galactic disc, suppressing star formation (e.g. Stinson et al., 2013; Hopkins et al., 2014; Keller et al., 2016).

The environmental mechanisms that are known to influence galaxy evolution are also numerous. A galaxy within the virial radius of a host halo can experience ram pressure stripping of cold gas from its disc (Gunn & Gott, 1972), reduced accretion of hot gas (e.g. Larson et al., 1980; Balogh et al., 2000; Kawata & Mulchaey, 2007), high-speed tidal interactions with nearby galaxies (Moore et al., 1996, 1998) as well as mergers (Toomre & Toomre,

1972; Makino & Hut, 1997), all of which can suppress star formation over varying timescales. Although first discovered in galaxy clusters, subsequent works have found that the environmental trends at fixed stellar mass extend to groups (e.g. Postman & Geller, 1984; Zabludoff & Mulchaey, 1998; Lewis et al., 2002; Gómez et al., 2003; McGee et al., 2011). This suggests that not only does the dense core of a galaxy cluster affect galaxy properties, but satellite galaxies may undergo significant pre-processing in groups and may already have begun experiencing environmental effects well before entering the cluster environment (e.g. Kodama et al., 2001; Balogh et al., 2002; Hou et al., 2014; Roberts & Parker, 2017). It is therefore important to understand the relative importance of these mechanisms not just in massive clusters but in low mass groups as well.

Although most galaxies are either blue, star-forming and disc-dominated or red, quiescent and early-type, there are exceptions. One way to investigate the mechanisms that dominate galaxy evolution is to search for objects outside of these two main populations. These exceptions may be transitional objects evolving from active and blue to passive and red or they may be one stage of a more complicated evolutionary picture. Numerous studies have examined the significant population of so-called 'passive red spirals', i.e. galaxies with late-type morphologies but red optical colours (e.g. Poggianti et al., 1999, 2004; Goto et al., 2003; Masters et al., 2010). Other examples of outlier populations in the literature include blue, late-type passive galaxies (e.g. Mahajan & Raychaudhury, 2009) and blue, star-forming early-type galaxies (e.g. Schawinski et al., 2009; Huertas-Company et al., 2010).

The aim of this work is to characterize galaxies that are red in optical colour but exhibiting significant star formation. Several authors have studied red, star-forming galaxies using a variety of colour and star formation metrics over a range of samples (e.g. Hammer et al., 1997; Coia et al., 2005; Demarco et al., 2005; Wolf et al., 2005, 2009; Davoodi et al., 2006; Weinmann et al.,

2006; Popesso et al., 2007; Koyama et al., 2008, 2011; Gallazzi et al., 2008; Saintonge et al., 2008; Haines et al., 2008; Verdugo et al., 2008; Brand et al., 2009; Mahajan & Raychaudhury, 2009). The majority of the above works, however, restricted their analysis to the cluster environment and few controlled for stellar mass to disentangle secular and environmental trends. These red star-forming galaxies have never been the sole focus of a study taking full advantage of the sample size and range of environments in the Sloan Digital Sky Survey and related data products.

In this work we investigate red, star-forming galaxies, hereafter referred to as Red Misfits, comparing them to the blue-and-active and red-and-quiescent populations in the Sloan Digital Sky Survey Data Release 7 (SDSS DR7; Abazajian et al., 2009). In particular, we examine the stellar mass and morphology distributions of Red Misfits as well as their dust content, AGN abundance and preferred environments as defined by their host group halo mass and halo-centric radius. We determine that Red Misfits represent a physically-distinct population separate from the typical blue-and-active and red-and-quiescent populations and can help constrain quenching mechanisms and timescales.

In Section 2 we describe our sample and the inclination-dependent colour corrections we apply. The properties of Red Misfits (stellar mass, morphology, dust content, AGN abundance, environmental trends) are described in Section 3. The discussion and implications of our findings are presented in Section 4 and we summarize in Section 5. Throughout this work we assume a flat ΛCDM cosmology with Ω_m=0.3, Ω_Λ=0.7, h=0.7.

2.2 Sample

2.2.1 Full Galaxy Catalogue

Our galaxy catalogue derives from the New York University Value-Added Galaxy Catalog (NYUVAGC; Blanton et al., 2005b) based on the Sloan Digital Sky Survey Data Release 7 (SDSS DR7; Abazajian et al., 2009). Specifically we use the *ugrizJHK* Petrosian absolute magnitudes, k-corrected to z=0.1 and corrected for Milky Way dust extinction (Schlegel et al., 1998) based on the `kcorrect` code of Blanton & Roweis (2007). We use emission line measurements from the Max Planck Institut für Astrophysik and Johns Hopkins University (MPA-JHU) collaboration[1]. We also use SDSS-derived catalogues providing galaxy specific star formation rates (sSFRs, Brinchmann et al., 2004) and stellar masses (Kauffmann et al., 2003b). Both the sSFR and stellar mass catalogues include updated prescriptions from Salim et al. (2007) for fiber aperture correction and active galactic nuclei (AGN) contamination. In the interest of completeness we restrict our sample to galaxies with stellar masses above $10^{9.5}$ $M_{\odot}$ and redshifts below 0.1.

Structural parameters are obtained by matching the Simard et al. (2011) morphology catalogue to our sample. The `GIM2D` (Simard et al., 2002) software was used to fit surface brightness profiles with parametric models. Three fits are provided: an n_b=4 de Vaucouleurs bulge+disc decomposition, a free n_b bulge+disc decomposition and a single-component pure Sérsic decomposition. We use the results from the single-component pure Sérsic decomposition in this study.

This sample is not volume-limited; as a result, it will suffer from the Malmquist bias (Malmquist, 1925), leading to a bias towards higher lumi-

[1] http://www.mpa-garching.mpg.de/SDSS/DR7/

nosity (and thus higher stellar mass) objects that increases with redshift. To correct for this we weight by $1/V_{max}$, where V_{max} is the comoving volume of the universe out to a comoving radius at which the galaxy would have met the selection criteria of the sample. V_{max} values are included in the Simard et al. (2011) catalogue. To prevent the contamination of our sample by extremely high-weight galaxies we remove from our sample the very few dim galaxies with V_{max}<1 Mpc.

2.2.2 Colour Correction

We correct for inclination-induced colour bias in our sample following the general method of Maller et al. (2009). In short, the magnitudes are corrected such that the average observed z=0.1 k-corrected $g-K$ and $r-K$ colours of inclined galaxies match the expected colours of a face-on galaxy with the same M_K and Sérsic index. We make modifications to the Maller et al. (2009) methodology to achieve better results with our sample. Most importantly, we adopt a different function to fit the g-r colour of a face-on galaxy to K-band magnitude and Sérsic index. See Section 2.7 for a more detailed explanation of our correction method. It is important to note that this correction is not intended to recover the dust-unaffected colour of a galaxy, rather it recovers the face-on colours of galaxies. The method simply reverses the additional effects of inclination on colour. The inclination-corrected colours of a sample of galaxies may still be significantly dust-reddened if there is a large amount of intrinsic dust within the sample (see Section 2.3.3).

To allow for accurate colour corrections we remove the ∼0.1 per cent galaxies in our sample with missing K-band magnitudes or Sérsic indices. Our full sample therefore consists of 277785 galaxies after all cuts have been applied. Inclination and z=0.1 k-corrected $g-r$ colours are denoted $(M_g^i - M_r^i)^{0.1}$ for the remainder of this work.

2.2.3 Emission Line Subsample

To determine the amount of intrinsic dust-induced reddening (see Section 2.3.3) and the abundance of AGN (see Section 2.3.5) in star-forming, red galaxies as compared to the general population, we require a sample of galaxies with reliable emission line strength measurements. We construct an emission-line subsample by selecting the $\simeq$42 per cent of galaxies in our full sample with a 3σ or greater detection in Hα, Hβ, NII λ_{6584} and OIII λ_{5007}. We also require z>0.05 to reduce the aperture bias of the SDSS 3" fibre. After this cut the emission line subsample is $\sim$1/3 of the total sample and is heavily biased towards galaxies with significant star formation and/or AGN components (see Section 2.2.5).

2.2.4 Environmental Catalogues

2.2.4.1 Group Catalogue

To study the distribution of Red Misfits in different environments in the Universe, we match our full catalogue to the DR7 group catalogue of Yang et al. (2007, hereafter Y07). The iterative algorithm for halo-based group finding is outlined in detail in Yang et al. (2005) and Y07. The brightest galaxy is defined to be the central galaxy and the reminder are satellites. The stellar mass of each group is defined as

$$M_{*,grp} = \frac{1}{g(L_{19.5},L_{lim})} \sum_i \frac{M_{*,i}}{C_i} \ , \tag{2.1}$$

where $M_{*,i}$ is the stellar mass of the i'th galaxy in the group, C_i is the completeness of the survey at the position of that galaxy, and $g(L_{19.5},L_{lim})$ is a correction factor accounting for the magnitude limit of the survey. The mass of each group's halo is estimated using abundance matching to $M_{*,grp}$ with

the halo mass function of Warren et al. (2006) and the transfer function of Eisenstein & Hu (1998).

After removing the 65.6 per cent of galaxies residing in either systems consisting of a single member or systems deemed too small by Y07 to be assigned a halo mass, our final group sample consists of 95648 galaxies in 29346 groups with halo masses ranging from $10^{11.75}\mathrm{M}_{\odot}$ to $10^{15.1}\mathrm{M}_{\odot}$. The highest mass systems are galaxy clusters, but we will refer to all galaxies in this catalogue as group galaxies for simplicity.

We use projected group-centric distance and halo mass as measures of galaxy environment, both of which have been shown to correlate with local overdensity (Peng et al., 2012; Haas et al., 2012; Woo et al., 2013; Carollo et al., 2013). We calculate the projected group-centric distance using the methods outlined in Hogg (1999) and normalize to r_{200} given by Tinker & Chen (2008) and Y07:

$$r_{200} = \left(\frac{3M_{halo}}{4\pi(200\overline{\rho_m})}\right)^{1/3} , \tag{2.2}$$

which in our cosmology becomes

$$r_{200} = 1.13h^{-1}\ \mathrm{Mpc}\left(\frac{M_{halo}}{10^{14}h^{-1}M_{\odot}}\right)^{1/3}(1+z_{group})^{-1} , \tag{2.3}$$

where z_{group} is the redshift of the centre of the group.

2.2.4.2 Field Catalogue

As a companion to the group catalogue, we identify a catalogue of isolated field galaxies to probe the population of Red Misfits in low-density environments. We construct our field catalogue using the N=1 groups in the Y07 catalogue with additional isolation criteria. To be included in our field catalogue, a galaxy must have no neighbour within 1 Mpc and 1000 kms^{-1} brighter

	Percent of Sample			
Sample	Full	Emission-line	Group	Field
Sample Size	277785	90000	95648	112614
Blue Active	42.3%	74.7%	27.2%	52.2%
Blue Passive	1.7%	1.0%	1.6%	1.7%
Red Active (Red Misfit)	10.9%	15.4%	11.0%	10.9%
Red Passive	45.1%	8.8%	60.2%	35.2%

Table 2.1 Populations of each of the four galaxy populations in the four samples.

than the SDSS magnitude limit at our redshift cut of z=0.1. To eliminate the possibility that galaxies in our field catalogue have close neighbours just outside our sample region, we remove galaxies within 1 Mpc of the SDSS coverage boundary or within 1000 km s^{-1} of z=0.1 as in Roberts & Parker (2017). Our field sample consists of 112614 galaxies.

2.2.5 Galaxy Classification

We separate galaxies into four populations based on their inclination-corrected colour and specific star formation rate. V_{max}-weighted sSFR and colour density plots can be seen in Fig. 2.1 and Fig. 2.2. The sSFR distribution shows clear bimodality with peaks near $10^{-11.5}$ yr^{-1} and 10^{-10} yr^{-1} and a local minimum at $\approx 10^{-10.8}$ yr^{-1}. We use this minimum to divide our sample into 'active' galaxies (sSFR$>10^{-10.8}$ yr^{-1}) and 'passive' ones (sSFR$<10^{-10.8}$ yr^{-1}). This bimodality in sSFR and the break in the vicinity of sSFR$\approx 10^{-11}$ yr^{-1} has been noted by several authors (e.g. Brinchmann et al., 2004; Kauffmann et al., 2004; Wetzel et al., 2012) and is largely independent of stellar mass and environment (Wetzel et al., 2012). We note that while the sSFR measurements of galaxies with strong emission are derived from several emission lines, particularly Hα (Brinchmann et al., 2004), the sSFRs of galaxies with weak or undetectable

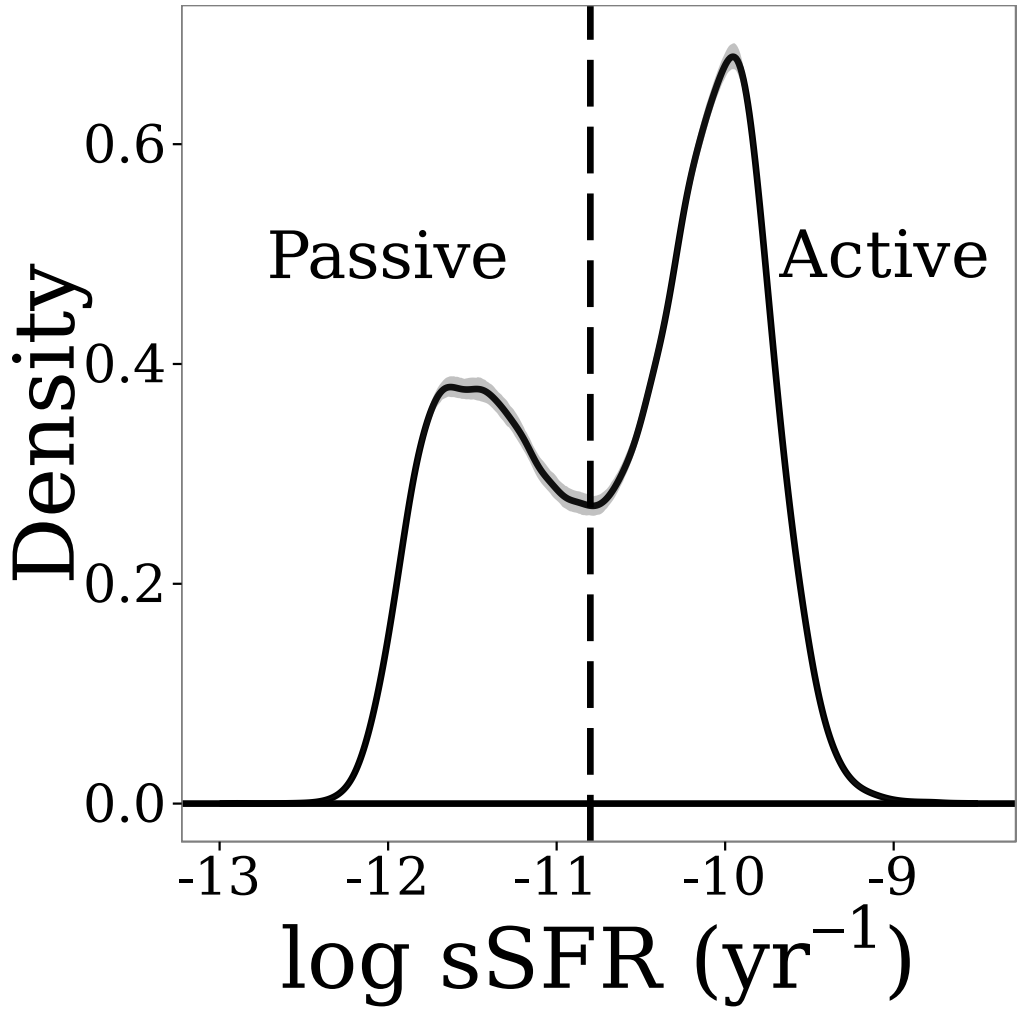

Figure 2.1 V_{max}-weighted specific star formation rate (sSFR) Gaussian kernal-smoothed distribution for galaxies in the full sample. The local minimum at log(SSFR)=-10.8 yr^{-1} defines our 'active' and 'passive' samples. Shaded regions in both plots show 99% confidence intervals from 1000 bootstrap resamplings.

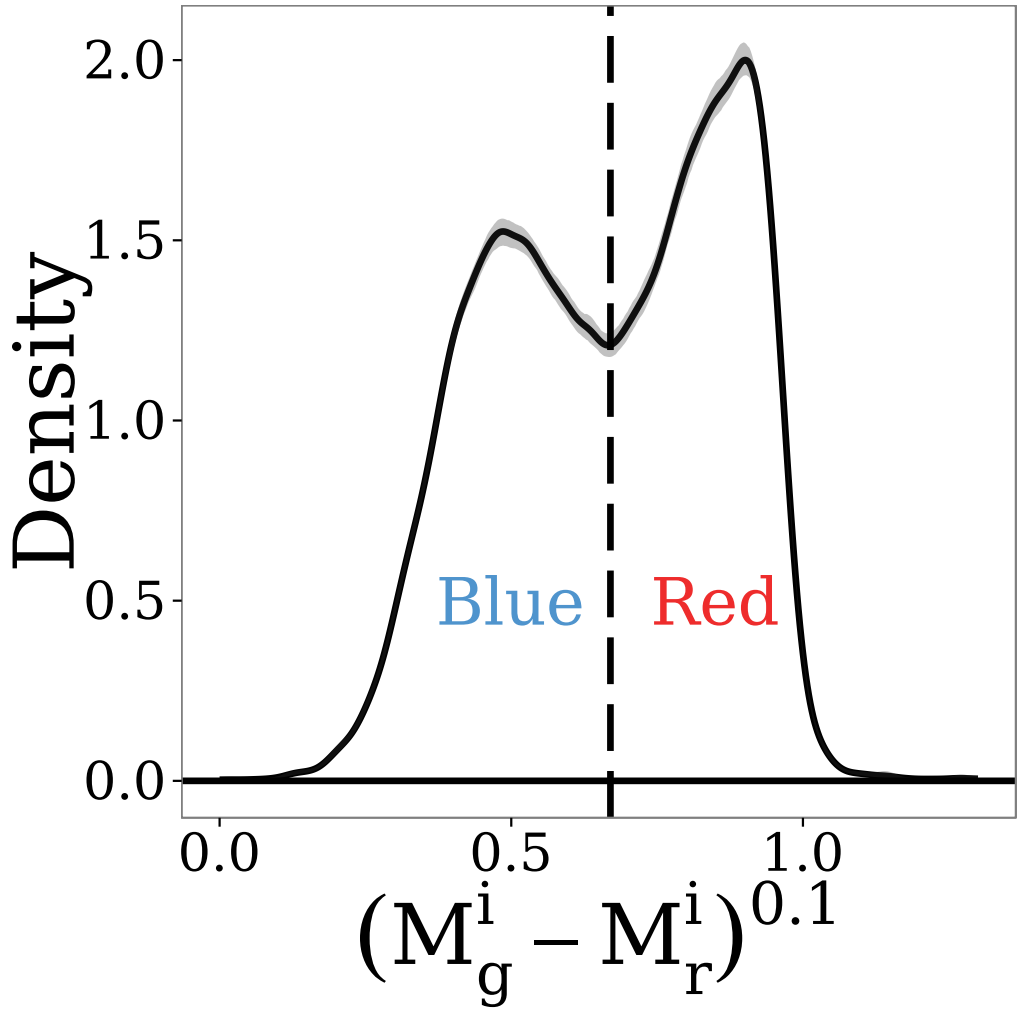

Figure 2.2 V_{max}-weighted $(M_g^i - M_r^i)^{0.1}$ colour distribution of galaxies in the full sample. A cut at $(M_g^i - M_r^i)^{0.1}$=0.67 mags defines our 'red' and 'blue' populations. Shaded regions in both plots show 99% confidence intervals from 1000 bootstrap resamplings.

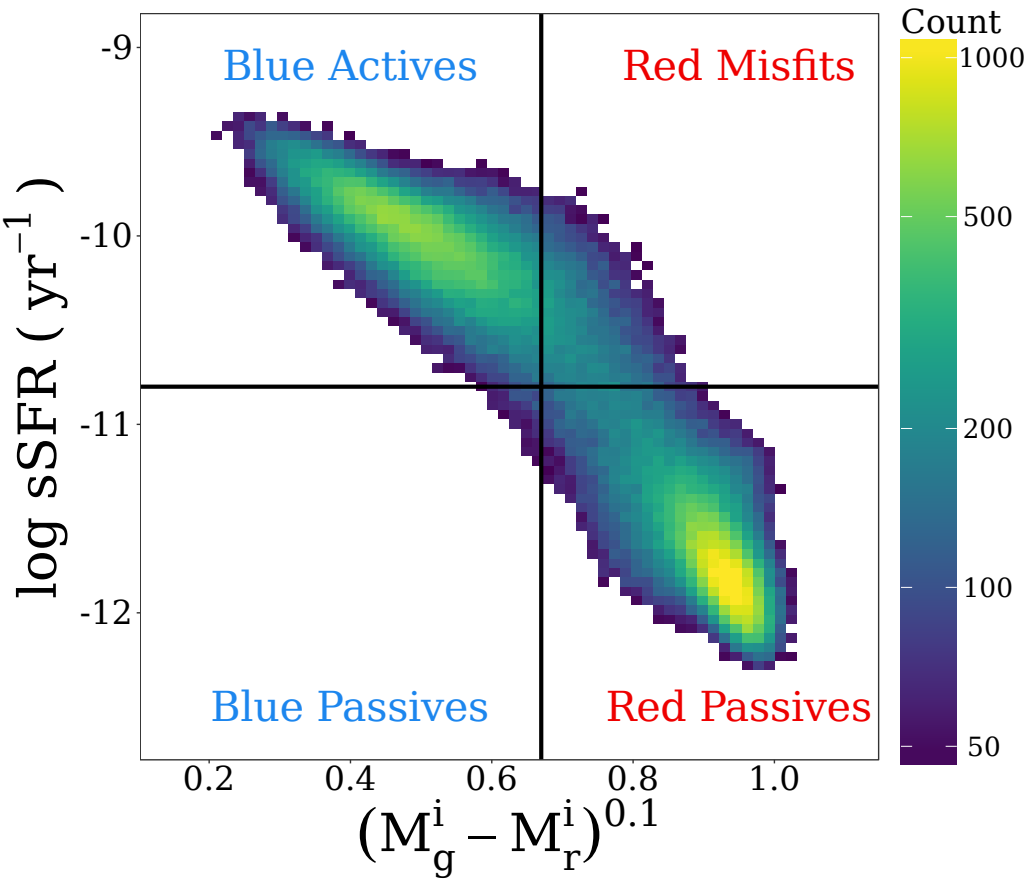

Figure 2.3 sSFR vs. inclination-corrected and k-corrected colour for galaxies in the full sample. Red/blue and active/passive cuts are shown. The Blue Active, Blue Passive, Red Active (Red Misfit) and Red Passive quadrants are shown based on divisions shown in Fig. 2.1 and Fig. 2.2.

emission lines are estimated primarily based on D_n4000 and very quiescent galaxies are assigned sSFRs in the vicinity of 10^{-12} yr^{-1} as an upper limit. Therefore while the active peak of the sSFR distribution in Fig. 2.1 is physical, the height of the quiescent peak is artificial, as the true distribution should tail off to lower sSFRs (Salim et al., 2007).

The distribution of inclination-corrected Petrosian $(M_g^i - M_r^i)^{0.1}$ colours can be seen in Fig. 2.2. The distribution is bimodal, in agreement with previous studies (e.g. Strateva et al., 2001; Baldry et al., 2004; Baldry et al., 2006; Balogh et al., 2004a; Blanton et al., 2005a; Coil et al., 2008). We divide our sample into 'red' and 'blue' populations by applying a cut at $(M_g^i - M_r^i)^{0.1} = 0.67$ mags. Defining our red and blue populations by fitting a red sequence on a colour-magnitude diagram does not change any of our results given that the slope of the red sequence is negligible, as was found by Mahajan & Raychaudhury (2009).

Fig. 2.3 shows the distribution of our sample in sSFR - intrinsic colour space with our sSFR and inclination-corrected colour cuts overlaid. We classify galaxies by the quadrant they occupy in Fig. 2.3: Blue Actives (blue and star-forming), Red Misfits (red and star-forming), Red Passives (red and quiescent) and Blue Passives (blue and quiescent). The relative populations of each quadrant in each of our samples are listed in Table 1. $\sim$87 per cent of galaxies in our full sample belong to either the Blue Active or Red Passive populations while a significant minority ($\sim$11) per cent of galaxies are Red Misfits.

We note that while these subpopulation sample sizes change depending on the colour and sSFR cuts used, the results in Section 2.3 are robust against the precise locations of these cuts.

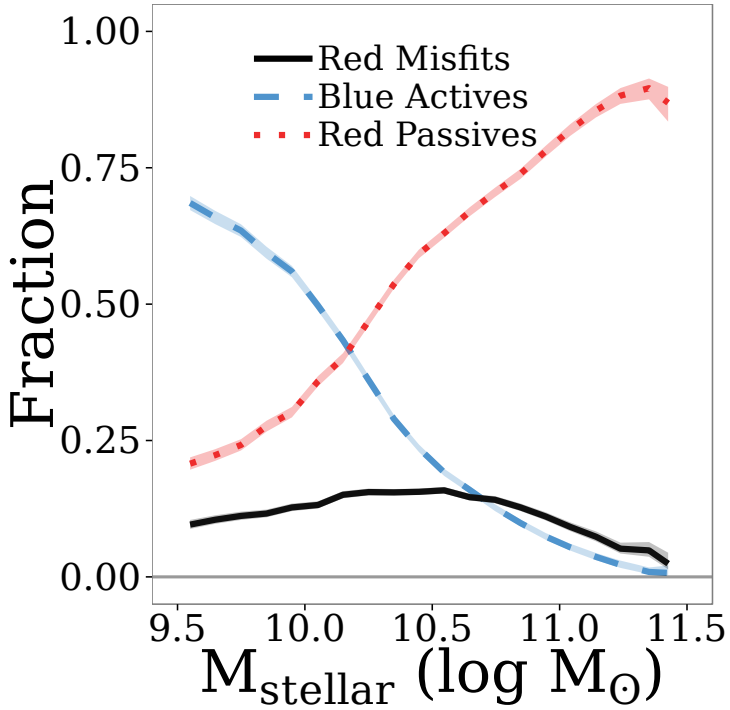

Figure 2.4 V_{max}-weighted relative populations of Blue Active, Red Passive and Red Misfit galaxies in the full sample binned by stellar mass. Shaded regions show 99% confidence intervals generated by the beta distribution as outlined by Cameron (2011).

2.3 Results

2.3.1 Stellar Mass

Many galaxy properties such as star formation rate (e.g. Salim et al., 2007; Noeske et al., 2007b; Poggianti et al., 2008), colour (e.g. Baldry et al., 2006; van den Bosch et al., 2008; Bamford et al., 2009) and morphology (e.g. van der Wel, 2008; Bamford et al., 2009; Bluck et al., 2014) correlate with stellar mass; we therefore compare the properties of Red Misfits, Blue Actives and Red Passives at fixed stellar mass.

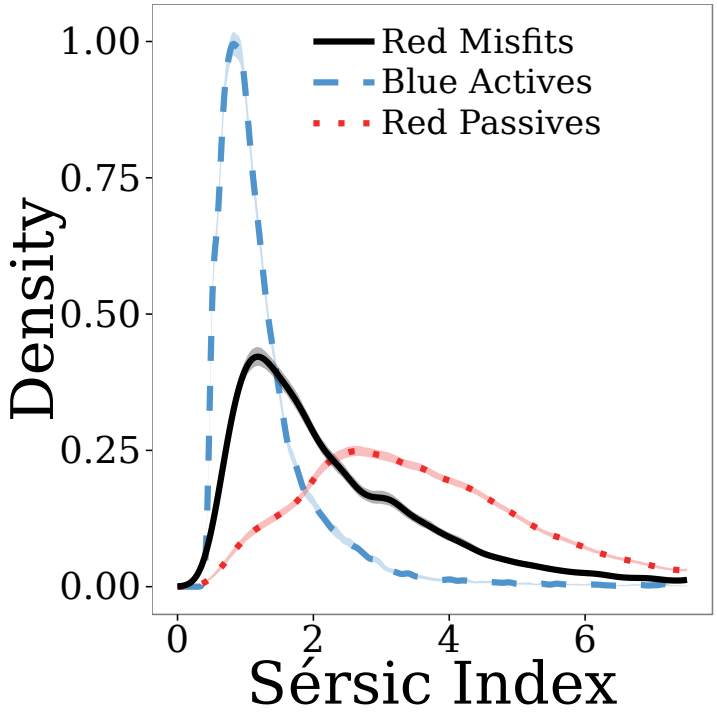

Figure 2.5 V_{max}-weighted density plot of the Sérsic index distribution of the Blue Active, Red Passive and Red Misfit populations in the full sample. 99% confidence interval from 1000 bootstrap resamplings shown in shaded regions.

Fig. 2.4 shows the relative populations of Blue Active, Red Passive and Red Misfit galaxies in different bins of stellar mass in the full sample. As expected (e.g. Weinmann et al., 2006; McGee et al., 2011) Blue Active galaxies dominate at low stellar mass while at high stellar mass Red Passives are the most common galaxy population. The proportion of Red Misfits, however, depends only weakly on stellar mass, comprising ∼10 per cent of galaxies at low stellar mass, peaking at ∼16 per cent at $M_{stellar} \simeq 10^{10.5} M_{\odot}$ before falling off to ∼5 per cent at high stellar mass.

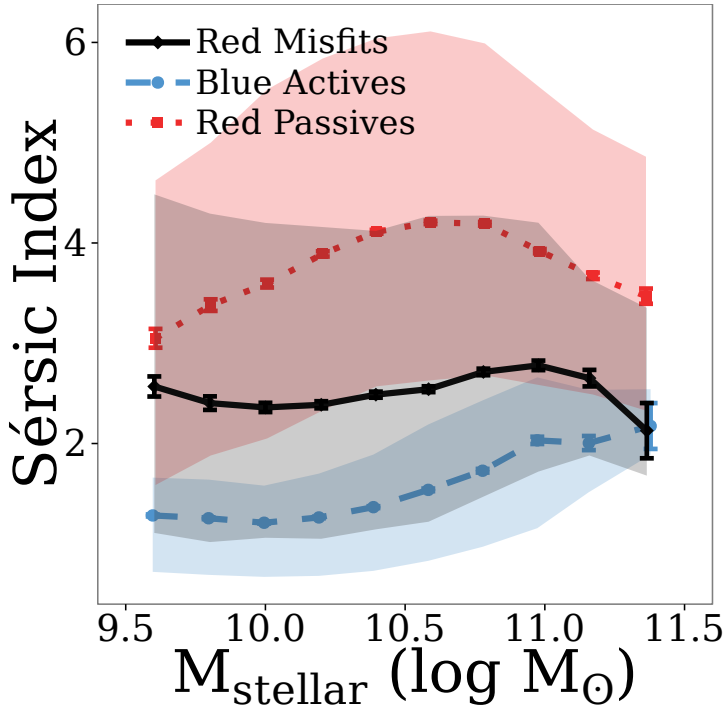

Figure 2.6 Mean Sérsic index of Blue Active, Red Passive and Red Misfit galaxies against stellar mass. Error bars indicate 1σ errors on the V_{max}-weighted mean value. Shaded regions span the 16th to 84th percentiles of each bin.

2.3.2 Morphology

The correspondence between colour and morphology (e.g. Strateva et al., 2001; Baldry et al., 2004) and star formation rate and morphology (e.g. Kauffmann et al., 2003c; Bell et al., 2012) indicate that the same processes that control a galaxy's star formation history may also control its structure. In Fig. 2.5 we show the distribution of Sérsic indices for each of the three populations in the full sample. The Red Passive population tends toward more early-type morphologies than the Blue Active population. Red Misfits have morphologies intermediate between the Blue Active and Red Passive populations. Qualitative results remain the same if we use alternate morphology proxies such as concentration ($c \equiv r_{90}/r_{50}$) or bulge-to-total light ratio: Red Misfits are more

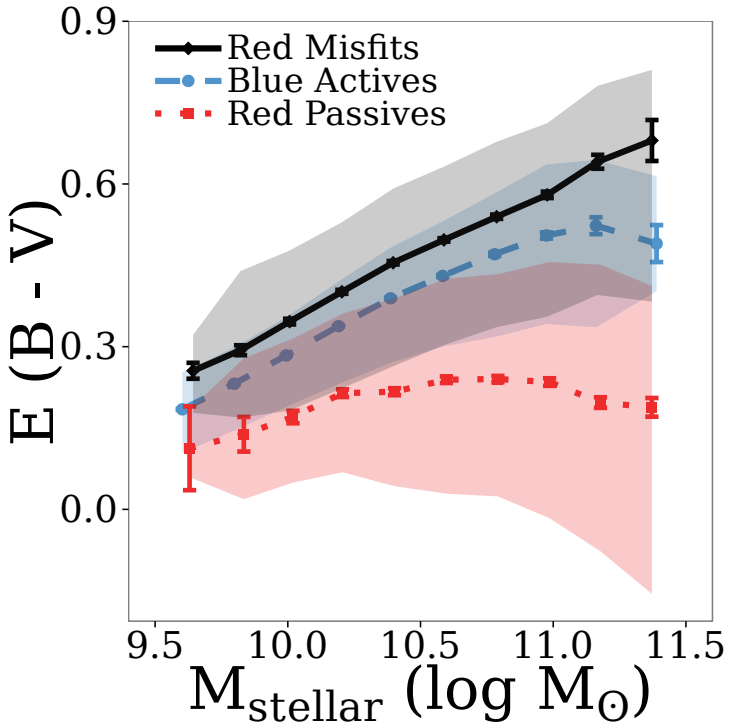

Figure 2.7 Optical colour excess due to intrinsic dust against stellar mass for non-edge-on (e<0.75) Blue Active, Red Passive and Red Misfit galaxies in the emission-line sample. Error bars indicate 1σ errors on the V_{max}-weighted mean value of each bin. Shaded regions span the 16th to 84th percentile of each bin.

(less) bulge-dominated and concentrated than Blue Actives (Red Passives). This intermediate morphology persists even at fixed stellar mass. In Fig. 2.6 we show the V_{max}-weighted mean Sérsic index for each population binned by stellar mass. Despite significant scatter, Red Misfits exhibit higher (lower) mean Sérsic indices than Blue Actives (Red Passives) at all stellar masses. Red Misfit morphologies also exhibit the weakest dependence on stellar mass out of the three populations.

2.3.3 Dust Content

We have selected Red Misfits using inclination-corrected colours to mitigate the impact of inclination on dust reddening, but the possibility still exists that Red Misfits have been significantly reddened due to large amounts of intrinsic dust. Dusty, star-forming red galaxies have been widely studied in the literature (e.g. Coia et al., 2005; Wolf et al., 2005, 2009; Gallazzi et al., 2008; Saintonge et al., 2008; Brand et al., 2009). In this section we explore the fraction of Red Misfits whose colours could be explained with significant reddening by intrinsic dust.

We quantify the amount of dust extinction using the Balmer decrement, comparing the fluxes of Hα and Hβ in our emission line catalogue. It is possible to determine the expected ratio between these lines depending on the properties of the absorbing medium (Menzel & Baker, 1937; Baker & Menzel, 1938). The flux ratio depends weakly on gas temperature and density (Osterbrock & Ferland, 2006) but is strongly affected by dust. The colour excess in the visible band due to dust is characterized by

$$E(B-V) = 1.97 \log\left(\frac{(H\alpha/H\beta)_{obs}}{2.86}\right), \tag{2.4}$$

where $(H\alpha/H\beta)_{obs}$ is the observed flux ratio, 2.86 is the unreddened ideal flux ratio corresponding to a medium at 10,000 K with an electron density of 100 cm^{-3} (Osterbrock, 1989) and 1.97 is a constant derived using the reddening curve of Calzetti et al. (2000). The choice of 2.86 for the unreddened flux ratio is common in the literature (e.g. Domínguez et al., 2013; Xiao et al., 2012). We note that since Balmer decrements are measured based on the Hα and Hβ emission lines, extinction is estimated based solely on the star-forming regions of a galaxy and therefore may not be representative of the galaxy as a whole.

In Fig. 2.7 we plot the Balmer decrement as a function of stellar mass for Blue Actives, Red Passives and Red Misfits in our sample of emission-

line galaxies (see Sec. 2.2.3). Since the Balmer decrements in our emission-line sample show only a mild trend with axis ratio (similar to Yip et al., 2010; Xiao et al., 2012), we remove edge-on (e>0.75) galaxies from the emission-line sample in Fig. 2.7 to capture intrinsic dust-reddening only; however, the results are consistent if the entire sample is used. The optical colour excess due to intrinsic dust reddening is on average larger in Red Misfits than Blue Actives across the entire stellar mass range of our sample in Fig. 2.7. This enhancement in colour excess is small: Red Misfits are dust-reddened in B-V colour by only 0.056 mags more than Blue Actives on average across all stellar mass bins. Applying the corresponding g-r colour offset based on the transformation of Jester et al. (2005) results in only $\sim$7 per cent of Red Misfits being reclassified as Blue Actives and does not qualitatively change any results of this study.

The scatter in Fig. 2.7 across each population and all stellar masses is significant: only 26 per cent of Red Misfits exhibit colour excesses 1σ over the colour excess for a typical Blue Active galaxy with the same stellar mass. The removal of these most-reddened Red Misfits does not qualitatively change any results presented in this work. We therefore conclude that although dust reddening can account for a small proportion of Red Misfits, the entire population cannot be dismissed as dust-reddened Blue Active galaxies.

2.3.4 Age and Metallicity

Although Red Misfits are star-forming by construction, a stellar population that is overall older than the Blue Actives can significantly contribute to their red colours. To characterize the mean stellar age of each population we use the D_n4000 index as defined by Balogh et al. (1999) provided in the MPA-JHU emission-line catalogue.

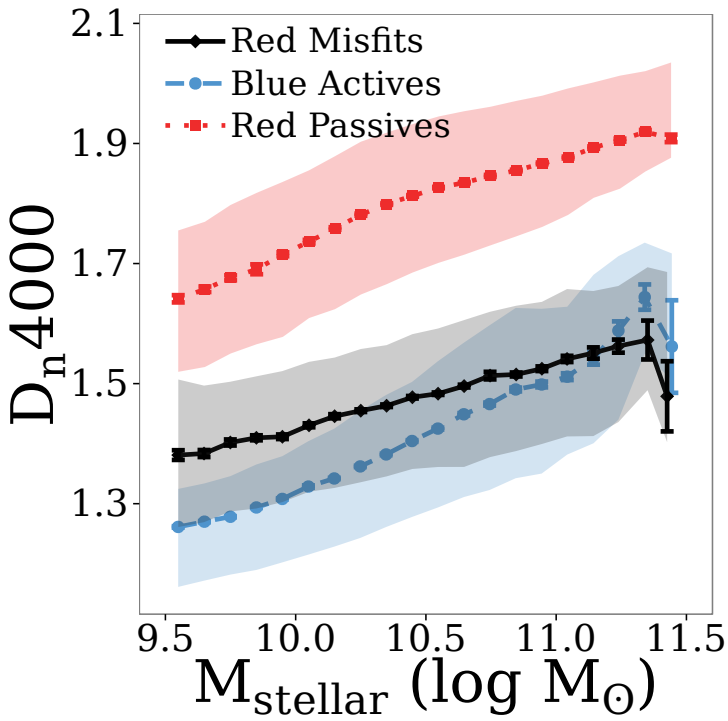

Figure 2.8 D_n4000 index measurement for each population in the full sample binned by stellar mass. Error bars indicate 1σ errors on the V_{max}-weighted mean value. Shaded regions span the 16th to 84th percentile of each bin.

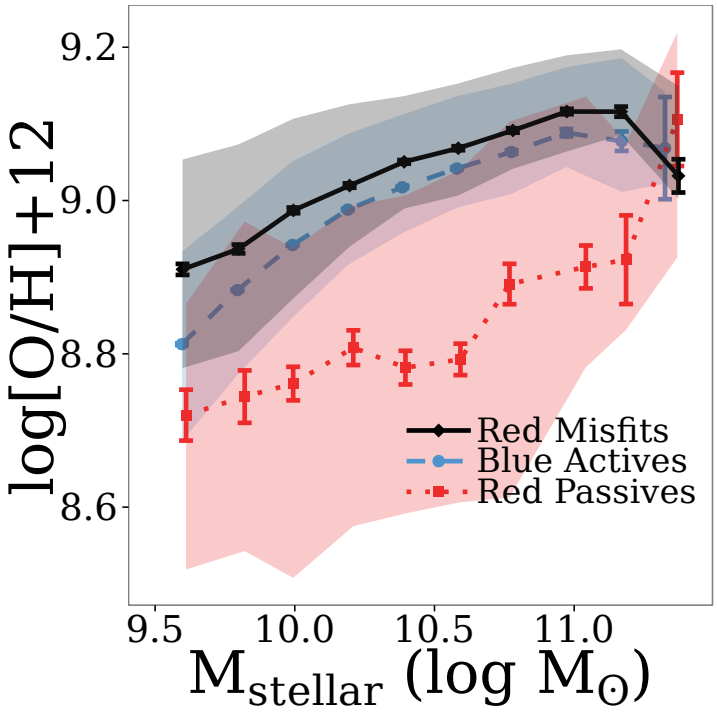

Figure 2.9 Gas-phase metallicity of each population in the full sample binned by stellar mass. Error bars indicate 1σ errors on the V_{max}-weighted mean value. Shaded regions span the 16th to 84th percentile of each bin.

Fig. 2.8 shows the relationship between D_n4000 and stellar mass for Blue Actives, Red Passives and Red Misfits in the full sample. Red Passive galaxies show high values of D_n4000, confirming them as galaxies with an old stellar population and relatively little recent star formation. Conversely, Blue Actives exhibit low D_n4000 values, indicating that they have comparatively younger stellar populations. Both populations tend towards larger D_n4000 at higher stellar mass. At low and moderate stellar mass, Red Misfits exhibit an intermediate D_n4000 measurement between the Blue Active and Red Passive populations. Toward high stellar mass, the Red Misfit D_n4000 measurements approach the same value as the Blue Actives', indicating that their stellar populations are of comparable age.

The redness of Red Misfits can therefore not be attributed to any single factor. Rather, their colours are due to contributions from increased dust (as measured by the Balmer decrement) and aged stellar populations (as measured by D_n4000) when compared to Blue Actives.

The Red Misfits could have atypical sSFRs for their stellar mass because of differences in gas-phase metallicity (e.g. Ellison et al., 2008; Yates et al., 2012; Lara-López et al., 2013). To probe metallicity we use the gas-phase metallicity ($\log[O/H]+12$) measurements in the MPA-JHU catalogue based on Tremonti et al. (2004). We stress that only a small fraction (30 per cent) of our full sample has metallicity measurements, as Tremonti et al. (2004) only estimate $\log[O/H]$ for galaxies with a 5σ detection or greater in Hα, Hβ and NII. The sample of galaxies with metallicity measurements will therefore be dominated by Blue Actives ($\sim$90 per cent) and Red Passives will be extremely underrepresented ($\sim$0.5 per cent). Fig. 2.9 shows the relationship between $\log[O/H]+12$ for the Red Misfits, Blue Actives and Red Passives that meet these criteria. For all three populations, gas-phase metallicity increases with stellar mass. As the most metal-rich population by a slight margin, Red Misfits are on average $\simeq$0.03 dex more metal-rich than Blue Actives.

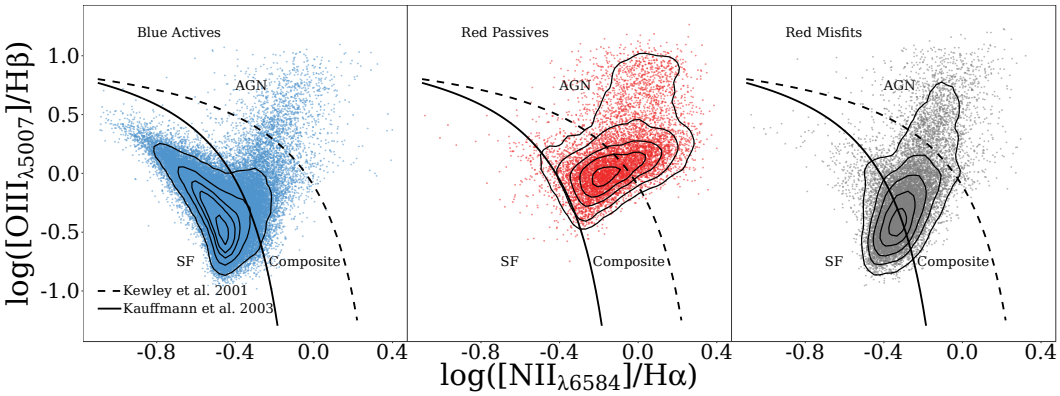

Figure 2.10 Distribution of Blue Actives (left), Red Passives (centre) and Red Misfits (right) in the emission-line sample on the BPT diagram. Contours encompass 10%, 30%, 50%, 70% and 90% of the unweighted distributions. Lines from Kewley et al. (2001) and Kauffmann et al. (2003c) define star-forming and AGN regions of the diagram as well as the composite region where emission from stellar and non-stellar processes are comparable.

2.3.5 AGN Abundance

It has been known for some time that active galactic nuclei (AGN) play a significant role in galaxy evolution. To match observations in the local Universe, galaxy evolution models typically invoke AGN feedback – heating central gas and suppressing star formation in massive galaxies (e.g. Granato et al., 2004; Bower et al., 2006). Nuclear star formation associated with an AGN (e.g. Goto, 2006; Bildfell et al., 2008; Reichard et al., 2009) may help reconcile the significant star formation in Red Misfits with their red colours.

We identify AGN in our three populations using the 'BPT' emission line diagnostic diagram of Baldwin et al. (1981). The BPT diagram identifies the dominant source of ionization in a galaxy by its position in $\log_{10}([\text{NII}]/\text{H}\beta)$ vs. $\log_{10}([\text{OIII}]/\text{H}\alpha)$ space. The distributions of Red Misfits, Blue Actives and Red Passives in the emission-line sample on the BPT diagram are illustrated in Fig. 2.10. The solid line of Kauffmann et al. (2003a), based on the observed distribution of SDSS galaxies, provides the upper limit for galaxies whose emission is

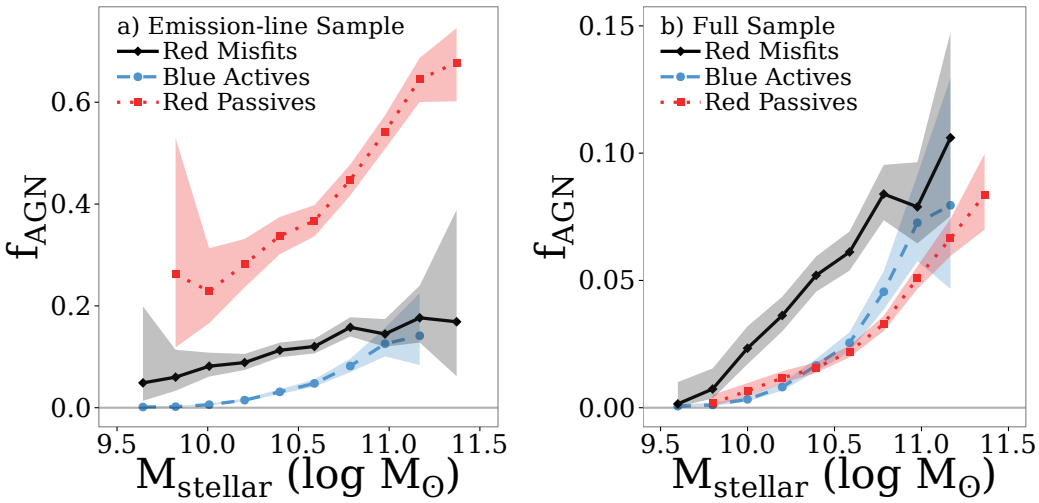

Figure 2.11 a) Fraction of each population in our emission-line subsample identified as hosting an AGN (i.e. fraction lying above the Ke01 line) in bins of stellar mass. b) AGN fraction of each population in our *full* sample (i.e. fraction satisfying the emission-line criteria of Section 2.2.3 and lying above the Ke01 line). Shaded regions are 99% confidence intervals generated by the beta distribution as outlined by Cameron (2011).

dominated by ongoing star formation (i.e. ionization from O and B stars). The dashed line of Kewley et al. (2001), hereafter Ke01, based on the region which can reasonably be described by maximal starburst emission, provides the lower limit for galaxies whose emission is dominated by non-stellar processes. These non-stellar heating processes may include shocks and evolved stellar populations (e.g. Stasińska et al., 2008), but the major source of non-stellar heating will be AGN, so for simplicity we choose to call all objects above the Ke01 line 'AGN'. The region between the Ke01 and Kauffmann et al. (2003a) lines encompasses objects for which stellar and non-stellar emission are comparable. We refer to these objects as 'composites'.

The vast majority of emission-line Blue Active galaxies reside in the star-forming region of Fig. 2.10. Conversely, there are very few (∼5 per cent) emission-line Red Passive galaxies in the star-forming region. Rather, most

emission-line Red Passive galaxies reside in the composite and AGN region of the diagram. Finally, emission-line Red Misfits are concentrated in the star-forming and composite regions but have a significant tail ($\sim$12 per cent) in the AGN region.

Fig. 2.11a shows the fraction of galaxies identified as hosting an AGN (i.e. fraction of galaxies lying above the Ke01 line on a BPT diagram) in the emission-line sample binned by stellar mass. Across the entire stellar mass range of our emission-line sample, emission-line Red Passives are the most likely of the three populations to be located above the Ke01 line on a BPT diagram, especially toward higher stellar masses. Emission-line Red Misfits are significantly more likely to host an AGN than Blue Actives, especially at low stellar mass where there are virtually no AGN hosted by Blue Active emission-line galaxies.

We stress that the emission-line sample is not representative of the full sample. The vast majority of Red Passives do not exhibit strong emission and are underrepresented in the emission-line sample as described in Section 2.2.3 (see Table 2.1). The Red Passives that are included in the emission-line sample are going to be the ones with significant non-stellar emission, hence the high f_{AGN} in Fig. 2.11a. Conversely, the significant emission from star formation means nearly all Blue Actives are included in the emission-line sample and consequently a relatively small fraction of them will host an AGN.

Fig. 2.11b shows the fraction of galaxies hosting AGN in the full sample, i.e. the fraction of galaxies in the full sample that satisfy our emission-line criteria outlined in Section 2.2.3 and lie above the Ke01 line on a BPT diagram. At all stellar masses, we find Red Misfits are more likely to host an AGN than Blue Actives or Red Passives in the full sample. The f_{AGN} enhancement in Red Misfits is particularly strong towards low stellar mass, where the fraction

of Red Passive galaxies hosting AGN is low and the fraction of Blue Actives hosting AGN is nearly zero.

We point out that despite the fact that Red Passives are significantly less likely to host a BPT-identified AGN when compared to Red Misfits across the entire stellar mass range, Red Passives are still the most common hosts of AGN in our full sample (particularly at high stellar mass) due to the sheer size of the population (see Table 2.1). However, below a stellar mass of $\sim 10^{10.3}$ $M_{\odot}$, Red Misfits are the most common hosts of BPT-identified AGN in the local Universe.

2.3.6 Environmental Trends

Having explored the stellar masses, morphologies, dust content and AGN abundance of Red Misfits compared to Blue Actives and Red Passives, we now consider how the proportions of these populations change with environment. We characterize environment by both group halo mass, given in the Y07 catalogue, and group-centric distance scaled by the characteristic radius R_{200} described in Section 2.2.4.1. Given that star formation trends with environment are dominated by the changing fraction of passive galaxies rather than the changing sSFR of star-forming galaxies themselves (e.g. McGee et al., 2011; Wijesinghe et al., 2012; Schaefer et al., 2017), exploring how population proportions vary with environment can help constrain the physical processes responsible for quenching.

We show the V_{max}-weighted relative fractions of each population against group halo mass in Fig. 2.12. Results are shown for samples binned by group-centric distance and by stellar mass. The Blue Active population fraction decreases with increasing group halo mass in all bins with a stronger halo mass dependence at low stellar mass. Correspondingly, the Red Passive fraction in-

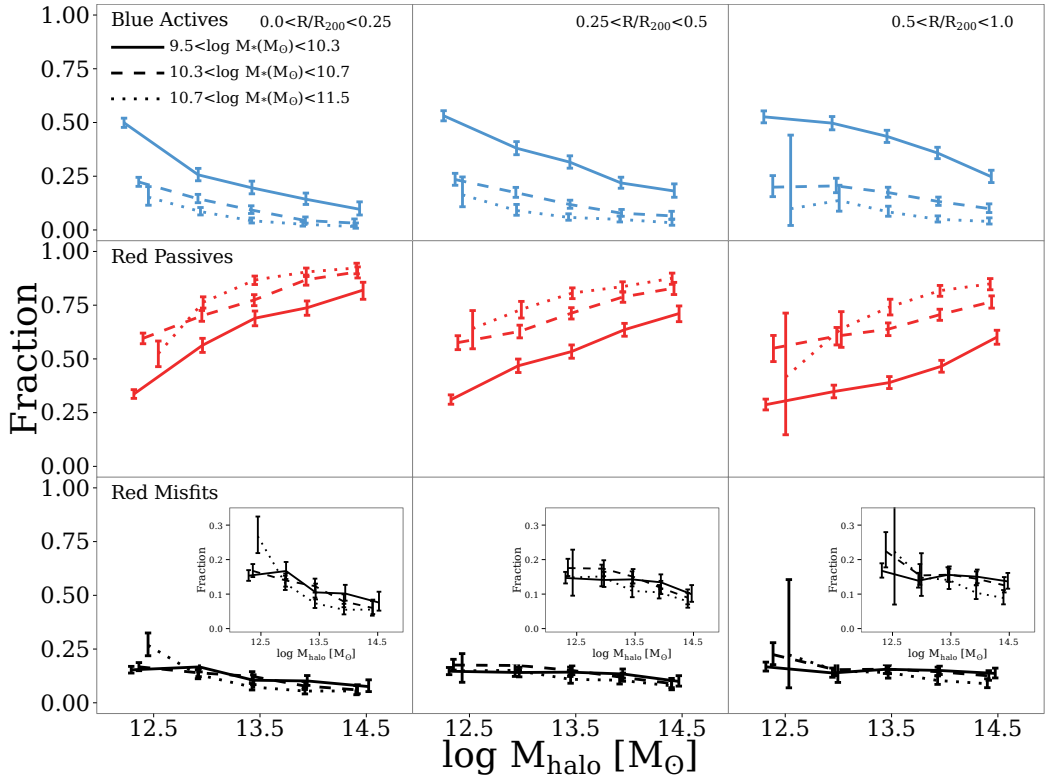

Figure 2.12 V_{max}-weighted satellite fractions of Blue Actives (top), Red Passives (middle) and Red Misfits (bottom) in our group sample against group halo mass. Fractions are shown for galaxies in the inner third (left column), middle third (middle column) and outer third (right column) of the R/R_{200} distribution. Results are also shown in three bins of stellar mass as different line styles corresponding to the upper, middle and lower thirds of the stellar mass distribution. Insets zoom in on the Red Misfit results. Error bars are 99% confidence intervals generated by the beta distribution as outlined by (Cameron, 2011).

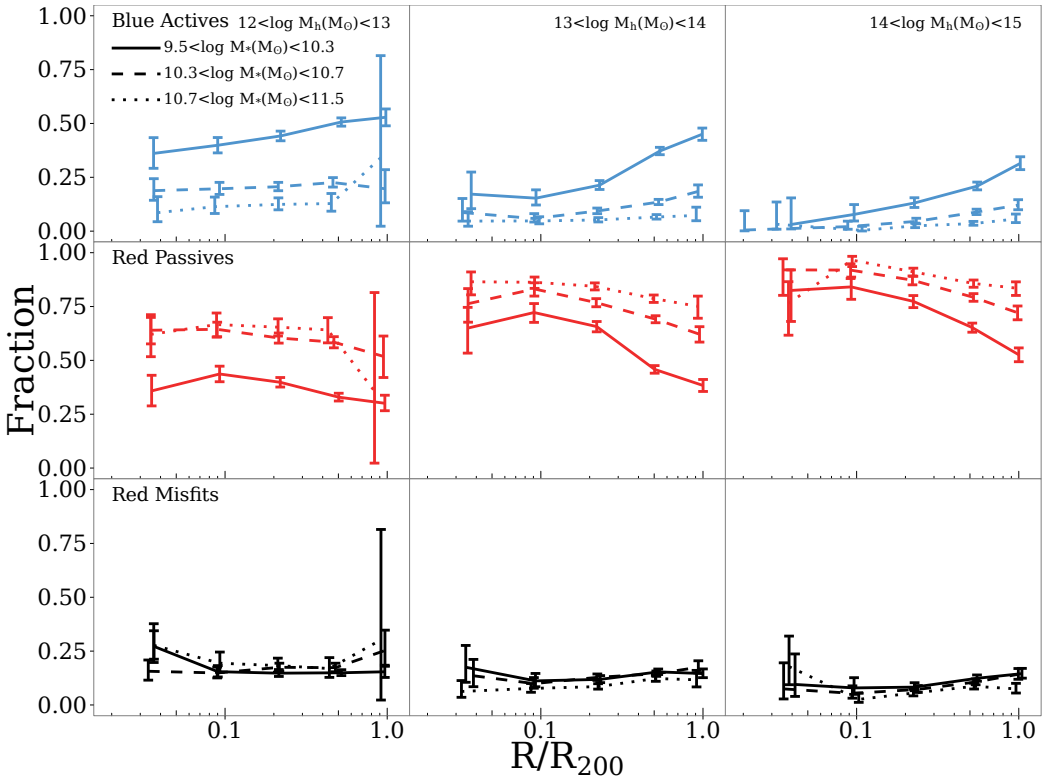

Figure 2.13 Same as Fig. 2.12 except we plot fractions against R/R_{200} and bin by group halo mass in the columns.

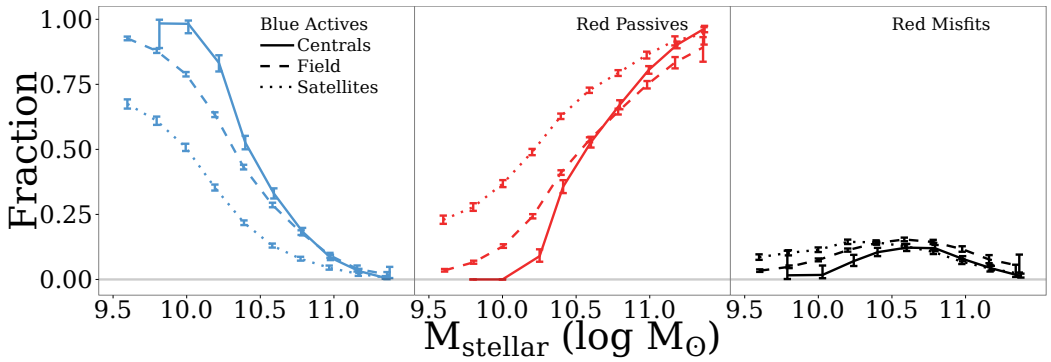

Figure 2.14 V_{max}-weighted fractions of Red Misfit, Blue Active and Red Passive galaxies with stellar mass in our field sample, the sample of centrals in our group catalogue and the sample of satellites in our group catalogue. The fraction of Red Misfits depends only weakly on stellar mass and environment. Error bars are 99% confidence intervals generated by the beta distribution as outlined by (Cameron, 2011).

creases with halo mass. The Red Misfit dependence on halo mass is much weaker, but the inset shows that the fraction of Red Misfits decreases weakly with halo mass in all bins of stellar mass and group-centric distance with little dependence on stellar mass.

To see radial trends more clearly, Fig. 2.13 shows population fractions plotted against group-centric distance and binned in columns by group halo mass. The fraction of Blue Actives (Red Passives) increases (decreases) with increasing group-centric distance with a stronger dependence at low stellar mass, though generally the trends are weaker than the trends with halo mass, particularly at low halo mass. The Red Misfit dependence on group-centric distance is very weak.

There are two important environments not shown in Figs. 2.12 and 2.13: field galaxies (described in Section 2.2.4.2) and central galaxies (here defined as the brightest galaxy in the group). Population fractions with stellar mass in our field, central and satellite samples are shown in Fig. 2.14. Blue Active and Red Passive fractions depend most strongly on stellar mass in our sample

of centrals and most weakly in our sample of satellites. Red Misfit fractions, however, are remarkably flat with both stellar mass and environment. With the exception of very low stellar mass, where the fraction of Red Misfit centrals drops to zero, there is an ∼11 per cent chance of a galaxy in a given sample being a Red Misfit, independent of its stellar mass or whether it is a central, satellite or field galaxy. We note that the overwhelming majority of low-stellar mass centrals are centrals of galaxy pairs or triplets rather than richer groups and in very low mass groups there is a risk of misidentifying the central galaxy (e.g. Peng et al., 2012; Knobel et al., 2013).

2.4 Discussion

In the previous sections we have shown that there exists a small but significant population of red and star-forming galaxies in the Sloan Digital Sky Survey. These 'Red Misfit' galaxies exhibit intermediate morphologies relative to the more common Blue Active and Red Passive populations, show a slight excess of attenuation due to intrinsic dust, and have an enhanced probability of hosting an AGN, This population represents ∼11 per cent of $z < 0.1$ galaxies, varying only weakly with stellar mass, halo mass, and group-centric radius. In this section we interpret these results to try and elucidate the physical origin of Red Misfits and compare our results to previous investigations of optically-red galaxies exhibiting measurable star formation.

2.4.1 Red Misfits as Having Poorly-Constrained Star Formation

Red Misfits are defined based on their colours and sSFRs. Earlier SDSS catalogues estimated sSFR based on optical emission lines (particularly Hα) and the sSFRs for AGN and low S/N galaxies were poorly constrained (Brinchmann et al., 2004). The overestimation of Red Misfits' sSFRs due to AGN

contamination or low S/N emission lines is a therefore a valid concern, especially considering the preponderance of AGN in Red Misfits. We use the updated, UV-based sSFRs of Salim et al. (2007). Whereas AGN can contaminate Hα, the contribution to the UV continuum from AGN is low (Salim et al., 2007; Kauffmann et al., 2007).

2.4.2 Red Misfits as a Combination of Blue Actives and Red Passives

In Section 2.3.3 we show that Red Misfits are not entirely dusty star-forming galaxies. It is possible, however, that Red Misfits could be a mix of dusty Blue Actives and Red Passives with overestimated sSFRs. Indeed, inclination-induced dust reddening significantly inflates the population of Red Misfits if inclination-corrected colours are not used (see Section 2.7). However, if the Red Misfits that remain after inclination correction are dominated by Blue Actives or Red Passives, their properties should closely match one of the two populations. Red Misfits and Blue Actives are similar in their Balmer decrements (see Fig. 2.7), mean stellar ages and gas-phase metallicities (see Fig. 2.8 and Fig. 2.9). On the other hand, the stellar masses, morphologies and AGN fractions of Red Misfits are typical of neither Blue Actives nor Red Passives.

Authors (e.g. Gallazzi et al., 2008; Mahajan & Raychaudhury, 2009) find bimodality in properties of their red star-forming samples and interpret this as evidence that their populations of star-forming red galaxies are a mix of two distinct populations. We stress that we do not see evidence of multiple components for any property of our Red Misfits – they appear to be a single population. Although there may be some contamination of our Red Misfit sample by dusty Blue Actives and overestimated-sSFR Red Passives, it is impossible to combine these populations in a way that reproduces the properties

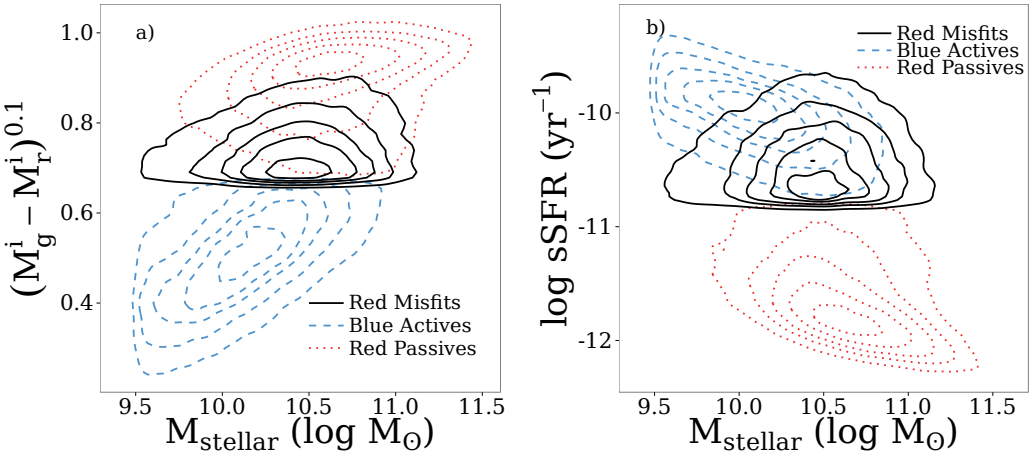

Figure 2.15 *a):* Inclination-corrected $g-r$ colour against stellar mass for Red Misfits, Blue Actives and Red Passives. *b*: sSFR against stellar mass for Red Misfits, Blue Actives and Red Passives. Contours in both plots encompass 10%, 30%, 50%, 70% and 90% of the unweighted distributions.

of Red Misfits. The properties of Red Misfits remain the same even if the most intrinsically-dusty galaxies are removed and if the sSFR cutoff defining Red Misfits is raised.

2.4.3 Red Misfits as Their Own Distinct Population

Given that the morphologies, AGN abundances, dust content and environmental trends of SDSS Red Misfits are inconsistent with them being dusty/edge-on Blue Actives or Red Passives with overestimated sSFRs (or a combination thereof) and there is little evidence they have particularly ill-constrained sSFRs, we suggest instead that Red Misfits are in fact their own separate population of galaxies in the local Universe distinct from the Blue Active and Red Passive populations. Here we explore the possible physical origins of Red Misfits, their connection to other known populations and how they fit into the broad picture of galaxy evolution.

2.4.3.1 Connection with the Green Valley

Red Misfits exhibit many intermediate properties which indicate they might be a transition population between the blue star-forming cloud and the red sequence. They may be similar to previously identified intermediate populations such as the green valley – the sparsely-populated transition region between the red sequence and the blue cloud (e.g. Bell et al., 2004; Faber et al., 2007; Wyder et al., 2007). In corrected colour-stellar mass space (Fig. 2.15a), the distribution of Red Misfits seems to be a high-mass continuation of the Blue Active distribution and its locus lies primarily in the green valley. The intermediate morphologies of Red Misfits are also consistent with the green valley (Mendez et al., 2011). We note that the green valley is typically defined with uncorrected UV-optical CMDs so direct comparisons are difficult.

In Fig. 2.15b, it is clear that sSFRs and stellar masses of Blue Actives are tightly correlated, forming the star-forming main sequence found in samples of star-forming galaxies (e.g. Brinchmann et al., 2004; Noeske et al., 2007a; Elbaz et al., 2007). Red Misfits, however, do not exhibit this correlation and instead lie below the main sequence of star formation.

The Red Misfit distributions in Fig. 2.15 therefore support a scenario in which Red Misfits are in fact transition galaxies similar to green valley galaxies in the midst of being quenched gradually on their way to the red sequence. Star formation is suppressed but not entirely zero in these galaxies, therefore their stellar mass continues to increase as they fall off the specific star-forming main sequence and gradually redden in colour, explaining the older mean stellar age when compared to Blue Actives.

This scheme of gradual quenching is qualitatively similar to the late-type quenching model of Schawinski et al. (2014). An important distinction is that Schawinski et al. (2014) infer a significant environmental contribution to this quenching model as they find a dearth of Galaxy Zoo-selected late-type green

valley galaxies in halos below M_{halo}=10^{12} $h^{-1}M_{\odot}$. The proportion of Red Misfits, however, is flat with M_{halo}.

It is this (near) equal abundance of Red Misfits in all environments that suggests the processes that govern/create them are driven by secular evolution. The prevalence of AGN in Red Misfits suggests they play a role, either as a mechanism of secular quenching or a byproduct of it. AGN feedback can suppress gas cooling on 1-2 Gyr timescales (e.g. Croton et al., 2006), inhibiting star formation after the cool gas supply is exhausted. The more dominant bulges of Red Misfits when compared to Blue Actives may indicate more massive central black holes (Magorrian et al., 1998; Häring & Rix, 2004) and thus stronger feedback. AGN have been found to prefer similar regions in parameter space as Red Misfits, i.e. in the green valley (e.g. Nandra et al., 2007; Silverman et al., 2008; Schawinski et al., 2014) and below the massive end of the specific star-forming main sequence (Salim et al., 2007).

AGN feedback is far from the only secular mechanism capable of quenching star formation. Strong bars are efficient at driving gas inwards (e.g. Knapen et al., 1995; Sheth et al., 2005), exhausting cold gas supply by spurring central star formation (e.g. Martin & Friedli, 1997), building a pseudobulge (e.g. Kormendy & Kennicutt, 2004; Athanassoula, 2005) and perhaps coupling to an AGN. The deep potential well of a significant bulge created by internal processes or minor mergers combined with the declining self-gravity of the cool gas as the gas supply dwindles can prevent the fragmentation of the disk and thus suppress its star formation efficiency (Martig et al., 2009).

2.4.3.2 Connection with S0s/S0 Projenitors

Previous work studying anomalously red galaxies (e.g. Goto et al., 2003; Wolf et al., 2009; Koyama et al., 2011) have suggested that they are the pro-

jenitors of the S0 population. S0s have also been discussed as a transition population in the context of transforming infalling blue galaxies (e.g. Poggianti et al., 1999; Kodama et al., 2001; Wilman & Erwin, 2012).

At a glance there are many similarities between Red Misfits and S0s: their red colours (Roberts & Haynes, 1994), enhanced sSFR over elliptical galaxies (e.g. Amblard et al., 2014), overlap with the green valley (Salim et al., 2012) intermediate bulge-total ratio relative to early-type and late-types (e.g. Simien & de Vaucouleurs, 1986), enhanced AGN fraction (e.g. Schawinski et al., 2007; Wilman & Erwin, 2012; Amblard et al., 2014) over ellipticals and an enhanced dust mass relative to ellipticals as well (Amblard et al., 2014). Their sizable abundance in diverse environments, i.e. in both massive clusters (e.g. Dressler, 1980; Moran et al., 2007) and the field (e.g. van den Bergh, 2009; Wilman et al., 2009) and their flat radial gradients in clusters (e.g. Dressler, 1980; Dressler et al., 1997) are all consistent with behaviour seen in the Red Misfit population; however, their preference for the cluster environment (Dressler, 1980) and their rather strong population trends with halo mass and stellar mass (Wilman & Erwin, 2012) are not. So while the Red Misfit population may include some S0 projenitors, it cannot explain the whole population.

2.4.3.3 Connection with Red Spirals

The red colours and early-disc morphologies of Red Misfits are reminiscent of the significant 'red spiral' population in the Universe (van den Bergh, 1976; Dressler et al., 1999; Poggianti et al., 1999). Indeed, some authors investigating a red star-forming population (e.g. Gallazzi et al., 2008; Wolf et al., 2009; Crossett et al., 2014) treat red spirals and their star-forming red population as largely the same thing. Red spirals are often referred to as passive (e.g. Poggianti et al., 1999; Goto et al., 2003) yet many can still exhibit significant star formation (Cortese, 2012) and many of the galaxies in the Galaxy Zoo-

selected red spiral catalogue of Masters et al. (2010) qualify as star-forming by our definitions (see Section 2.2.5). Red Misfits and red spirals both show intermediate star formation rates (Tojeiro et al., 2013) and enhanced AGN fraction (Masters et al., 2010). Red spirals, however, show dust and environment properties (e.g. Goto et al., 2003; Skibba, 2009; Bamford et al., 2009; Masters et al., 2010; Tojeiro et al., 2013) which are distinct from Red Misfits. These red spirals have been suggested as a projenitor of S0s (Goto et al., 2003; Wolf et al., 2009) and as a evolutionary stage on the way to the red sequence (Moran et al., 2007; Bundy et al., 2010; Tojeiro et al., 2013). It is possible that Red spirals represent Red Misfits which have finished quenching.

2.5 Summary & Conclusions

We investigate a population of red, star-forming galaxies (Red Misfits) in the Sloan Digital Sky Survey Data Release 7. We identify them as star-forming based on their MPA-JHU specific star formation rates and red using NYU-VAGC $g-r$ colours, k-corrected to z=0.1 and corrected for attenuation due to inclination. This population represents $\sim$11 per cent of galaxies in the local Universe. Selecting galaxy populations using *both* sSFR and colour allows more robust identification of intermediate or transition galaxies than using only one or the other. The use of inclination-corrected colours reduces contamination of intermediate populations by highly-inclined galaxies, allowing more physically meaningful classification of galaxy populations.

To elucidate the physical origin of Red Misfits and their role in galaxy evolution, we study the properties and halo occupation statistics of Red Misfits, comparing them to Blue Active and Red Passives and finding the following:

1. The fraction of Red Misfits is nearly flat with stellar mass (Fig. 2.4). This is in stark contrast to Blue Actives and Red Passives, which dominate demographics in low and high stellar mass samples respectively.

2. Compared to Blue Actives and Red Passives, Red Misfits are more likely to be fit by an intermediate Sérsic index (Fig. 2.5, Fig. 2.6). Red Misfits are therefore not universally early-type or late-type but rather exhibit a range of morphologies and prefer intermediate morphologies.

3. At fixed stellar mass, Red Misfits show slightly larger levels of intrinsic dust-reddening than Blue Actives as measured by the Balmer decrement (Fig. 2.10). This excess, however, is not enough to attribute the colours of Red Misfits entirely to dust. Rather, their colours are due to contributions from increased dust (as measured by the Balmer decrement) and aged stellar populations (as measured by D_n4000) when compared to Blue Actives.

4. Overall, Red Misfits in our smaller emission-line sample are twice as likely to be classified on a BPT diagram as hosting an AGN than Red Passives and 5.5 times more likely to host one than Blue Actives (Fig. 2.11). This enhanced AGN likelihood persists at fixed stellar mass and is especially strong at low stellar mass.

5. Red Misfits exhibit only very weak environmental trends. Their proportion declines slightly with increasing host halo mass but is flat with increasing group-centric separation (Fig. 2.13, 2.12). Blue Actives and Red Passives, by comparison, exhibit much stronger environmental trends in our group sample. Additionally, Red Misfits are found in equal proportion in our field and group samples. Conversely, Blue Actives are more abundant in the field sample and Red Passives more abundant in the group sample when compared to our total sample.

6. Red Misfits overlap with previously identified intermediate populations (e.g. green valley galaxies, S0s) although they show different trends with environment.

We interpret these results as evidence that Red Misfits are a transition population of galaxies between the blue cloud and the red sequence. These galaxies are being gradually quenched; their sSFRs slowly moving off the star-forming main sequence as they continue to grow in stellar mass and their stellar population ages. Red Misfits' agnosticism towards environment indicates that this gradual quenching is primarily driven by secular processes, particularly AGN feedback.

2.6 Acknowledgements

FAE acknowledges support from an Ontario Graduate Scholarship. LCP and IDR acknowledge support from the Natural Sciences and Engineering Research Council of Canada.

Funding for the SDSS and SDSS-II has been provided by the Alfred P. Sloan Foundation, the Participating Institutions, the National Science Foundation, the U.S. Department of Energy, the National Aeronautics and Space Administration, the Japanese Monbukagakusho, the Max Planck Society, and the Higher Education Funding Council for England. The SDSS Web Site is http://www.sdss.org/. The SDSS is managed by the Astrophysical Research Consortium for the Participating Institutions. The Participating Institutions are the American Museum of Natural History, Astrophysical Institute Potsdam, University of Basel, University of Cambridge, Case Western Reserve University, University of Chicago, Drexel University, Fermilab, the Institute for Advanced Study, the Japan Participation Group, Johns Hopkins University, the Joint Institute for Nuclear Astrophysics, the Kavli Institute for Particle As-

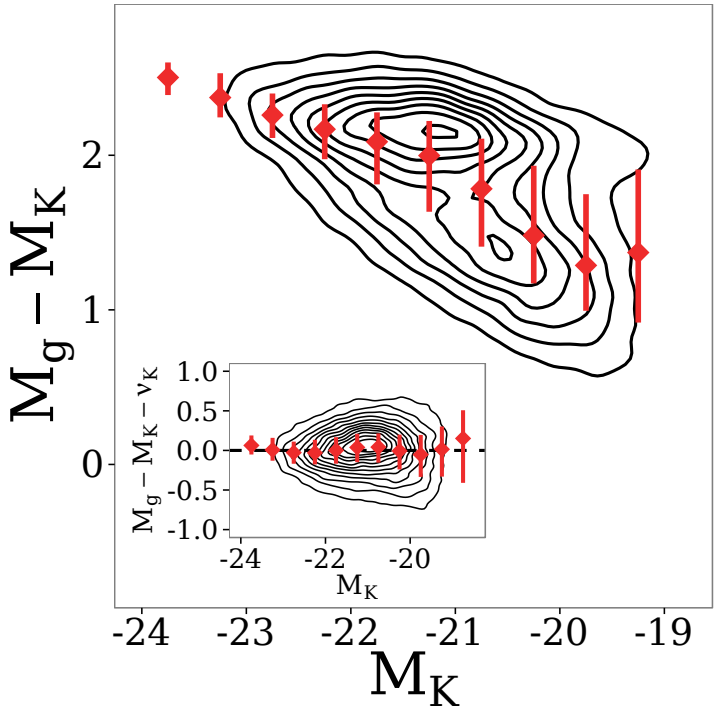

Figure 2.16 M_g - M_K colour of face-on (b/a>0.85) galaxies against M_K. Points show median value and interquartile range in each bin. Inset shows residuals between M_g - M_K colour and Eq. 2.5.

trophysics and Cosmology, the Korean Scientist Group, the Chinese Academy of Sciences (LAMOST), Los Alamos National Laboratory, the Max-Planck-Institute for Astronomy (MPIA), the Max-Planck-Institute for Astrophysics (MPA), New Mexico State University, Ohio State University, University of Pittsburgh, University of Portsmouth, Princeton University, the United States Naval Observatory, and the University of Washington.

2.7 Appendix: Intrinsic Galaxy Colours

The classification of the galaxies in our catalogue into different populations depends in part on their observed M_g-M_r colour, a property known to vary with inclination (e.g. Tully et al., 1998). Intrinsic dust extinction through the disc

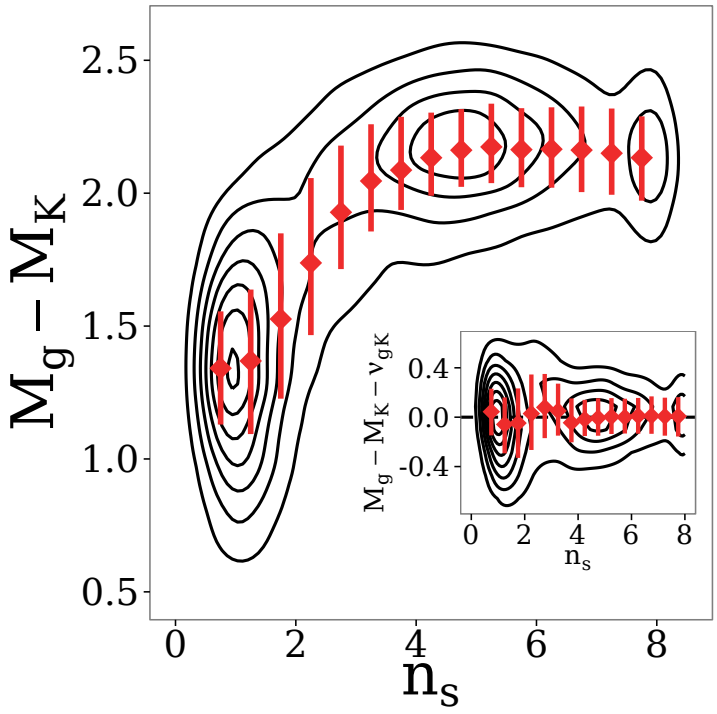

Figure 2.17 M_g - M_K colour of face-on (b/a>0.85) galaxies against Sérsic index. Points show median value and interquartile range in each bin. Inset shows residuals between M_g - M_K colour and Eq. 2.5.

of a galaxy will cause highly-inclined galaxies to appear redder than identical galaxies viewed face-on. It is therefore possible that many galaxies identified as being red in photometric colour are highly-inclined blue galaxies. We correct out the inclination dependence of optical colour to obtain intrinsic colours. Since inclination angles provided by Simard et al. (2011) are reliable only for disc-dominated galaxies, we opt to use axis ratios provided by Simard et al. (2011) as our inclination proxy to calculate intrinsic colours for our full sample.

It is important to note that a galaxy's colour does not depend on inclination alone, nor is colour the only property to vary with inclination. Any colour dependence on inclination may be primarily due to dependence on a separate property that is also varying with inclination. To isolate the attenuating effect of inclination it is crucial that we compare galaxies at different inclinations that are as intrinsically identical as possible. This is typically done by matching samples by a property known not to vary with inclination, such as K band magnitude (Bell & de Jong, 2001).

Since inclination-dependent attenuation affects both the g and r bands, comparing $g - r$ colours of galaxies at different inclinations will couple these effects and may lead to complicated dependencies. To disentangle the effects of attenuation on M_g and M_r we find the correlation between observed M_g - M_K and M_r - M_K colours and inclination. Assuming inclination-induced attenuation in the K band is negligible (Bell & de Jong, 2001), the attenuation in the g or r band is then whatever correction is needed to remove the $g/r - K$ colour dependence on inclination. The g and r attenuations can then be used to correct each galaxy's observed M_g-M_r colour to what it would be if the galaxy were observed face-on. The advantage to this approach is that no prior knowledge or assumptions about dust properties or stellar populations are required to perform the correction.

This general method of measuring inclination-induced attenuation or correcting colours has been applied by several groups (Tully et al., 1998; Masters et al., 2003; Shao et al., 2007; Padilla & Strauss, 2008, e.g.) but we follow closely the specific methodology of Maller et al. (2009), who identify samples of galaxies that are intrinsically the same using galaxies closely matched in both M_K and Sérsic Index (n_s). Thus the attenuation in the g and r bands will be functions not only of inclination but also of M_K and n_s.

To correct the *g/r-K* colours of inclined galaxies to their face-on colours we must first determine what these face-on colours actually are. Fig. 2.16 and Fig. 2.17 show the M_g - M_K colours of face-on (b/a>0.85) galaxies against M_K and n_s. We see that the median colour of face-on galaxies is linear in M_K. The dependence of colour on n_s appears more complicated. We find that the median face-on colour is linear in n_s for $n_s<4$ and constant in n_s for $n_s \geq 4$. Furthermore, we find the dependence of M_g - M_K on M_K differs between $n_s<4$ and $n_s \geq 4$ galaxies. We do not show similar analysis for M_r - M_K colours but the trends are the same. We fit the median galaxy colour by a function of the form:

$$\nu_{g/r-K} = \nu_{g/r,0} + \nu_{g/r,K}(M_K + 20) + \nu_{g/r,n}(n_s) \qquad \text{for } n_s < 4 \qquad (2.5a)$$

$$\nu_{g/r-K} = \nu'_{g/r,0} + \nu'_{g/r,K}(M_K + 20) \qquad \text{for } n_s \geq 4 \qquad (2.5b)$$

where $\nu_{g/r-K}$ is the median $g-K$ or $r-K$ colour of a face-on galaxy and $\nu_{g/r,0}$, $\nu_{g/r,K}$ and $\nu_{g/r,n}$ are fitting parameters. Residuals to this fit are shown in insets in Fig. 2.16 and Fig. 2.17, demonstrating that our model fits the galaxy colours well.

With a successful model for face-on $g-K$ and $r-K$ galaxy colours, we can examine how axis ratio affects the observed colours of samples of intrinsically identical galaxies. Fig 2.18 shows the residual between the M_g-M_K colour and ν_{g-K} as a function of axis ratio binned into quartiles of M_K and n_s. With varying strength across parameter space, the trend remains the same: highly-

inclined galaxies are systematically redder than identical face-on ones. Despite significant scatter, the trend is linear in log(b/a). We therefore express the attenuation as

$$A_{g/r-K} = \gamma_{g/r} \log(b/a) \ , \tag{2.6}$$

where γ_g and γ_r are slopes of a linear fit of $M_{g/r} - M_K - \nu_{g/r-K}$ to $\log(b/a)$. Values for γ_g are shown in Fig. 2.18 for each bin of M_K and n_s. We notice that γ_g depends on both M_K and n_s. We obtain our best fit when we express γ_g and γ_r as

$$\gamma_\lambda = \gamma_{\lambda,0} + \gamma_{\lambda,K}(M_K + 20) + \gamma_{\lambda,n} n_s \qquad \text{for } \mathrm{n}_s < 3 \tag{2.7a}$$

$$\gamma_\lambda = \gamma'_{\lambda,0} + \gamma'_{\lambda,K}(M_K + 20) \qquad \text{for } \mathrm{n}_s \geq 3 \tag{2.7b}$$

We find the best-fitting parameters for this model using a Monte Carlo Markov Chain to minimize

$$\chi^2 = \sum \left[\frac{M_{g/r} - M_K - \nu_{g/r-K} - A_{g/r-K}}{\sigma_{g/r-K}} \right]^2 \ , \tag{2.8}$$

where $A_{g/r-K}$ is given by Eq. 2.6 and 2.7 and $\sigma_{g/r-K}$ is the variance of $M_g/r - M_K - \nu_{g/r-K}$. We see no evidence of $\sigma_{\lambda-K}$ varying across parameter space so it is taken as a constant for both the n_s <3 and n_s ≥3 samples.

With a model for the attenuation and best-fit parameters for that model, Fig. 2.19 shows the data from Fig. 2.18 with A_{g-K} subtracted. We see that the correction is successful at removing any trend between galaxy colour and axis ratio matching the M_g - M_K colours of edge-on galaxies to face-on ones. The correction is equally successful with M_r - M_K colours.

With an A_{g-K} and A_{r-K} that successfully reverse the attenuating effect of inclination, we can finally obtain intrinsic $g - r$ colours for each galaxy:

$$(M_g - M_r)^i = (M_g^0 - A_{g-K}) - (M_r^0 - A_{r-K}) \ . \tag{2.9}$$

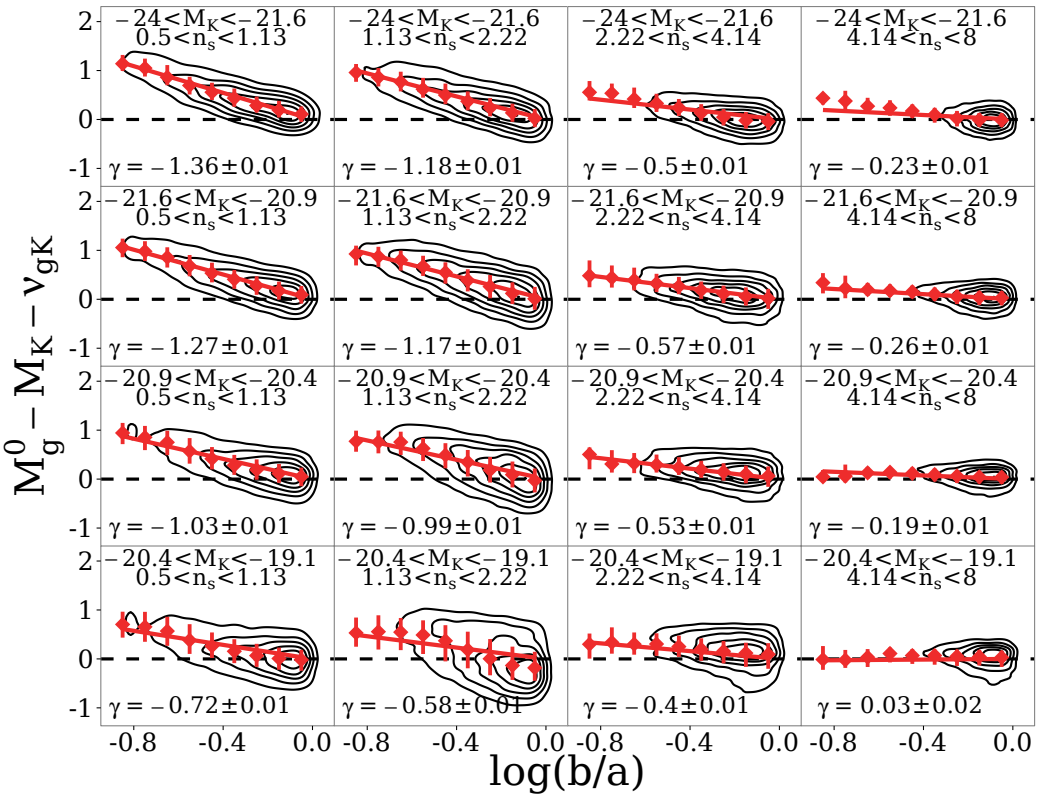

Figure 2.18 Difference between M_g - M_K colour and the expected M_g - M_K colour of a face-on galaxy with the same M_K and n_s as a function of axis ratio. Results are binned by the quartiles of M_K and n_s. Points show median values and interquartile ranges in log(b/a) bins. The best-fit slopes γ for each panel are shown.

Defining our populations using the local minima of the colour and sSFR distributions as described in 2.2.5, 46818 galaxies are classified as Red Misfits when we use uncorrected $(M_g - M_r)^0$. When using corrected $(M_g - M_r)^i$, the local minimum shifts bluewards by 0.02 mags and the Red Misfit population drops by 35 per cent, the rest being re-classified as Blue Actives. This correction is successful at mitigating the contamination of the Red Misfit population by highly-inclined Blue Actives.

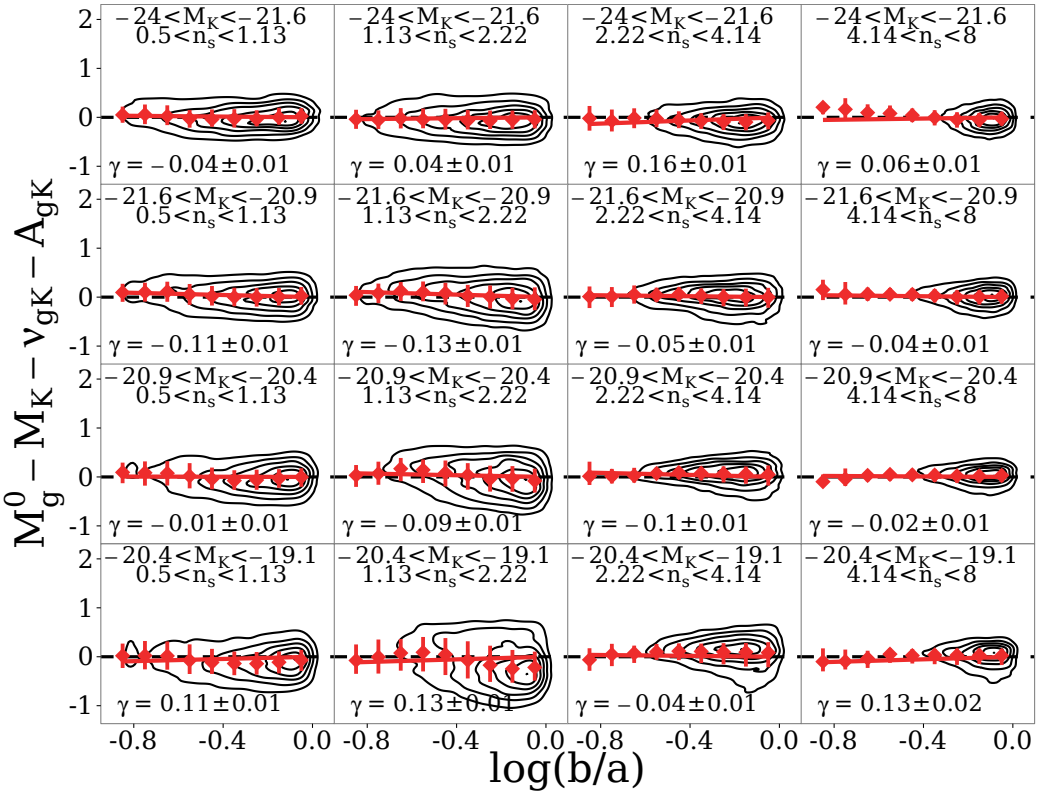

Figure 2.19 Difference between *corrected* M_g - M_K colour and the expected M_g - M_K colour of a face-on galaxy with the same M_K and n_s as a function of axis ratio. Results are binned by the quartiles of M_K and n_s. Points show median values and interquartile ranges in log(b/a) bins.

Bibliography

Abazajian, K. N., Adelman-McCarthy, J. K., Agüeros, M. A., Allam, S. S., Prieto, C. A., An, D., Anderson, K. S. J., Anderson, S. F., Annis, J., Bahcall, N. A., Bailer-Jones, C. A. L., Barentine, J. C., Bassett, B. A., Becker, A. C., Beers, T. C., Bell, E. F., Belokurov, V., Berlind, A. A., Berman, E. F., Bernardi, M., Bickerton, S. J., Bizyaev, D., Blakeslee, J. P., Blanton, M. R., Bochanski, J. J., Boroski, W. N., Brewington, H. J., Brinchmann, J., Brinkmann, J., Brunner, R. J., Budavári, T., Carey, L. N., Carliles, S., Carr, M. A., Castander, F. J., Cinabro, D., Connolly, A. J., Csabai, I., Cunha, C. E., Czarapata, P. C., Davenport, J. R. A., de Haas, E., Dilday, B., Doi, M., Eisenstein, D. J., Evans, M. L., Evans, N. W., Fan, X., Friedman, S. D., Frieman, J. A., Fukugita, M., Gänsicke, B. T., Gates, E., Gillespie, B., Gilmore, G., Gonzalez, B., Gonzalez, C. F., Grebel, E. K., Gunn, J. E., Györy, Z., Hall, P. B., Harding, P., Harris, F. H., Harvanek, M., Hawley, S. L., Hayes, J. J. E., Heckman, T. M., Hendry, J. S., Hennessy, G. S., Hindsley, R. B., Hoblitt, J., Hogan, C. J., Hogg, D. W., Holtzman, J. A., Hyde, J. B., ichi Ichikawa, S., Ichikawa, T., Im, M., Ivezić, Ž., Jester, S., Jiang, L., Johnson, J. A., Jorgensen, A. M., Jurić, M., Kent, S. M., Kessler, R., Kleinman, S. J., Knapp, G. R., Konishi, K., Kron, R. G., Krzesinski, J., Kuropatkin, N., Lampeitl, H., Lebedeva, S., Lee, M. G., Lee, Y. S., Leger, R. F., Lépine, S., Li, N., Lima, M., Lin, H., Long, D. C., Loomis, C. P., Loveday, J., Lupton, R. H., Magnier, E., Malanushenko, O., Malanushenko, V., Mandelbaum, R., Margon, B., Marriner, J. P., Martínez-Delgado, D., Matsubara, T., McGehee, P. M., McKay, T. A., Meiksin, A., Morrison, H. L., Mullally, F., Munn, J. A., Murphy, T., Nash, T., Nebot, A., Neilsen, E. H., Newberg, H. J., Newman, P. R., Nichol, R. C., Nicinski, T., Nieto-Santisteban, M., Nitta,

A., Okamura, S., Oravetz, D. J., Ostriker, J. P., Owen, R., Padmanabhan, N., Pan, K., Park, C., Pauls, G., Peoples, J., Percival, W. J., Pier, J. R., Pope, A. C., Pourbaix, D., Price, P. A., Purger, N., Quinn, T., Raddick, M. J., Fiorentin, P. R., Richards, G. T., Richmond, M. W., Riess, A. G., Rix, H.-W., Rockosi, C. M., Sako, M., Schlegel, D. J., Schneider, D. P., Scholz, R.-D., Schreiber, M. R., Schwope, A. D., Seljak, U., Sesar, B., Sheldon, E., Shimasaku, K., Sibley, V. C., Simmons, A. E., Sivarani, T., Smith, J. A., Smith, M. C., Smolčić, V., Snedden, S. A., Stebbins, A., Steinmetz, M., Stoughton, C., Strauss, M. A., SubbaRao, M., Suto, Y., Szalay, A. S., Szapudi, I., Szkody, P., Tanaka, M., Tegmark, M., Teodoro, L. F. A., Thakar, A. R., Tremonti, C. A., Tucker, D. L., Uomoto, A., Berk, D. E. V., Vandenberg, J., Vidrih, S., Vogeley, M. S., Voges, W., Vogt, N. P., Wadadekar, Y., Watters, S., Weinberg, D. H., West, A. A., White, S. D. M., Wilhite, B. C., Wonders, A. C., Yanny, B., Yocum, D. R., York, D. G., Zehavi, I., Zibetti, S., & Zucker, D. B. 2009, ApJS, 182, 543

Amblard, A., Riguccini, L., Temi, P., Im, S., Fanelli, M., & Serra, P. 2014, ApJ, 783, 135

Athanassoula, E. 2005, MNRAS, 358, 1477

Baker, J. G. & Menzel, D. H. 1938, ApJ, 88, 52

Baldry, I. K., Balogh, M. L., Bower, R. G., Glazebrook, K., Nichol, R. C., Bamford, S. P., & Budavari, T. 2006, MNRAS, 373, 469

Baldry, I. K., Glazebrook, K., Brinkmann, J., Ivezić, Ž., Lupton, R. H., Nichol, R. C., & Szalay, A. S. 2004, ApJ, 600, 681

Baldwin, J. A., Phillips, M. M., & Terlevich, R. 1981, PASP, 93, 5

Balogh, M., Bower, R. G., Smail, I., Ziegler, B. L., Davies, R. L., Gaztelu, A., & Fritz, A. 2002, MNRAS, 337, 256

Balogh, M., Eke, V., Miller, C., Lewis, I., Bower, R., Couch, W., Nichol, R., Bland-Hawthorn, J., Baldry, I. K., Baugh, C., Bridges, T., Cannon, R., Cole, S., Colless, M., Collins, C., Cross, N., Dalton, G., Propris, R. D., Driver, S. P., Efstathiou, G., Ellis, R. S., Frenk, C. S., Glazebrook, K., Gomez, P., Gray, A., Hawkins, E., Jackson, C., Lahav, O., Lumsden, S., Maddox, S., Madgwick, D., Norberg, P., Peacock, J. A., Percival, W., Peterson, B. A., Sutherland, W., & Taylor, K. 2004a, MNRAS, 348, 1355

Balogh, M. L., Baldry, I. K., Nichol, R., Miller, C., Bower, R., & Glazebrook, K. 2004b, ApJ, 615, L101

Balogh, M. L., Morris, S. L., Yee, H. K. C., Carlberg, R. G., & Ellingson, E. 1999, ApJ, 527, 54

Balogh, M. L., Navarro, J. F., & Morris, S. L. 2000, ApJ, 540, 113

Bamford, S. P., Nichol, R. C., Baldry, I. K., Land, K., Lintott, C. J., Schawinski, K., Slosar, A., Szalay, A. S., Thomas, D., Torki, M., Andreescu, D., Edmondson, E. M., Miller, C. J., Murray, P., Raddick, M. J., & Vandenberg, J. 2009, MNRAS, 393, 1324

Bell, E. F. & de Jong, R. S. 2001, ApJ, 550, 212

Bell, E. F., van der Wel, A., Papovich, C., Kocevski, D., Lotz, J., McIntosh, D. H., Kartaltepe, J., Faber, S. M., Ferguson, H., Koekemoer, A., Grogin, N., Wuyts, S., Cheung, E., Conselice, C. J., Dekel, A., Dunlop, J. S., Giavalisco, M., Herrington, J., Koo, D. C., McGrath, E. J., de Mello, D., Rix, H.-W., Robaina, A. R., & Williams, C. C. 2012, ApJ, 753, 167

Bell, E. F., Wolf, C., Meisenheimer, K., Rix, H.-W., Borch, A., Dye, S., Kleinheinrich, M., Wisotzki, L., & McIntosh, D. H. 2004, ApJ, 608, 752

Bildfell, C., Hoekstra, H., Babul, A., & Mahdavi, A. 2008, MNRAS, 389, 1637

Blanton, M. R., Brinkmann, J., Csabai, I., Doi, M., Eisenstein, D., Fukugita, M., Gunn, J. E., Hogg, D. W., & Schlegel, D. J. 2003, AJ, 125, 2348

Blanton, M. R., Eisenstein, D., Hogg, D. W., Schlegel, D. J., & Brinkmann, J. 2005a, ApJ, 629, 143

Blanton, M. R. & Roweis, S. 2007, AJ, 133, 734

Blanton, M. R., Schlegel, D. J., Strauss, M. A., Brinkmann, J., Finkbeiner, D., Fukugita, M., Gunn, J. E., Hogg, D. W., Ivezić, Ž., Knapp, G. R., Lupton, R. H., Munn, J. A., Schneider, D. P., Tegmark, M., & Zehavi, I. 2005b, AJ, 129, 2562

Bluck, A. F. L., Mendel, J. T., Ellison, S. L., Moreno, J., Simard, L., Patton, D. R., & Starkenburg, E. 2014, MNRAS, 441, 599

Bower, R. G., Benson, A. J., Malbon, R., Helly, J. C., Frenk, C. S., Baugh, C. M., Cole, S., & Lacey, C. G. 2006, MNRAS, 370, 645

Brand, K., Moustakas, J., Armus, L., Assef, R. J., Brown, M. J. I., Cool, R. R., Desai, V., Dey, A., Floc'h, E. L., Jannuzi, B. T., Kochanek, C. S., Melbourne, J., Papovich, C. J., & Soifer, B. T. 2009, ApJ, 693, 340

Brinchmann, J., Charlot, S., White, S. D. M., Tremonti, C., Kauffmann, G., Heckman, T., & Brinkmann, J. 2004, MNRAS, 351, 1151

Bundy, K., Scarlata, C., Carollo, C. M., Ellis, R. S., Drory, N., Hopkins, P., Salvato, M., Leauthaud, A., Koekemoer, A. M., Murray, N., Ilbert, O., Oesch, P., Ma, C.-P., Capak, P., Pozzetti, L., & Scoville, N. 2010, ApJ, 719, 1969

Calzetti, D., Armus, L., Bohlin, R. C., Kinney, A. L., Koornneef, J., & Storchi-Bergmann, T. 2000, ApJ, 533, 682

Cameron, E. 2011, PASP, 28, 128

Carollo, C. M., Cibinel, A., Lilly, S. J., Miniati, F., Norberg, P., Silverman, J. D., van Gorkom, J., Cameron, E., Finoguenov, A., Peng, Y., Pipino, A., & Rudick, C. S. 2013, ApJ, 776, 71

Cheung, E., Athanassoula, E., Masters, K. L., Nichol, R. C., Bosma, A., Bell, E. F., Faber, S. M., Koo, D. C., Lintott, C., Melvin, T., Schawinski, K., Skibba, R. A., & Willett, K. W. 2013, ApJ, 779, 162

Coia, D., McBreen, B., Metcalfe, L., Biviano, A., Altieri, B., Ott, S., Fort, B., Kneib, J.-P., Mellier, Y., Miville-Deschênes, M.-A., O'Halloran, B., & Sanchez-Fernandez, C. 2005, A&A, 431, 433

Coil, A. L., Newman, J. A., Croton, D., Cooper, M. C., Davis, M., Faber, S. M., Gerke, B. F., Koo, D. C., Padmanabhan, N., Wechsler, R. H., & Weiner, B. J. 2008, ApJ, 672, 153

Cooper, M. C., Newman, J. A., Coil, A. L., Croton, D. J., Gerke, B. F., Yan, R., Davis, M., Faber, S. M., Guhathakurta, P., Koo, D. C., Weiner, B. J., & Willmer, C. N. A. 2007, MNRAS, 376, 1445

Cortese, L. 2012, A&A, 543, A132

Crossett, J. P., Pimbblet, K. A., Stott, J. P., & Jones, D. H. 2014, MNRAS, 437, 2521

Croton, D. J., Springel, V., White, S. D. M., De Lucia, G., Frenk, C. S., Gao, L., Jenkins, A., Kauffmann, G., Navarro, J. F., & Yoshida, N. 2006, MNRAS, 365, 11

Davoodi, P., Pozzi, F., Oliver, S., Polletta, M., Afonso-Luis, A., Farrah, D., Hatziminaoglou, E., Rodighiero, G., Berta, S., Waddington, I., Lonsdale, C., Rowan-Robinson, M., Shupe, D. L., Evans, T., Fang, F., Smith, H. E., & Surace, J. 2006, MNRAS, 371, 1113

Demarco, R., Rosati, P., Lidman, C., Homeier, N. L., Scannapieco, E., Benítez, N., Mainieri, V., Nonino, M., Girardi, M., Stanford, S. A., Tozzi, P., Borgani, S., Silk, J., Squires, G., & Broadhurst, T. J. 2005, A&A, 432, 381

Domínguez, A., Siana, B., Henry, A. L., Scarlata, C., Bedregal, A. G., Malkan, M., Atek, H., Ross, N. R., Colbert, J. W., Teplitz, H. I., Rafelski, M., McCarthy, P., Bunker, A., Hathi, N. P., Dressler, A., Martin, C. L., & Masters, D. 2013, ApJ, 763, 145

Dressler, A. 1980, ApJ, 236, 351

Dressler, A., Oemler, Jr., A., Couch, W. J., Smail, I., Ellis, R. S., Barger, A., Butcher, H., Poggianti, B. M., & Sharples, R. M. 1997, ApJ, 490, 577

Dressler, A., Smail, I., Poggianti, B. M., Butcher, H., Couch, W. J., Ellis, R. S., & Oemler, Jr., A. 1999, ApJS, 122, 51

Dubois, Y., Pichon, C., Welker, C., Le Borgne, D., Devriendt, J., Laigle, C., Codis, S., Pogosyan, D., Arnouts, S., Benabed, K., Bertin, E., Blaizot, J., Bouchet, F., Cardoso, J.-F., Colombi, S., de Lapparent, V., Desjacques, V., Gavazzi, R., Kassin, S., Kimm, T., McCracken, H., Milliard, B., Peirani, S., Prunet, S., Rouberol, S., Silk, J., Slyz, A., Sousbie, T., Teyssier, R., Tresse, L., Treyer, M., Vibert, D., & Volonteri, M. 2014, MNRAS, 444, 1453

Eisenstein, D. J. & Hu, W. 1998, ApJ, 496, 605

Elbaz, D., Daddi, E., Le Borgne, D., Dickinson, M., Alexander, D. M., Chary, R.-R., Starck, J.-L., Brandt, W. N., Kitzbichler, M., MacDonald, E., Nonino, M., Popesso, P., Stern, D., & Vanzella, E. 2007, A&A, 468, 33

Ellison, S. L., Patton, D. R., Simard, L., & McConnachie, A. W. 2008, AJ, 135, 1877

Faber, S. M., Willmer, C. N. A., Wolf, C., Koo, D. C., Weiner, B. J., Newman, J. A., Im, M., Coil, A. L., Conroy, C., Cooper, M. C., Davis, M., Finkbeiner, D. P., Gerke, B. F., Gebhardt, K., Groth, E. J., Guhathakurta, P., Harker, J., Kaiser, N., Kassin, S., Kleinheinrich, M., Konidaris, N. P., Kron, R. G., Lin, L., Luppino, G., Madgwick, D. S., Meisenheimer, K., Noeske, K. G., Phillips, A. C., Sarajedini, V. L., Schiavon, R. P., Simard, L., Szalay, A. S., Vogt, N. P., & Yan, R. 2007, ApJ, 665, 265

Gallazzi, A., Bell, E. F., Wolf, C., Gray, M. E., Papovich, C., Barden, M., Peng, C. Y., Meisenheimer, K., Heymans, C., van Kampen, E., Gilmour, R., Balogh, M., McIntosh, D. H., Bacon, D., Barazza, F. D., Böhm, A., Caldwell, J. A. R., Häußler, B., Jahnke, K., Jogee, S., Lane, K., Robaina, A. R., Sanchez, S. F., Taylor, A., Wisotzki, L., & Zheng, X. 2008, ApJ, 690, 1883

Gómez, P. L., Nichol, R. C., Miller, C. J., Balogh, M. L., Goto, T., Zabludoff, A. I., Romer, A. K., Bernardi, M., Sheth, R., Hopkins, A. M., Castander, F. J., Connolly, A. J., Schneider, D. P., Brinkmann, J., Lamb, D. Q., SubbaRao, M., & York, D. G. 2003, ApJ, 584, 210

Goto, T. 2006, MNRAS, 369, 1765

Goto, T., Okamura, S., Sekiguchi, M., Bernardi, M., Brinkmann, J., Gómez, P. L., Harvanek, M., Kleinman, S. J., Krzesinski, J., Long, D., Loveday, J., Miller, C. J., Neilsen, E. H., Newman, P. R., Nitta, A., Sheth, R. K., Snedden, S. A., & Yamauchi, C. 2003, PASJ, 55, 757

Granato, G. L., Zotti, G. D., Silva, L., Bressan, A., & Danese, L. 2004, ApJ, 600, 580

Gunn, J. E. & Gott, J. R. 1972, ApJ, 176, 1

Haas, M. R., Schaye, J., & Jeeson-Daniel, A. 2012, MNRAS, 419, 2133

Haines, C. P., Gargiulo, A., & Merluzzi, P. 2008, MNRAS, 385, 1201

Hammer, F., Flores, H., Lilly, S. J., Crampton, D., Le Fèvre, O., Rola, C., Mallen-Ornelas, G., Schade, D., & Tresse, L. 1997, ApJ, 481, 49

Häring, N. & Rix, H.-W. 2004, ApJ, 604, L89

Hogg, D. W. 1999, ArXiv Astrophysics e-prints

Hogg, D. W., Blanton, M. R., Eisenstein, D. J., Gunn, J. E., Schlegel, D. J., Zehavi, I., Bahcall, N. A., Brinkmann, J., Csabai, I., Schneider, D. P., Weinberg, D. H., & York, D. G. 2003, ApJ, 585, L5

Hopkins, P. F., Hernquist, L., Cox, T. J., Di Matteo, T., Robertson, B., & Springel, V. 2006, ApJS, 163, 1

Hopkins, P. F., Kereš, D., Oñorbe, J., Faucher-Giguère, C.-A., Quataert, E., Murray, N., & Bullock, J. S. 2014, MNRAS, 445, 581

Hou, A., Parker, L. C., & Harris, W. E. 2014, MNRAS, 442, 406

Huertas-Company, M., Aguerri, J. A. L., Tresse, L., Bolzonella, M., Koekemoer, A. M., & Maier, C. 2010, A&A, 515, A3

Jester, S., Schneider, D. P., Richards, G. T., Green, R. F., Schmidt, M., Hall, P. B., Strauss, M. A., Vanden Berk, D. E., Stoughton, C., Gunn, J. E., Brinkmann, J., Kent, S. M., Smith, J. A., Tucker, D. L., & Yanny, B. 2005, AJ, 130, 873

Kauffmann, G., Heckman, T. M., Budavári, T., Charlot, S., Hoopes, C. G., Martin, D. C., Seibert, M., Barlow, T. A., Bianchi, L., Conrow, T., Donas, J., Forster, K., Friedman, P. G., Lee, Y.-W., Madore, B. F., Milliard, B., Morrissey, P. F., Neff, S. G., Rich, R. M., Schiminovich, D., Small, T., Szalay, A. S., Wyder, T. K., & Yi, S. K. 2007, ApJS, 173, 357

Kauffmann, G., Heckman, T. M., Tremonti, C., Brinchmann, J., Charlot, S., White, S. D. M., Ridgway, S. E., Brinkmann, J., Fukugita, M., Hall, P. B., Ivezić, Ž., Richards, G. T., & Schneider, D. P. 2003a, MNRAS, 346, 1055

Kauffmann, G., Heckman, T. M., White, D. M. S., Charlot, S., Tremonti, C., Brinchmann, J., Bruzual, G., Peng, E. W., Seibert, M., Bernardi, M., Blanton, M., Brinkmann, J., Castander, F., Csábai, I., Fukugita, M., Ivezic, Z., Munn, J. A., Nichol, R. C., Padmanabhan, N., Thakar, A. R., Weinberg, D. H., & York, D. 2003b, MNRAS, 341, 33

Kauffmann, G., Heckman, T. M., White, S. D. M., Charlot, S., Tremonti, C., Peng, E. W., Seibert, M., Brinkmann, J., Nichol, R. C., SubbaRao, M., & York, D. 2003c, MNRAS, 341, 54

Kauffmann, G., White, S. D. M., Heckman, T. M., Ménard, B., Brinchmann, J., Charlot, S., Tremonti, C., & Brinkmann, J. 2004, MNRAS, 353, 713

Kawata, D. & Mulchaey, J. S. 2007, ApJ, 672, L103

Keller, B. W., Wadsley, J., & Couchman, H. M. P. 2016, MNRAS, 463, 1431

Kewley, L. J., Dopita, M. A., Sutherland, R. S., Heisler, C. A., & Trevena, J. 2001, ApJ, 556, 121

Knapen, J. H., Beckman, J. E., Heller, C. H., Shlosman, I., & de Jong, R. S. 1995, ApJ, 454, 623

Knobel, C., Lilly, S. J., Kovač, K., Peng, Y., Bschorr, T. J., Carollo, C. M., Contini, T., Kneib, J.-P., Le Fevre, O., Mainieri, V., Renzini, A., Scodeggio, M., Zamorani, G., Bardelli, S., Bolzonella, M., Bongiorno, A., Caputi, K., Cucciati, O., de la Torre, S., de Ravel, L., Franzetti, P., Garilli, B., Iovino, A., Kampczyk, P., Lamareille, F., Le Borgne, J.-F., Le Brun, V., Maier, C., Mignoli, M., Pello, R., Perez Montero, E., Presotto, V., Silverman, J., Tanaka, M., Tasca, L., Tresse, L., Vergani, D., Zucca, E., Barnes,

L., Bordoloi, R., Cappi, A., Cimatti, A., Coppa, G., Koekemoer, A. M., López-Sanjuan, C., McCracken, H. J., Moresco, M., Nair, P., Pozzetti, L., & Welikala, N. 2013, ApJ, 769, 24

Kodama, T., Smail, I., Nakata, F., Okamura, S., & Bower, R. G. 2001, ApJ, 562, L9

Kormendy, J. & Kennicutt, R. C. 2004, Annual Review of Astronomy and Astrophysics, 42, 603

Koyama, Y., Kodama, T., Nakata, F., Shimasaku, K., & Okamura, S. 2011, ApJ, 734, 66

Koyama, Y., Kodama, T., Shimasaku, K., Okamura, S., Tanaka, M., Lee, H. M., Im, M., Matsuhara, H., Takagi, T., Wada, T., & Oyabu, S. 2008, MNRAS, 391, 1758

Lara-López, M. A., Hopkins, A. M., López-Sánchez, A. R., Brough, S., Gunawardhana, M. L. P., Colless, M., Robotham, A. S. G., Bauer, A. E., Bland-Hawthorn, J., Cluver, M., Driver, S., Foster, C., Kelvin, L. S., Liske, J., Loveday, J., Owers, M. S., Ponman, T. J., Sharp, R. G., Steele, O., Taylor, E. N., & Thomas, D. 2013, MNRAS, 434, 451

Larson, R. B., Tinsley, B. M., & Caldwell, C. N. 1980, ApJ, 237, 692

Lewis, I., Balogh, M., Propris, R. D., Couch, W., Bower, R., Offer, A., Bland-Hawthorn, J., Baldry, I. K., Baugh, C., Bridges, T., Cannon, R., Cole, S., Colless, M., Collins, C., Cross, N., Dalton, G., Driver, S. P., Efstathiou, G., Ellis, R. S., Frenk, C. S., Glazebrook, K., Hawkins, E., Jackson, C., Lahav, O., Lumsden, S., Maddox, S., Madgwick, D., Norberg, P., Peacock, J. A., Percival, W., Peterson, B. A., Sutherland, W., & Taylor, K. 2002, MNRAS, 334, 673

Magorrian, J., Tremaine, S., Richstone, D., Bender, R., Bower, G., Dressler, A., Faber, S. M., Gebhardt, K., Green, R., Grillmair, C., Kormendy, J., & Lauer, T. 1998, AJ, 115, 2285

Mahajan, S. & Raychaudhury, S. 2009, MNRAS, 400, 687

Makino, J. & Hut, P. 1997, ApJ, 481, 83

Maller, A. H., Berlind, A. A., Blanton, M. R., & Hogg, D. W. 2009, ApJ, 691, 394

Malmquist, K. G. 1925, Meddelanden fran Lunds Astronomiska Observatorium Serie I, 106, 1

Martig, M., Bournaud, F., Teyssier, R., & Dekel, A. 2009, ApJ, 707, 250

Martin, P. & Friedli, D. 1997, A&A, 326, 449

Masters, K. L., Giovanelli, R., & Haynes, M. P. 2003, AJ, 126, 158

Masters, K. L., Mosleh, M., Romer, A. K., Nichol, R. C., Bamford, S. P., Schawinski, K., Lintott, C. J., Andreescu, D., Campbell, H. C., Crowcroft, B., Doyle, I., Edmondson, E. M., Murray, P., Raddick, M. J., Slosar, A., Szalay, A. S., & Vandenberg, J. 2010, MNRAS, 405, 783

McGee, S. L., Balogh, M. L., Wilman, D. J., Bower, R. G., Mulchaey, J. S., Parker, L. C., & Oemler, A. 2011, MNRAS, 413, 996

Mendez, A. J., Coil, A. L., Lotz, J., Salim, S., Moustakas, J., & Simard, L. 2011, ApJ, 736, 110

Menzel, D. H. & Baker, J. G. 1937, ApJ, 86, 70

Moore, B., Katz, N., Lake, G., Dressler, A., & Oemler, A. 1996, Nature, 379, 613

Moore, B., Lake, G., & Katz, N. 1998, ApJ, 495, 139

Moran, S. M., Ellis, R. S., Treu, T., Smith, G. P., Rich, R. M., & Smail, I. 2007, ApJ, 671, 1503

Nandra, K., Georgakakis, A., Willmer, C. N. A., Cooper, M. C., Croton, D. J., Davis, M., Faber, S. M., Koo, D. C., Laird, E. S., & Newman, J. A. 2007, ApJ, 660, L11

Noeske, K. G., Faber, S. M., Weiner, B. J., Koo, D. C., Primack, J. R., Dekel, A., Papovich, C., Conselice, C. J., Le Floc'h, E., Rieke, G. H., Coil, A. L., Lotz, J. M., Somerville, R. S., & Bundy, K. 2007a, ApJ, 660, L47

Noeske, K. G., Weiner, B. J., Faber, S. M., Papovich, C., Koo, D. C., Somerville, R. S., Bundy, K., Conselice, C. J., Newman, J. A., Schiminovich, D., Le Floc'h, E., Coil, A. L., Rieke, G. H., Lotz, J. M., Primack, J. R., Barmby, P., Cooper, M. C., Davis, M., Ellis, R. S., Fazio, G. G., Guhathakurta, P., Huang, J., Kassin, S. A., Martin, D. C., Phillips, A. C., Rich, R. M., Small, T. A., Willmer, C. N. A., & Wilson, G. 2007b, ApJ, 660, L43

Oemler, A. 1974, ApJ, 194, 1

Osterbrock, D. E. 1989, Astrophysics of gaseous nebulae and active galactic nuclei

Osterbrock, D. E. & Ferland, G. J. 2006, Astrophysics of gaseous nebulae and active galactic nuclei

Padilla, N. D. & Strauss, M. A. 2008, MNRAS, 388, 1321

Peng, Y., Lilly, S. J., Kovač, K., Bolzonella, M., Pozzetti, L., Renzini, A., Zamorani, G., Ilbert, O., Knobel, C., Iovino, A., Maier, C., Cucciati, O., Tasca, L., Carollo, C. M., Silverman, J., Kampczyk, P., de Ravel, L., Sanders,

D., Scoville, N., Contini, T., Mainieri, V., Scodeggio, M., Kneib, J.-P., Fèvre, O. L., Bardelli, S., Bongiorno, A., Caputi, K., Coppa, G., de la Torre, S., Franzetti, P., Garilli, B., Lamareille, F., Borgne, J.-F. L., Brun, V. L., Mignoli, M., Montero, E. P., Pello, R., Ricciardelli, E., Tanaka, M., Tresse, L., Vergani, D., Welikala, N., Zucca, E., Oesch, P., Abbas, U., Barnes, L., Bordoloi, R., Bottini, D., Cappi, A., Cassata, P., Cimatti, A., Fumana, M., Hasinger, G., Koekemoer, A., Leauthaud, A., Maccagni, D., Marinoni, C., McCracken, H., Memeo, P., Meneux, B., Nair, P., Porciani, C., Presotto, V., & Scaramella, R. 2010, ApJ, 721, 193

Peng, Y., Lilly, S. J., Renzini, A., & Carollo, M. 2012, ApJ, 757, 4

Poggianti, B. M., Bridges, T. J., Komiyama, Y., Yagi, M., Carter, D., Mobasher, B., Okamura, S., & Kashikawa, N. 2004, ApJ, 601, 197

Poggianti, B. M., Desai, V., Finn, R., Bamford, S., De Lucia, G., Varela, J., Aragón-Salamanca, A., Halliday, C., Noll, S., Saglia, R., Zaritsky, D., Best, P., Clowe, D., Milvang-Jensen, B., Jablonka, P., Pelló, R., Rudnick, G., Simard, L., von der Linden, A., & White, S. 2008, ApJ, 684, 888

Poggianti, B. M., Smail, I., Dressler, A., Couch, W. J., Barger, A. J., Butcher, H., Ellis, R. S., & Oemler, Jr., A. 1999, ApJ, 518, 576

Popesso, P., Biviano, A., Romaniello, M., & Böhringer, H. 2007, A&A, 461, 411

Postman, M. & Geller, M. J. 1984, ApJ, 281, 95

Reichard, T. A., Heckman, T. M., Rudnick, G., Brinchmann, J., Kauffmann, G., & Wild, V. 2009, ApJ, 691, 1005

Roberts, I. D. & Parker, L. C. 2017, MNRAS, 467, 3268

Roberts, M. S. & Haynes, M. P. 1994, ARA&A, 32, 115

Saintonge, A., Tran, K.-V. H., & Holden, B. P. 2008, ApJ, 685, L113

Salim, S., Fang, J. J., Rich, R. M., Faber, S. M., & Thilker, D. A. 2012, ApJ, 755, 105

Salim, S., Rich, R. M., Charlot, S., Brinchmann, J., Johnson, B. D., Schiminovich, D., Seibert, M., Mallery, R., Heckman, T. M., Forster, K., Friedman, P. G., Martin, D. C., Morrissey, P., Neff, S. G., Small, T., Wyder, T. K., Bianchi, L., Donas, J., Lee, Y.-W., Madore, B. F., Milliard, B., Szalay, A. S., Welsh, B. Y., & Yi, S. K. 2007, ApJS, 173, 267

Schaefer, A. L., Croom, S. M., Allen, J. T., Brough, S., Medling, A. M., Ho, I.-T., Scott, N., Richards, S. N., Pracy, M. B., Gunawardhana, M. L. P., Norberg, P., Alpaslan, M., Bauer, A. E., Bekki, K., Bland-Hawthorn, J., Bloom, J. V., Bryant, J. J., Couch, W. J., Driver, S. P., Fogarty, L. M. R., Foster, C., Goldstein, G., Green, A. W., Hopkins, A. M., Konstantopoulos, I. S., Lawrence, J. S., López-Sánchez, A. R., Lorente, N. P. F., Owers, M. S., Sharp, R., Sweet, S. M., Taylor, E. N., van de Sande, J., Walcher, C. J., & Wong, O. I. 2017, MNRAS, 464, 121

Schawinski, K., Lintott, C., Thomas, D., Sarzi, M., Andreescu, D., Bamford, S. P., Kaviraj, S., Khochfar, S., Land, K., Murray, P., Nichol, R. C., Raddick, M. J., Slosar, A., Szalay, A., Vandenberg, J., & Yi, S. K. 2009, MNRAS, 396, 818

Schawinski, K., Thomas, D., Sarzi, M., Maraston, C., Kaviraj, S., Joo, S.-J., Yi, S. K., & Silk, J. 2007, MNRAS, 382, 1415

Schawinski, K., Urry, C. M., Simmons, B. D., Fortson, L., Kaviraj, S., Keel, W. C., Lintott, C. J., Masters, K. L., Nichol, R. C., Sarzi, M., Skibba, R., Treister, E., Willett, K. W., Wong, O. I., & Yi, S. K. 2014, MNRAS, 440, 889

Schlegel, D. J., Finkbeiner, D. P., & Davis, M. 1998, ApJ, 500, 525

Shao, Z., Xiao, Q., Shen, S., Mo, H. J., Xia, X., & Deng, Z. 2007, ApJ, 659, 1159

Sheth, K., Vogel, S. N., Regan, M. W., Thornley, M. D., & Teuben, P. J. 2005, ApJ, 632, 217

Sijacki, D., Vogelsberger, M., Genel, S., Springel, V., Torrey, P., Snyder, G. F., Nelson, D., & Hernquist, L. 2015, MNRAS, 452, 575

Silverman, J. D., Mainieri, V., Lehmer, B. D., Alexander, D. M., Bauer, F. E., Bergeron, J., Brandt, W. N., Gilli, R., Hasinger, G., Schneider, D. P., Tozzi, P., Vignali, C., Koekemoer, A. M., Miyaji, T., Popesso, P., Rosati, P., & Szokoly, G. 2008, ApJ, 675, 1025

Simard, L., Mendel, J. T., Patton, D. R., Ellison, S. L., & McConnachie, A. W. 2011, ApJS, 196, 11

Simard, L., Willmer, C. N. A., Vogt, N. P., Sarajedini, V. L., Phillips, A. C., Weiner, B. J., Koo, D. C., Im, M., Illingworth, G. D., & Faber, S. M. 2002, ApJS, 142, 1

Simien, F. & de Vaucouleurs, G. 1986, ApJ, 302, 564

Skibba, R. A. 2009, MNRAS, 392, 1467

Springel, V., Di Matteo, T., & Hernquist, L. 2005, MNRAS, 361, 776

Stasińska, G., Vale Asari, N., Cid Fernandes, R., Gomes, J. M., Schlickmann, M., Mateus, A., Schoenell, W., Sodré, Jr., L., & Seagal Collaboration. 2008, MNRAS, 391, L29

Stinson, G. S., Brook, C., Macciò, A. V., Wadsley, J., Quinn, T. R., & Couchman, H. M. P. 2013, MNRAS, 428, 129

Strateva, I., Ivezić, Ž., Knapp, G. R., Narayanan, V. K., Strauss, M. A., Gunn, J. E., Lupton, R. H., Schlegel, D., Bahcall, N. A., Brinkmann, J., Brunner, R. J., Budavári, T., Csabai, I., Castander, F. J., Doi, M., Fukugita, M., Győry, Z., Hamabe, M., Hennessy, G., Ichikawa, T., Kunszt, P. Z., Lamb, D. Q., McKay, T. A., Okamura, S., Racusin, J., Sekiguchi, M., Schneider, D. P., Shimasaku, K., & York, D. 2001, AJ, 122, 1861

Tinker, J. L. & Chen, H.-W. 2008, ApJ, 679, 1218

Tojeiro, R., Masters, K. L., Richards, J., Percival, W. J., Bamford, S. P., Maraston, C., Nichol, R. C., Skibba, R., & Thomas, D. 2013, MNRAS, 432, 359

Toomre, A. & Toomre, J. 1972, ApJ, 178, 623

Tremonti, C. A., Heckman, T. M., Kauffmann, G., Brinchmann, J., Charlot, S., White, S. D. M., Seibert, M., Peng, E. W., Schlegel, D. J., Uomoto, A., Fukugita, M., & Brinkmann, J. 2004, ApJ, 613, 898

Tully, R. B., Pierce, M. J., Huang, J.-S., Saunders, W., Verheijen, M. A. W., & Witchalls, P. L. 1998, AJ, 115, 2264

van den Bergh, S. 1976, ApJ, 206, 883

—. 2009, ApJ, 702, 1502

van den Bosch, F. C., Aquino, D., Yang, X., Mo, H. J., Pasquali, A., McIntosh, D. H., Weinmann, S. M., & Kang, X. 2008, MNRAS, 387, 79

van der Wel, A. 2008, ApJ, 675, L13

Verdugo, M., Ziegler, B. L., & Gerken, B. 2008, A&A, 486, 9

Warren, M. S., Abazajian, K., Holz, D. E., & Teodoro, L. 2006, ApJ, 646, 881

Weinmann, S. M., van den Bosch, F. C., Yang, X., & Mo, H. J. 2006, MNRAS, 366, 2

Wetzel, A. R., Tinker, J. L., & Conroy, C. 2012, MNRAS, 424, 232

Wijesinghe, D. B., Hopkins, A. M., Brough, S., Taylor, E. N., Norberg, P., Bauer, A., Brown, M. J. I., Cameron, E., Conselice, C. J., Croom, S., Driver, S., Grootes, M. W., Jones, D. H., Kelvin, L., Loveday, J., Pimbblet, K. A., Popescu, C. C., Prescott, M., Sharp, R., Baldry, I., Sadler, E. M., Liske, J., Robotham, A. S. G., Bamford, S., Bland-Hawthorn, J., Gunawardhana, M., Meyer, M., Parkinson, H., Drinkwater, M. J., Peacock, J., & Tuffs, R. 2012, MNRAS, 423, 3679

Wilman, D. J. & Erwin, P. 2012, ApJ, 746, 160

Wilman, D. J., Oemler, Jr., A., Mulchaey, J. S., McGee, S. L., Balogh, M. L., & Bower, R. G. 2009, ApJ, 692, 298

Wolf, C., Aragón-Salamanca, A., Balogh, M., Barden, M., Bell, E. F., Gray, M. E., Peng, C. Y., Bacon, D., Barazza, F. D., Böhm, A., Caldwell, J. A. R., Gallazzi, A., Häußler, B., Heymans, C., Jahnke, K., Jogee, S., van Kampen, E., Lane, K., McIntosh, D. H., Meisenheimer, K., Papovich, C., Sánchez, S. F., Taylor, A., Wisotzki, L., & Zheng, X. 2009, MNRAS, 393, 1302

Wolf, C., Gray, M. E., & Meisenheimer, K. 2005, Astronomy and Astrophysics, 443, 435

Woo, J., Dekel, A., Faber, S. M., Noeske, K., Koo, D. C., Gerke, B. F., Cooper, M. C., Salim, S., Dutton, A. A., Newman, J., Weiner, B. J., Bundy, K., Willmer, C. N. A., Davis, M., & Yan, R. 2013, MNRAS, 428, 3306

Wyder, T. K., Martin, D. C., Schiminovich, D., Seibert, M., Budavári, T., Treyer, M. A., Barlow, T. A., Forster, K., Friedman, P. G., Morrissey, P.,

Neff, S. G., Small, T., Bianchi, L., Donas, J., Heckman, T. M., Lee, Y.-W., Madore, B. F., Milliard, B., Rich, R. M., Szalay, A. S., Welsh, B. Y., & Yi, S. K. 2007, ApJS, 173, 293

Xiao, T., Wang, T., Wang, H., Zhou, H., Lu, H., & Dong, X. 2012, MNRAS, 421, 486

Yang, X., Mo, H. J., van den Bosch, F. C., & Jing, Y. P. 2005, MNRAS, 356, 1293

Yang, X., Mo, H. J., van den Bosch, F. C., Pasquali, A., Li, C., & Barden, M. 2007, ApJ, 671, 153

Yates, R. M., Kauffmann, G., & Guo, Q. 2012, MNRAS, 422, 215

Yip, C.-W., Szalay, A. S., Wyse, R. F. G., Dobos, L., Budavári, T., & Csabai, I. 2010, ApJ, 709, 780

York, D. G., Adelman, J., John E. Anderson, J., Anderson, S. F., Annis, J., Bahcall, N. A., Bakken, J. A., Barkhouser, R., Bastian, S., Berman, E., Boroski, W. N., Bracker, S., Briegel, C., Briggs, J. W., Brinkmann, J., Brunner, R., Burles, S., Carey, L., Carr, M. A., Castander, F. J., Chen, B., Colestock, P. L., Connolly, A. J., Crocker, J. H., Csabai, I., Czarapata, P. C., Davis, J. E., Doi, M., Dombeck, T., Eisenstein, D., Ellman, N., Elms, B. R., Evans, M. L., Fan, X., Federwitz, G. R., Fiscelli, L., Friedman, S., Frieman, J. A., Fukugita, M., Gillespie, B., Gunn, J. E., Gurbani, V. K., de Haas, E., Haldeman, M., Harris, F. H., Hayes, J., Heckman, T. M., Hennessy, G. S., Hindsley, R. B., Holm, S., Holmgren, D. J., hao Huang, C., Hull, C., Husby, D., Ichikawa, S.-I., Ichikawa, T., Ivezić, Ž., Kent, S., Kim, R. S. J., Kinney, E., Klaene, M., Kleinman, A. N., Kleinman, S., Knapp, G. R., Korienek, J., Kron, R. G., Kunszt, P. Z., Lamb, D. Q., Lee, B., Leger, R. F., Limmongkol, S., Lindenmeyer, C., Long, D. C., Loomis, C., Loveday, J., Lucinio, R., Lupton, R. H., MacKinnon, B., Mannery, E. J., Mantsch, P. M., Margon, B.,

McGehee, P., McKay, T. A., Meiksin, A., Merelli, A., Monet, D. G., Munn, J. A., Narayanan, V. K., Nash, T., Neilsen, E., Neswold, R., Newberg, H. J., Nichol, R. C., Nicinski, T., Nonino, M., Okada, N., Okamura, S., Ostriker, J. P., Owen, R., Pauls, A. G., Peoples, J., Peterson, R. L., Petravick, D., Pier, J. R., Pope, A., Pordes, R., Prosapio, A., Rechenmacher, R., Quinn, T. R., Richards, G. T., Richmond, M. W., Rivetta, C. H., Rockosi, C. M., Ruthmansdorfer, K., Sandford, D., Schlegel, D. J., Schneider, D. P., Sekiguchi, M., Sergey, G., Shimasaku, K., Siegmund, W. A., Smee, S., Smith, J. A., Snedden, S., Stone, R., Stoughton, C., Strauss, M. A., Stubbs, C., SubbaRao, M., Szalay, A. S., Szapudi, I., Szokoly, G. P., Thakar, A. R., Tremonti, C., Tucker, D. L., Uomoto, A., Berk, D. V., Vogeley, M. S., Waddell, P., i Wang, S., Watanabe, M., Weinberg, D. H., Yanny, B., & Yasuda, N. 2000, The Astronomical Journal, 120, 1579

Zabludoff, A. I. & Mulchaey, J. S. 1998, ApJ, 496, 39

Chapter 3

Further Properties of Red Misfits

In the previous chapter, I examined many properties of Red Misfits in an effort to determine whether and in which ways Red Misfits were distinct from Blue Actives and Red Passives. Here I revisit two of those properties, morphology and AGN fraction, in greater detail, drawing upon a more detailed BPT (Baldwin et al., 1981) classification in the literature and obtaining full morphological classifications for our Red Misfits. However, I first also explore whether Red Misfits are preferentially found in close galaxy pairs.

3.1 Are Red Misfits in Close Galaxy Pairs?

Recent results suggest that close pairs of galaxies can trigger AGN activity (e.g. Ellison et al., 2011; Satyapal et al., 2014; Gordon et al., 2017) and an enhancement in star formation (e.g. Patton et al., 2011; Scudder et al., 2012). Given that Red Misfits show enhanced sSFR compared to Red Passives and an enhanced AGN fraction relative to both Blue Actives and Red Passives (see Chapter 2), it is worthwhile to explore whether Red Misfits prefer to be in close galaxy pairs. This may not be captured in our measures of environment, M_{halo} and r/r_{200}, as they probe environment at a larger scale – we cannot identify close pairs embedded in groups or clusters using these metrics. If Red Misfits preferred to be in groups, the proportion of Red Misfits in my field sample (which consists of non-paired galaxies by definition) should be lower than in

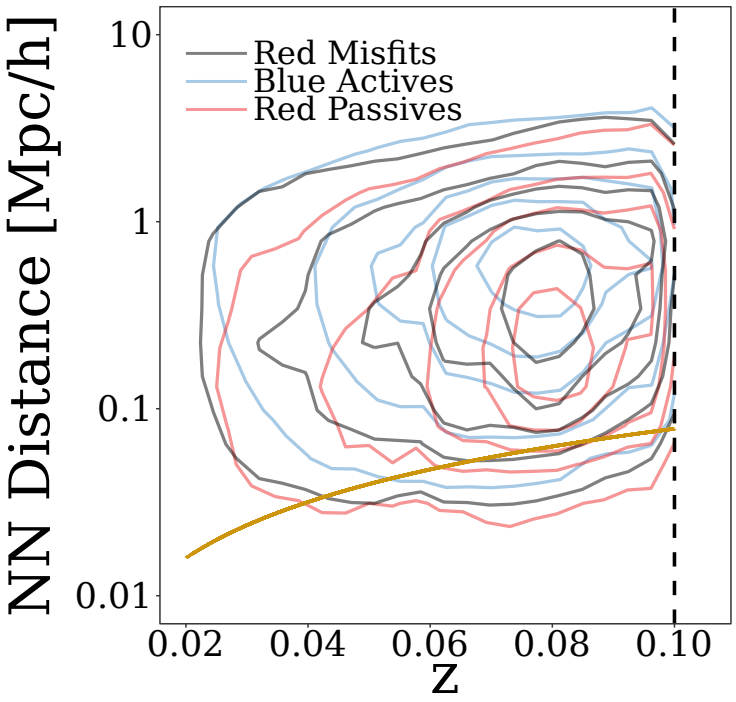

Figure 3.1 Distribution of nearest-neighbour-distances for Red Misfits, Blue Actives and Red Passives against redshift. Vertical dashed line shows z=0.1 redshift limit of our sample. Solid gold curve corresponds to the 55" SDSS fibre collision limit.

my group sample, which is not the case (see Table 2.1). I note, however, that if Red Misfits were found in abundance in close pairs it would be difficult to reconcile their enhanced gas-phase metallicities (see Fig. 2.9) with the results of Ellison et al. (2008) finding a metallicity decrement in close pair galaxies at fixed stellar mass.

In Fig. 3.1 I show the distribution of projected distances to a nearest neighbour galaxy within Δv=500kms^{-1} for each population. More conservative Δv restrictions do not qualitatively change results. See Patton et al. (2000) for a discussion regarding choosing the best Δv cut to select pairs. The projected separation is calculated as $\Delta\theta \mathrm{D}_M$, where $\Delta\theta$ is the angular separation of the two galaxies on the sky and D_M is the transverse comoving distance in our Ω_m=0.3, Ω_Λ=0.7 cosmology (see Hogg (1999)). We see in Fig. 3.1 that Red Passives peak towards smaller nearest neighbour separations while Blue Actives extend out to further separations. Red Misfits, however, are intermediate between the two; since the close pair fraction of Red Misfits is not enhanced over Red Passives, there is no clear indication that interactions between close galaxy pairs are responsible for the Red Misfit population.

There is a worry that close Red Misfit pairs could remain unresolved in my sample. Pairs with angular separations less than 55" cannot be distinguished by a single SDSS fibre, therefore nearest-neighbour separations below this limit are underdetected. This issue is mitigated by repeated observations of some sky regions and overlap between spectroscopic plates. The gold curve in Fig. 3.1 is the transverse comoving distance corresponding to an angular separation of 55" at each redshift. This limit is comfortably below the D_{NN} peak for all three populations at all redshifts. Discarding all pairs below this limit would not change my conclusions, therefore I am able to confirm that spectroscopic incompleteness does not influence my position that close galaxy pairs are not responsible for Red Misfits and their interesting properties.

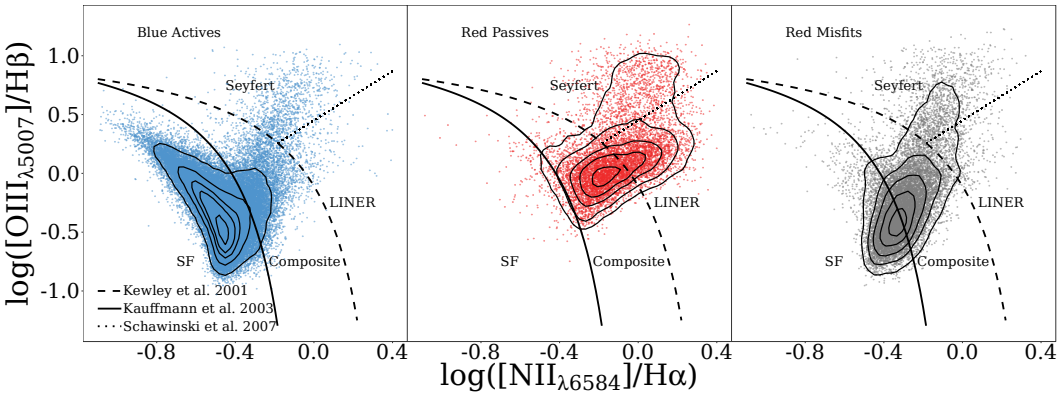

Figure 3.2 Distribution of Blue Actives (left), Red Passives (centre) and Red Misfits (right) in the emission-line sample on the BPT diagram. Contours encompass 10%, 30%, 50%, 70% and 90% of the unweighted distributions. Lines from Kewley et al. (2001) and Kauffmann et al. (2003) define star-forming and AGN regions of the diagram as well as the composite region. Schawinski et al. (2007) line splits the AGN region into a Seyfert region and a LINER region.

For posterity, I looked at how the nearest neighbour distance distribution changes if I restrict myself to pairs with stellar mass ratios closer than 1:10. Again I do not find an excess of Red Misfits in close pairs relative to Blue Actives and Red Passives. I also find that paired Red Misfits do not prefer Blue Actives, Red Passives or Red Misfits as partners, nor do they prefer to be the more massive or less massive partner in the pair.

3.2 AGN Revisited: Seyfert and LINER Emission

In Section 2.3.5 I referred to the region above the Kewley et al. (2001) line on a BPT diagram (Fig. 2.10) as the 'AGN' region for brevity. In a stricter sense, this region simply represents galaxies whose emission cannot be explained by star formation. I investigate this region to explore and further interpret the enhanced fraction of Red Misfits hosting AGN (see Fig. 2.11).

Specifically, we can further divide the AGN region into a 'Seyfert' region and a 'LINER' (low ionization nuclear emission line regions; Heckman, 1980) region and explore the occupation of these regions by Red Misfits, Blue Actives and Red Passives.

Galaxies in the Seyfert region are objects whose emission is dominated by a luminous AGN. The LINER region, however, is more controversial. A variety of physical processes can be invoked as an explanation of LINER emission, from low-luminosity, radiatively-inefficient AGN (e.g. Ho et al., 1993, 1997a; Kewley et al., 2006), fast radiative shocks (e.g. Dopita & Sutherland, 1995; Dopita et al., 2015), photoionization from young stars (e.g. Filippenko & Terlevich, 1992; Shields, 1992). See Ho (2008) for a review of suspected LINER sources.

Of interest to Red Misfits is the mounting observational evidence of LINER-like emission from evolved stellar populations (mainly post-AGB stars) in optically red galaxies, particularly over the last decade (e.g. Binette et al., 1994; Stasińska et al., 2008; Cid Fernandes et al., 2011; Yan & Blanton, 2012). Recent spatially-resolved observations of LINERs support this picture, showing that the LINER emission can be spread over kpc scales instead of confined to the nucleus (Sarzi et al., 2006, 2010; Belfiore et al., 2016). If the non-SF emission of Red Misfits can be explained by non-nuclear emission from evolved populations I will need to amend my interpretation of their enhanced AGN fraction.

Fig. 3.2 shows the distribution of Red Misfits, Blue Actives and Red Passives on a BPT diagram. This is the same as Fig. 2.10 except now I split the AGN region into a Seyfert region and a LINER region using the line of Schawinski et al. (2007) (hereafter S07). The S07 line is derived empirically based on the location of Seyferts and LINERs identified on [OIII]λ_{5007}/Hβ vs [OI]λ_{6300}/Hα and [OIII]λ_{5007}/Hβ vs [SII]$\lambda_{6717,6731}$/Hα BPT diagrams, where the use of the low ionization species [SII] and [OI] separate Seyferts and LIN-

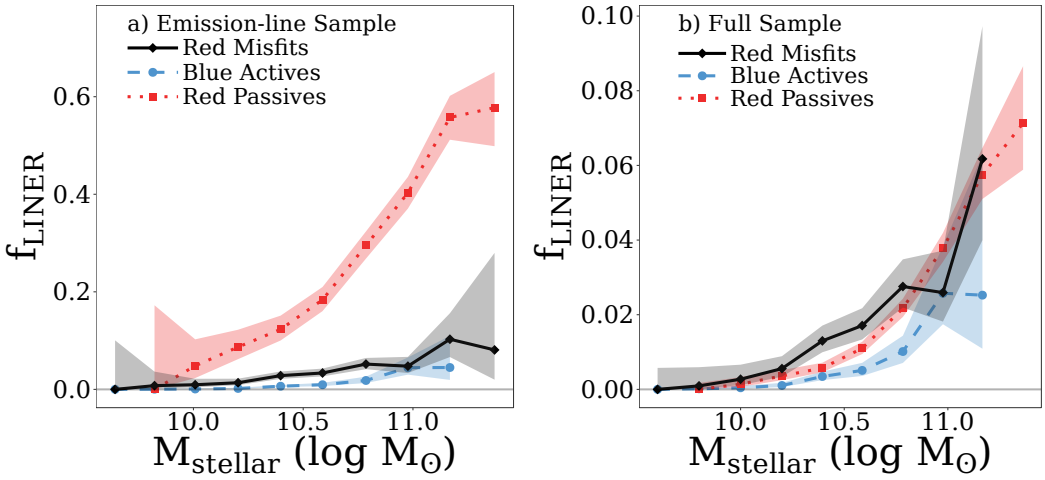

Figure 3.3 a) Fraction of each population in my emission-line subsample identified as LINERs (i.e. fraction lying above the Ke01 line and below the S07 line) in bins of stellar mass. b) Seyfert fraction for each population in my *full* sample (i.e. fraction satisfying the emission-line criteria of Section 2.2.3 and lying above the Ke01 line and below the S07 line). Shaded regions are 99% confidence intervals generated by the beta distribution as outlined by Cameron (2011).

ERs more clearly (see Kewley et al., 2006). Emission-line Red Misfits seem to prefer the Seyfert region over the LINER region; however, it is important to take a closer look and carefully compare the LINER fraction at fixed stellar mass.

Reminiscent of Fig. 2.11, Fig. 3.3a shows the fraction of galaxies identified as LINERs (i.e. fraction of galaxies lying above the Ke01 line but below the S07 line) in the emission-line sample against stellar mass. While a significant fraction of emission-line Red Passives are identified as LINERs, particularly at high stellar mass, the fraction of emission-line Blue Actives and Red Misfits that are LINERs is nearly negligible except at high stellar mass. Emission-line Red Misfits, however, are slightly more likely to be LINERs than Blue Actives at fixed stellar mass.

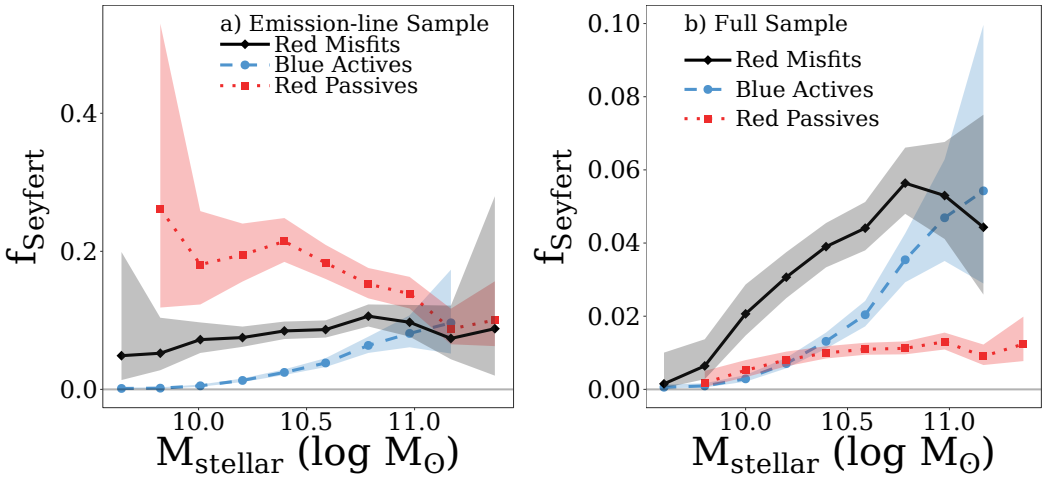

Figure 3.4 a) Fraction of each population in my emission-line subsample identified as Seyferts (i.e. fraction lying above both the Ke01 and S07 lines) in bins of stellar mass. b) Seyfert fraction for each population in my *full* sample (i.e. fraction satisfying the emission-line criteria of Section 2.2.3 and lying above the Ke01 and S07 lines). Shaded regions are 99% confidence intervals generated by the beta distribution as outlined by Cameron (2011).

Again, since my emission-line sample presents a biased look at galaxy populations, in Fig. 3.3b I show the fraction of LINERs for each population in the full sample, i.e. the fraction of galaxies in the full sample that satisfy my emission-line criteria outlined in Section 2.2.3 *and* lie in the LINER region. We only see a noticeable f_{LINER} enhancement for Red Misfits in a narrow range of stellar mass. However, this enhancement is slight, especially compared to the much clearer f_{AGN} enhancement seen in Fig. 2.11b.

Correspondingly, Fig. 3.4 shows the fraction of each population in both the emission-line and full samples identified as Seyferts (i.e. fraction lying above both the Ke01 line and S07 line) against stellar mass. While once again emission-line Red Passives are the most likely to be Seyferts over most of the stellar mass range in Fig. 3.4a, in Fig. 3.4b we see a significant enhancement in the fraction of Seyfert Red Misfits over Blue Actives and Red Passives. This enhancement is much stronger than the f_{LINER} boost and is more similar to

the f_{AGN} increase we saw in Fig. 2.11b. In summary, it appears that the non-SF emission from Red Misfits is dominated by classical Seyfert nuclear emission and not the more contentious LINER emission. It seems the increased AGN fraction of Red Misfits is genuine. I note that this represents a notable distinction between Red Misfits and the red spirals of Masters et al. (2011) discussed in Section 2.4.3 – while Red Misfits clearly favour the Seyfert region over the LINER region, 82±12% of emission-line red spirals are LINERs while just 6±2% are Seyferts when emission-line red spirals are selected with a S/N>2 cut on the BPT lines.

3.3 Galaxy Zoo: A Second Look at Red Misfit Morphologies

Proxies for galaxy morphology such as the Sérsic index, concentration parameter or B/T fraction are useful, providing a quantified metric of what can be a complex galaxy property. The price of using these is that the more subtle morphological features of each individual galaxy are lost and each proxy can introduce its own bias to the sample. For example, disk galaxies with prominent bulges can have Sérsic indices more typical of early-types as the surface brightness profile fit will be dominated by the bulge light. When available, a full morphological classification for each galaxy can provide extra insight over using these proxies.

3.3.1 Morphological Classification

To revisit Red Misfit morphologies, I match my catalogue to Galaxy Zoo (GZ1; Lintott et al., 2008) project. GZ1 provides multiple independent visual morphological classifications of nearly one million galaxies in the Sloan Digital Sky Survey (a review of the GZ1 results can be found in Lintott et al. (2011)).

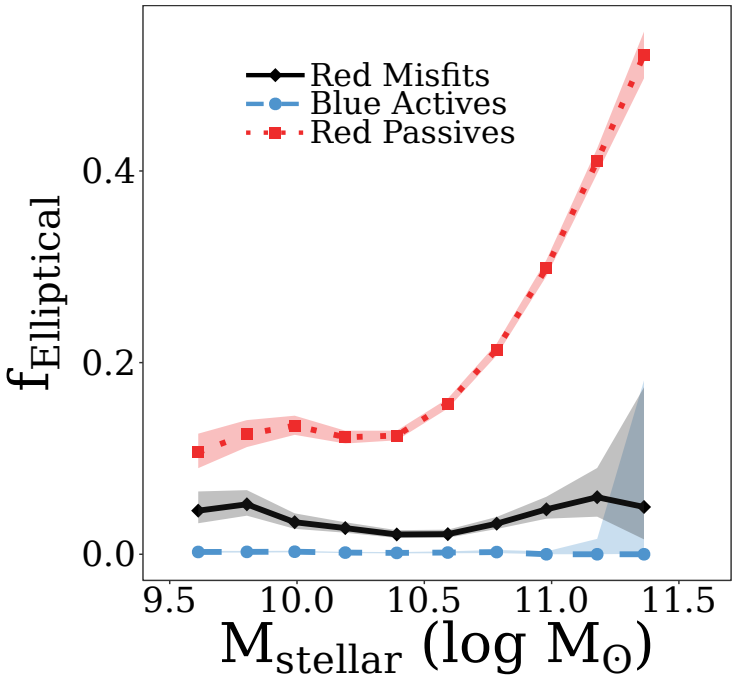

Figure 3.5 V_{max}-weighted fraction of Blue Actives, Red Passives and Red Misfits identified as elliptical ($p_{elliptical}$>0.8) by Galaxy Zoo binned by stellar mass. Shaded regions show 99% confidence intervals generated by the beta distribution as outlined by Cameron (2011).

While traditional visual classification of galaxies relied on a small number of experts (e.g. Sandage, 1961; de Vaucouleurs et al., 1991; Nair & Abraham, 2010), the scale of GZ1 is made possible by the participation of more than 100,000 volunteer citizen scientists classifying galaxies via a web-based interface. The fraction of volunteers identifying each galaxy as elliptical, spiral, edge-on or in the midst of a merger can then be used as a measure of morphology.

272205 galaxies in my full catalogue (98 per cent) have GZ1 morphology classifications. I classify a galaxy as early-type if $p_{elliptical} > 0.8$, i.e. 80 per cent or more of the Galaxy Zoo users (after vote re-weighting) categorized the galaxy as elliptical. The conservative threshold of 0.8 is common when using Galaxy Zoo classifications (e.g. see Lintott et al., 2008; Bamford et al., 2009; Schawinski et al., 2009; Masters et al., 2010; Willett et al., 2013). Fig. 3.5

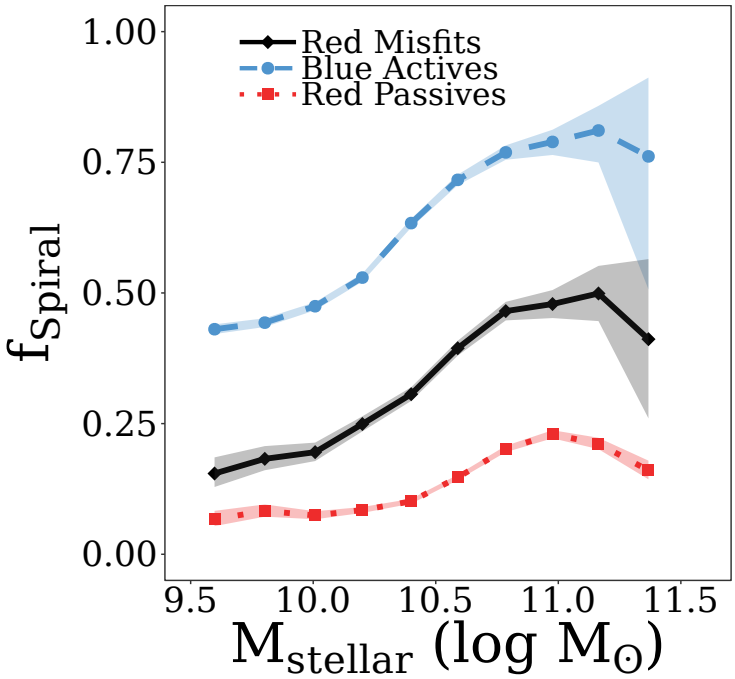

Figure 3.6 V_{max}-weighted fraction of Blue Actives, Red Passives and Red Misfits identified as spiral (p_{CS}>0.8) by Galaxy Zoo binned by stellar mass. Shaded regions show 99% confidence intervals generated by the beta distribution as outlined by Cameron (2011).

shows how this fraction changes for each population with stellar mass. Red Passives are most likely to be designated as elliptical, especially at high stellar mass while conversely a near negligible amount of Blue Actives are given this classification. Red Misfits are slightly more likely than Blue Actives to be elliptical but nowhere near as likely to be elliptical as Red Passives and don't show the strong $f_{elliptical}$ trend with stellar mass seen in Red Passives.

Fig. 3.6, on the other hand, shows the fraction of each populations classified as spirals. GZ1 offers users three options for classifying late-type galaxies: clockwise, counter clockwise and edge-on. To be a spiral, the debiased 'Combined Spiral' probability ($p_{CW}+p_{CCW}+p_{edge}$) must exceed 0.8. Although f_{spiral} increases with stellar mass in all three populations, Red Misfits are intermediate between Blue Actives and Red Passives in their likelihood of being desig-

nated as a spiral across the entire stellar mass range of my sample. Figs. 3.5 and 3.6 are consistent with the results of Section 2.3.2 finding that Red Misfits have intermediate morphologies.

3.3.2 A Closer Look with Galaxy Zoo 2

In addition to simply classifying Red Misfits as ellipticals or spirals, I delve into more detailed aspects of Red Misfit morphologies by matching my full catalogue to Galaxy Zoo 2 (GZ2; Willett et al., 2013), the second phase of GZ1. 151843 galaxies in my full catalogue (55 per cent) have GZ2 classifications. This GZ2-matched subsample will be biased towards larger, brighter, more massive galaxies. While the principle goal of GZ1 was the categorization of galaxies as early-type or late-type, GZ2 expanded upon this by asking volunteers to identify and characterize more subtle morphological features for $\sim$300,000 of the largest and brightest GZ1 galaxies such as stellar bars, central bulge shapes/strengths and number/tightness of spiral arms. The GZ2 catalogue is therefore ideal for revisiting and expanding the results of Section 2.3.2. If Red Misfits do indeed prefer intermediate, bulge-dominated disk morphologies, this should manifest itself in their bulge prominence voting fractions. If some properties of Red Misfits can be attributed to central bars (see Section 2.4.3), one would expect an enhanced fraction of volunteers identifying bars in Red Misfits relative to Red Passives or Blue Actives.

3.3.3 Bulge Prominence

To investigate whether Red Misfit morphologies are predisposed towards disks with strong bulges, Fig. 3.7 shows the fraction of each population identified as having prominent bulges, i.e. the user answers 'dominant' or 'obvious' when asked how prominent the central bulge is compared to the rest of the

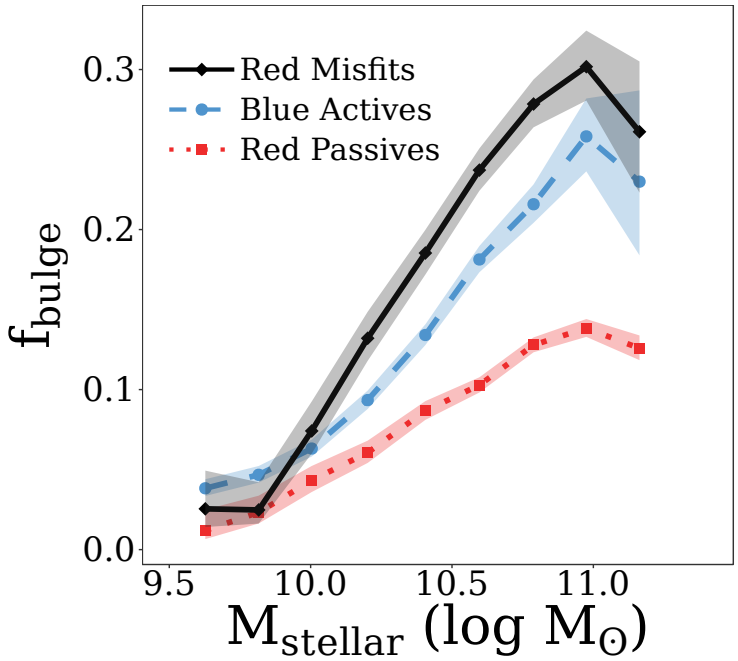

Figure 3.7 V_{max}-weighted fraction of Blue Actives, Red Passives and Red Misfits identified as hosting a prominent bulge ($p_{bulge,obvious} + p_{bulge,dominant}$>0.5) by Galaxy Zoo binned by stellar mass. Shaded regions show 99% confidence intervals generated by the beta distribution as outlined by Cameron (2011).

galaxy (as opposed to 'just noticeable' or 'no bulge'). I additionally require that a quarter or more of all classifications for a galaxy reach the bulge prominence question. To reach this question, a user must have first classified the galaxy as not edge-on and as having a disk or feature. Note that these galaxies will be biased towards late-type; the bulge prominence question will not often be reached for obviously early-type galaxies, i.e. users identifying strong bulges will more often select bulge-dominated disks, not ellipticals. This question is therefore perfect for identifying disk galaxies with significant bulges. I relax the p_{bulge} threshold from 0.8 to 0.5 otherwise bulge fractions among all three populations are very low. See e.g. Masters et al. (2011); Cheung et al. (2013) for a similar threshold relaxation when identifying bars. Retaining the 0.8 threshold does not materially alter the results. The bulge fraction for each population generally increases with stellar mass in Fig. 3.7. Across the majority of the entire stellar mass range, Red Misfits are more likely to display prominent bulges than Blue Actives or Red Passives. This supports my finding that Red Misfits have bulge-dominated disk morphologies – I see it not only in proxies for structural morphology but in visual morphology as well.

3.3.4 Bars

Another key aspect of galaxy morphology is the existence of a bar. Bars can efficiently drive gas towards central regions, possibly triggering central star formation (e.g. Knapen et al., 1995; Sheth et al., 2005) and facilitating bulge growth (e.g. Kormendy & Kennicutt, 2004). Therefore a large bar fraction in Red Misfits could reconcile their ongoing star formation with their red intrinsic colours and could explain their significant bulge components when compared to Blue Actives. Recent results find an increase in bar fraction in redder galaxies (Masters et al., 2011; Skibba et al., 2012; Lee et al., 2012). Bars may also explain the enhanced abundance of AGN in Red Misfits, however,

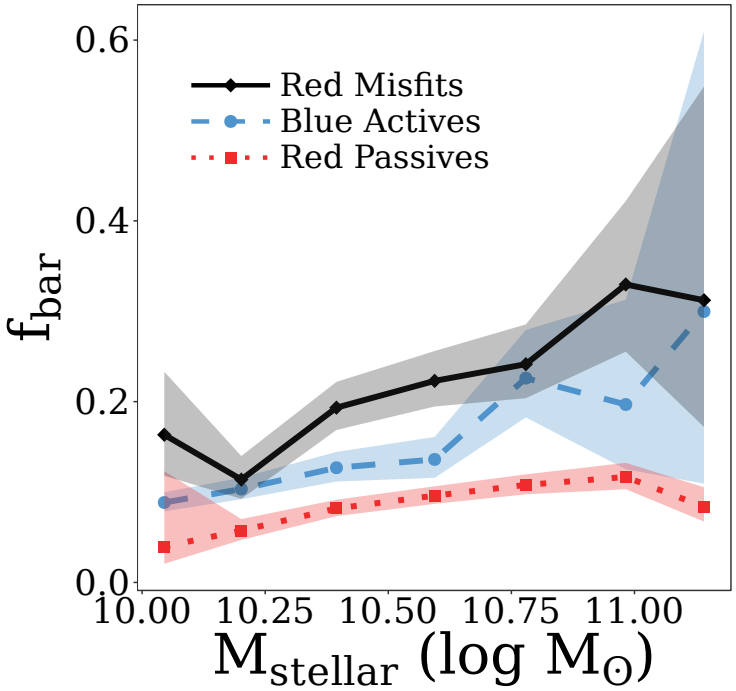

Figure 3.8 V_{max}-weighted fraction of Blue Actives, Red Passives and Red Misfits identified as hosting a bar (p_{bar}>0.5) by Galaxy Zoo binned by stellar mass. Shaded regions show 99% confidence intervals generated by the beta distribution as outlined by Cameron (2011).

results searching for an association between the presence of a bar and AGN activity have been mixed, with some groups establishing a link (e.g. Knapen et al., 2000; Laine et al., 2002; Galloway et al., 2015) and others finding no causal connection (e.g. Ho et al., 1997b; Cisternas et al., 2013, 2015; Cheung et al., 2015).

Fig. 3.8 shows how bar fraction changes with stellar mass for each population. Once again I use a p_{bar}>0.5 threshold and require that a quarter of users reach the bar question, having previously identified the galaxy as non edge-on and as having a feature or bar. I follow the philosophy of Masters et al. (2011) (see also Cheung et al., 2013) and only compute bar fractions among $0.01<z<0.06$, face-on ($b/a>0.5$) galaxies and ensure that my subsample is volume-limited by requiring $M_r^{0.1}$<-19.1. We see a slight enhancement in the bar likelihood for Red Misfits in this volume-limited subsample compared to Blue Actives. This enhancement may explain some of the properties of Red Misfits and is consistent with my conclusion that internal evolution processes are dominant in Red Misfits. Conclusively showing this bar fraction enhancement in Red Misfits has proven difficult as it depends quite strongly on the 25 per cent bar question threshold – the Red Misfit bar fraction enhancement increases as this criterion is relaxed and tends towards zero as I become more conservative with this threshold. Obtaining Hubble types for Red Misfits using expert visual classification, e.g. by matching to the morphology catalogue of Nair & Abraham (2010) might allow us to more easily determine the Red Misfit bar fraction.

I also matched my full sample to the bar length catalogue of Hoyle et al. (2011). To generate this catalogue, citizen scientists measured the bar lengths and widths of a subsample of ∼3000 strongly barred galaxies in GZ2. 2437 of those galaxies are in my full sample. Fig. 3.9 shows the distribution of bar lengths in barred Red Misfits, Blue Actives and Red Passives. The distribution of Red Misfit bar lengths peaks at a significantly greater length than the

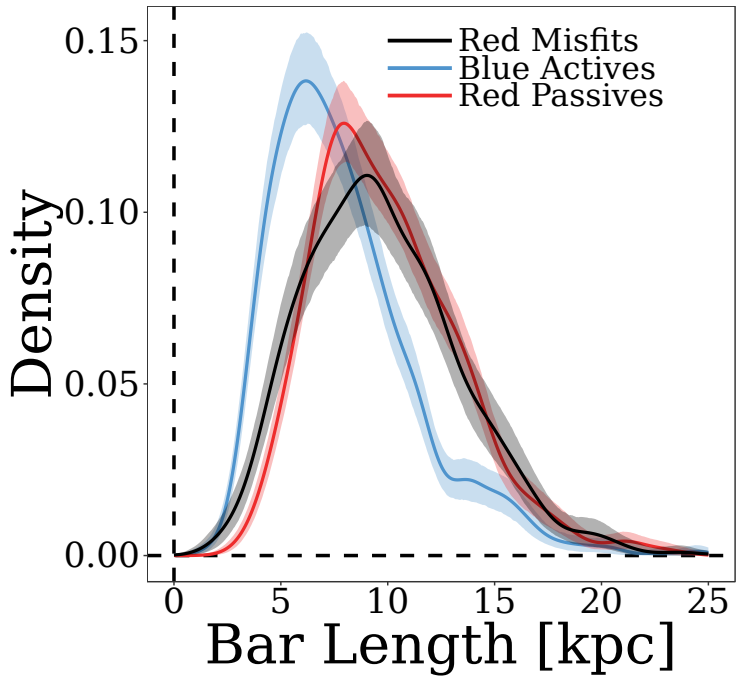

Figure 3.9 Distribution of bar lengths for each population when I match to the bar length catalogue of Hoyle et al. (2011). Shaded regions show 95% confidence interval from 1000 bootstrap resamplings.

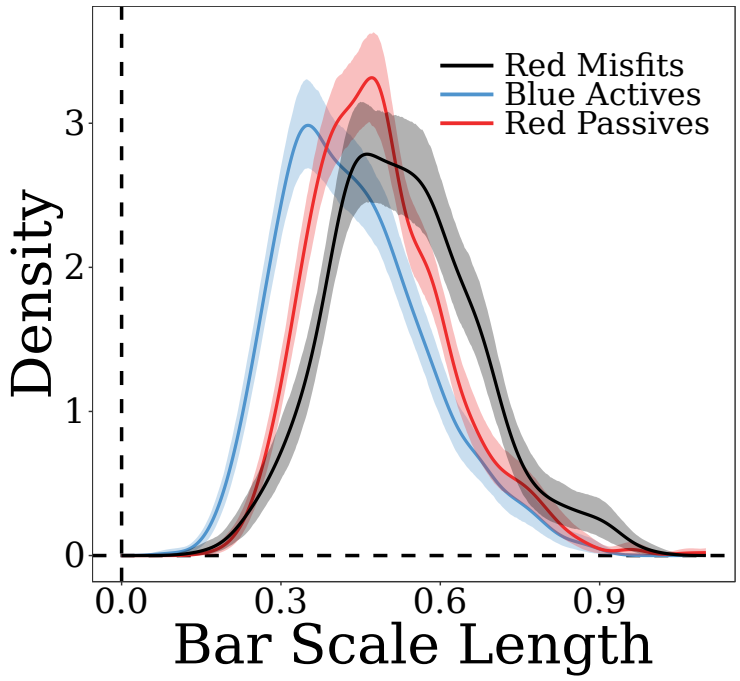

Figure 3.10 Distribution of scaled bar lengths ($L_{bar}/2 \cdot r_{90,Petro}$) for each population when I match to the bar length catalogue of Hoyle et al. (2011). Shaded regions show 95% confidence interval from 1000 bootstrap resamplings.

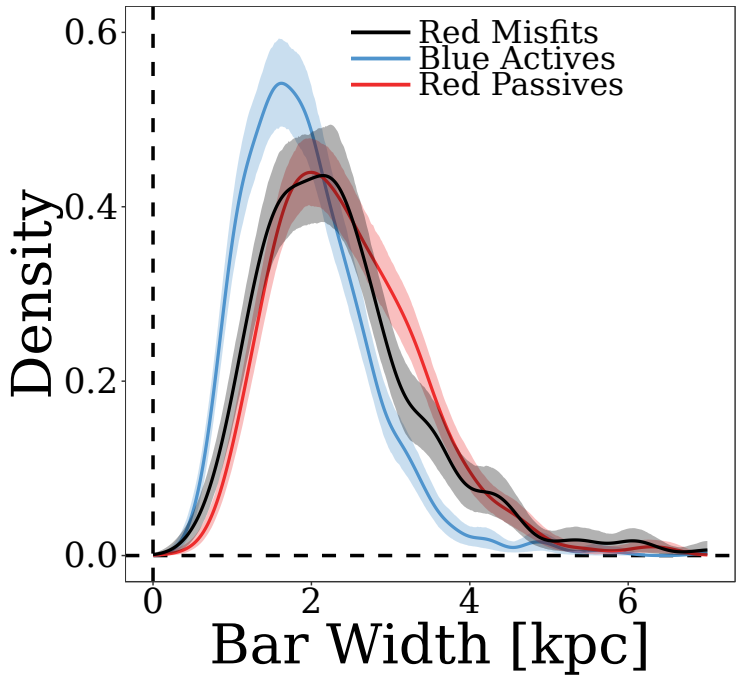

Figure 3.11 Distribution of bar widths for each population when I match to the bar length catalogue of Hoyle et al. (2011). Shaded regions show 95% confidence interval from 1000 bootstrap resamplings.

distribution for barred Blue Actives and at a slightly greater length than the distribution for barred Red Passives. Hoyle et al. (2011) also define a 'scaled bar length', the ratio of bar length to galaxy size (defined as twice the Petrosian r-band r_{90} in this case). Fig. 3.10 shows the distribution of scaled bar lengths for each population in my strongly barred subsample. Here, the distinction between the Red Misfit distribution and the Red Passive distribution is more significant – not only do barred Red Misfits peak towards longer bar scale lengths, the distribution is more broad, extending out to even longer scale lengths. Fig. 3.11 shows the distribution of bar *widths* for each population in my strongly barred subsample. There is no evidence that barred Red Misfits prefer wider bars than barred Blue Actives or Red Passives.

The reliability of the bar length trends I see is weakened by the limited size of the Hoyle et al. (2011) sample. Moreover, these results apply to the biased sample of bright, large, clearly barred Red Misfits, with limited applicability to the Red Misfit population as a whole. I therefore draw no conclusions about the bar geometry of barred Red Misfits.

In this chapter I looked in greater depth at the morphological and AGN results of Chapter 2. These more detailed investigations strengthened some key results and interpretations, i.e. that Red Misfits prefer intermediate, bulge-dominated disk morphologies, that they may host bars more often than Blue Actives and Red Passives, and that they more often show non-stellar emission characteristic of a central AGN. I additionally examined the close pair behaviour of Red Misfits and found that the population of Red Misfits cannot be explained by the enhanced star formation and AGN activity experienced by galaxies in close pairs.

Bibliography

Baldwin, J. A., Phillips, M. M., & Terlevich, R. 1981, PASP, 93, 5

Bamford, S. P., Nichol, R. C., Baldry, I. K., Land, K., Lintott, C. J., Schawinski, K., Slosar, A., Szalay, A. S., Thomas, D., Torki, M., Andreescu, D., Edmondson, E. M., Miller, C. J., Murray, P., Raddick, M. J., & Vandenberg, J. 2009, MNRAS, 393, 1324

Belfiore, F., Maiolino, R., Maraston, C., Emsellem, E., Bershady, M. A., Masters, K. L., Yan, R., Bizyaev, D., Boquien, M., Brownstein, J. R., Bundy, K., Drory, N., Heckman, T. M., Law, D. R., Roman-Lopes, A., Pan, K., Stanghellini, L., Thomas, D., Weijmans, A.-M., & Westfall, K. B. 2016, MNRAS, 461, 3111

Binette, L., Magris, C. G., Stasińska, G., & Bruzual, A. G. 1994, A&A, 292, 13

Cameron, E. 2011, PASP, 28, 128

Cheung, E., Athanassoula, E., Masters, K. L., Nichol, R. C., Bosma, A., Bell, E. F., Faber, S. M., Koo, D. C., Lintott, C., Melvin, T., Schawinski, K., Skibba, R. A., & Willett, K. W. 2013, ApJ, 779, 162

Cheung, E., Trump, J. R., Athanassoula, E., Bamford, S. P., Bell, E. F., Bosma, A., Cardamone, C. N., Casteels, K. R. V., Faber, S. M., Fang, J. J., Fortson, L. F., Kocevski, D. D., Koo, D. C., Laine, S., Lintott, C., Masters, K. L., Melvin, T., Nichol, R. C., Schawinski, K., Simmons, B., Smethurst, R., & Willett, K. W. 2015, MNRAS, 447, 506

Cid Fernandes, R., Stasińska, G., Mateus, A., & Vale Asari, N. 2011, MNRAS, 413, 1687

Cisternas, M., Gadotti, D. A., Knapen, J. H., Kim, T., Díaz-García, S., Laurikainen, E., Salo, H., González-Martín, O., Ho, L. C., Elmegreen, B. G., Zaritsky, D., Sheth, K., Athanassoula, E., Bosma, A., Comerón, S., Erroz-Ferrer, S., Gil de Paz, A., Hinz, J. L., Holwerda, B. W., Laine, J., Meidt, S., Menéndez-Delmestre, K., Mizusawa, T., Muñoz-Mateos, J. C., Regan, M. W., & Seibert, M. 2013, ApJ, 776, 50

Cisternas, M., Sheth, K., Salvato, M., Knapen, J. H., Civano, F., & Santini, P. 2015, ApJ, 802, 137

de Vaucouleurs, G., de Vaucouleurs, A., Corwin, Jr., H. G., Buta, R. J., Paturel, G., & Fouqué, P. 1991, Third Reference Catalogue of Bright Galaxies. Volume I: Explanations and references. Volume II: Data for galaxies between 0^h and 12^h. Volume III: Data for galaxies between 12^h and 24^h.

Dopita, M. A., Ho, I.-T., Dressel, L. L., Sutherland, R., Kewley, L., Davies, R., Hampton, E., Shastri, P., Kharb, P., Jose, J., Bhatt, H., Ramya, S., Scharwächter, J., Jin, C., Banfield, J., Zaw, I., James, B., Juneau, S., & Srivastava, S. 2015, ApJ, 801, 42

Dopita, M. A. & Sutherland, R. S. 1995, ApJ, 455, 468

Ellison, S. L., Patton, D. R., Mendel, J. T., & Scudder, J. M. 2011, MNRAS, 418, 2043

Ellison, S. L., Patton, D. R., Simard, L., & McConnachie, A. W. 2008, AJ, 135, 1877

Filippenko, A. V. & Terlevich, R. 1992, ApJ, 397, L79

Galloway, M. A., Willett, K. W., Fortson, L. F., Cardamone, C. N., Schawinski, K., Cheung, E., Lintott, C. J., Masters, K. L., Melvin, T., & Simmons, B. D. 2015, MNRAS, 448, 3442

Gordon, Y. A., Owers, M. S., Pimbblet, K. A., Croom, S. M., Alpaslan, M., Baldry, I. K., Brough, S., Brown, M. J. I., Cluver, M. E., Conselice, C. J., Davies, L. J. M., Holwerda, B. W., Hopkins, A. M., Gunawardhana, M. L. P., Loveday, J., Taylor, E. N., & Wang, L. 2017, MNRAS, 465, 2671

Heckman, T. M. 1980, A&A, 87, 152

Ho, L. C. 2008, ARA&A, 46, 475

Ho, L. C., Filippenko, A. V., & Sargent, W. L. W. 1993, ApJ, 417, 63

—. 1997a, ApJ, 487, 568

—. 1997b, ApJ, 487, 591

Hogg, D. W. 1999, ArXiv Astrophysics e-prints

Hoyle, B., Masters, K. L., Nichol, R. C., Edmondson, E. M., Smith, A. M., Lintott, C., Scranton, R., Bamford, S., Schawinski, K., & Thomas, D. 2011, MNRAS, 415, 3627

Kauffmann, G., Heckman, T. M., White, S. D. M., Charlot, S., Tremonti, C., Peng, E. W., Seibert, M., Brinkmann, J., Nichol, R. C., SubbaRao, M., & York, D. 2003, MNRAS, 341, 54

Kewley, L. J., Dopita, M. A., Sutherland, R. S., Heisler, C. A., & Trevena, J. 2001, ApJ, 556, 121

Kewley, L. J., Groves, B., Kauffmann, G., & Heckman, T. 2006, MNRAS, 372, 961

Knapen, J. H., Beckman, J. E., Heller, C. H., Shlosman, I., & de Jong, R. S. 1995, ApJ, 454, 623

Knapen, J. H., Shlosman, I., & Peletier, R. F. 2000, ApJ, 529, 93

Kormendy, J. & Kennicutt, R. C. 2004, Annual Review of Astronomy and Astrophysics, 42, 603

Laine, S., Shlosman, I., Knapen, J. H., & Peletier, R. F. 2002, ApJ, 567, 97

Lee, G.-H., Park, C., Lee, M. G., & Choi, Y.-Y. 2012, ApJ, 745, 125

Lintott, C., Schawinski, K., Bamford, S., Slosar, A., Land, K., Thomas, D., Edmondson, E., Masters, K., Nichol, R. C., Raddick, M. J., Szalay, A., Andreescu, D., Murray, P., & Vandenberg, J. 2011, MNRAS, 410, 166

Lintott, C. J., Schawinski, K., Slosar, A., Land, K., Bamford, S., Thomas, D., Raddick, M. J., Nichol, R. C., Szalay, A., Andreescu, D., Murray, P., & Vandenberg, J. 2008, MNRAS, 389, 1179

Masters, K. L., Mosleh, M., Romer, A. K., Nichol, R. C., Bamford, S. P., Schawinski, K., Lintott, C. J., Andreescu, D., Campbell, H. C., Crowcroft, B., Doyle, I., Edmondson, E. M., Murray, P., Raddick, M. J., Slosar, A., Szalay, A. S., & Vandenberg, J. 2010, MNRAS, 405, 783

Masters, K. L., Nichol, R. C., Hoyle, B., Lintott, C., Bamford, S. P., Edmondson, E. M., Fortson, L., Keel, W. C., Schawinski, K., Smith, A. M., & Thomas, D. 2011, MNRAS, 411, 2026

Nair, P. B. & Abraham, R. G. 2010, ApJS, 186, 427

Patton, D. R., Carlberg, R. G., Marzke, R. O., Pritchet, C. J., da Costa, L. N., & Pellegrini, P. S. 2000, ApJ, 536, 153

Patton, D. R., Ellison, S. L., Simard, L., McConnachie, A. W., & Mendel, J. T. 2011, MNRAS, 412, 591

Sandage, A. 1961, The Hubble Atlas of Galaxies

Sarzi, M., Falcón-Barroso, J., Davies, R. L., Bacon, R., Bureau, M., Cappellari, M., de Zeeuw, P. T., Emsellem, E., Fathi, K., Krajnović, D., Kuntschner, H., McDermid, R. M., & Peletier, R. F. 2006, MNRAS, 366, 1151

Sarzi, M., Shields, J. C., Schawinski, K., Jeong, H., Shapiro, K., Bacon, R., Bureau, M., Cappellari, M., Davies, R. L., de Zeeuw, P. T., Emsellem, E., Falcón-Barroso, J., Krajnović, D., Kuntschner, H., McDermid, R. M., Peletier, R. F., van den Bosch, R. C. E., van de Ven, G., & Yi, S. K. 2010, MNRAS, 402, 2187

Satyapal, S., Ellison, S. L., McAlpine, W., Hickox, R. C., Patton, D. R., & Mendel, J. T. 2014, MNRAS, 441, 1297

Schawinski, K., Lintott, C., Thomas, D., Sarzi, M., Andreescu, D., Bamford, S. P., Kaviraj, S., Khochfar, S., Land, K., Murray, P., Nichol, R. C., Raddick, M. J., Slosar, A., Szalay, A., Vandenberg, J., & Yi, S. K. 2009, MNRAS, 396, 818

Schawinski, K., Thomas, D., Sarzi, M., Maraston, C., Kaviraj, S., Joo, S.-J., Yi, S. K., & Silk, J. 2007, MNRAS, 382, 1415

Scudder, J. M., Ellison, S. L., Torrey, P., Patton, D. R., & Mendel, J. T. 2012, MNRAS, 426, 549

Sheth, K., Vogel, S. N., Regan, M. W., Thornley, M. D., & Teuben, P. J. 2005, ApJ, 632, 217

Shields, J. C. 1992, ApJ, 399, L27

Skibba, R. A., Masters, K. L., Nichol, R. C., Zehavi, I., Hoyle, B., Edmondson, E. M., Bamford, S. P., Cardamone, C. N., Keel, W. C., Lintott, C., & Schawinski, K. 2012, MNRAS, 423, 1485

Stasińska, G., Vale Asari, N., Cid Fernandes, R., Gomes, J. M., Schlickmann, M., Mateus, A., Schoenell, W., Sodré, Jr., L., & Seagal Collaboration. 2008, MNRAS, 391, L29

Willett, K. W., Lintott, C. J., Bamford, S. P., Masters, K. L., Simmons, B. D., Casteels, K. R. V., Edmondson, E. M., Fortson, L. F., Kaviraj, S., Keel, W. C., Melvin, T., Nichol, R. C., Raddick, M. J., Schawinski, K., Simpson, R. J., Skibba, R. A., Smith, A. M., & Thomas, D. 2013, MNRAS, 435, 2835

Yan, R. & Blanton, M. R. 2012, ApJ, 747, 61

Chapter 4

Summary & Conclusions

There are many previous investigations of galaxy colour, star formation rate and the correspondence between the two (e.g. Strateva et al., 2001; Blanton et al., 2003; Kauffmann et al., 2003; Baldry et al., 2004; Balogh et al., 2004a,b) and many works studying populations of galaxies which defy the correspondence between star formation, colour and morphology (e.g. Graham & Dey, 1996; Goto et al., 2003; Schawinski et al., 2009; Cardamone et al., 2009; Masters et al., 2010; Tojeiro et al., 2013). Although there are no works which define Red Misfits using MPA-JHU specific star formation rates and inclination- and k-corrected NYU-VAGC colours as I do, analogous populations of optically red but star-forming galaxies have been studied and some broad comparisons can be made. These studies have characterized star formation in a variety of ways. These include

- Mid-infrared flux (typically 24 μm) flux as a proxy for obscured SF (e.g. Coia et al., 2005; Davoodi et al., 2006; Saintonge et al., 2008; Gallazzi et al., 2008; Brand et al., 2009; Wolf et al., 2009; Zhu et al., 2011).
- UV flux (Gallazzi et al., 2008).
- NUV-r colour (e.g. Haines et al., 2008; Crossett et al., 2014)

- Emission-line measurements as SF proxies (e.g. Hammer et al., 1997; Homeier et al., 2005; Demarco et al., 2005; Franzetti et al., 2007; Verdugo et al., 2008; Koyama et al., 2008, 2010, 2011).
- Brinchmann et al. (2004) MPA-JHU sSFR based on emission lines (e.g. Weinmann et al., 2006; Popesso et al., 2007; Mahajan & Raychaudhury, 2009, this work).
- SED fitting using dust as a free parameter (e.g. Wolf et al., 2005, 2009).

These studies cover a wide variety of samples and different luminosity, mass, and redshift ranges. Detailed comparisons are therefore difficult; however, all these studies agree that a significant fraction of red sequence galaxies exhibit detectable levels of star formation whether obscured or not.

Many studies of red, star-forming galaxies, regardless of how they are defined, find them to have intermediate morphologies. The majority of studies characterizing their morphologies (Lane et al., 2007; Wolf et al., 2009; Verdugo et al., 2008; Gallazzi et al., 2008; Popesso et al., 2007; Crossett et al., 2014), whether by Sérsic decomposition, concentration, SED fitting, by-eye classification or Galaxy Zoo voting find them to exhibit a wide variety of morphologies, peaking at intermediate morphologies (typically Sa/Sb in those that provide Hubble Sequence classifications).

Environmental trends for starforming red populations in other works are generally also consistent with my results, although more difficult to interpret. Studies of red starforming galaxies in large surveys generally find their proportion to be constant with halo-centric radius, halo mass (Weinmann et al., 2006) and with local density (Verdugo et al., 2008). Mahajan & Raychaudhury (2009), however, find red starforming galaxies prefering the cluster core environment while the red starforming population of Haines et al. (2008) are more abundant in the field rather than the cluster or cluster outskirt environments.

Studies focusing on single or very few systems (e.g. Demarco et al., 2005; Wolf et al., 2005, 2009; Gallazzi et al., 2008; Koyama et al., 2010, 2011; Crossett et al., 2014) typically find starforming red galaxies to be most common in intermediate-density environments or groups on the outskirts of clusters, implying that cluster Red Misfit analogues may be related to pre-processing in galaxy groups. These results are consistent with my finding that Red Misfits slightly prefer low-mass haloes (Fig. 2.12) but not with my detection of Red Misfits even near the centres (in projection) of massive clusters. To complicate matters, the preferred environments of the red starforming population may change with z; Koyama et al. (2010) find red Hα emitters most abundant near the core of the $z = 0.81$ cluster RXJ1716.4+6708, yet in the $z = 0.41$ cluster CL0939+4713 Koyama et al. (2011) find red Hα emitters favouring the group environment on the outskirts of the cluster. These works are typically studying a small number of star-forming red galaxies in a single environment or a narrow range of environments, which makes direct comparisons with my large sample of Red Misfits (over a wide range of stellar mass and envrionments) difficult.

Comparing the dust content of Red Misfits to the literature is difficult as well, given that starforming red galaxies in the literature are often selected to be dusty in the first place (e.g. Wolf et al., 2005; Lane et al., 2007; Gallazzi et al., 2008; Wolf et al., 2009) or exhibiting significant dust-obscured star formation (e.g. Coia et al., 2005; Saintonge et al., 2008; Brand et al., 2009). Some works find sufficient dust attenuation (e.g. Davoodi et al., 2006; Brand et al., 2009) or edge-on inclinations (e.g. Verdugo et al., 2008) in their 'red' starforming populations to dismiss half or more of them as intrinsically blue. My use of inclination-corrected colours removes highly-inclined intrinsically-blue contaminants from my Red Misfit sample and I find that only $\sim$26 per cent of Red Misfits exhibit dust attenuation more than 1σ above that expected of a Blue Active at fixed stellar mass (see Fig. 2.7).

The fraction of AGN in Red Misfits is generally inconsistent with previous works finding no significant enhancement in the AGN fraction of red, star-forming galaxies, however they are defined (Weinmann et al., 2006; Verdugo et al., 2008; Mahajan & Raychaudhury, 2009), although direct comparisons are difficult due to sample selection. These works also do not control for stellar mass, which was important for identifying the f_{AGN} enhancement in Red Misfits (Fig. 2.11).

The possibility of multiple heterogeneous populations in star-forming red galaxies has surfaced in several works. Using IR-to-UV luminosity ratios as a proxy for dust attenuation, Gallazzi et al. (2008) find bimodality in the dust content of the Wolf et al. (2005) star-forming red galaxies and therefore split the population in two: ∼40 per cent are equally abundant at all environments, are fit by relatively large Sérsic indices (≈2.5), have low sSFR and experience dust attenuation roughly in line with the blue cloud. The other ∼60% are dusty, fit by smaller Sérsic indices (≈1.5), have systematically higher SSFRs and are most abundant at intermediate densities. Mahajan & Raychaudhury (2009) identify red, star-forming galaxies in Abell clusters (Abell et al., 1989) in SDSS DR4 using MPA-JHU star formation rates. They find bimodality in the dust extinction, Hδ EW and D_n4000 for their star-forming red galaxies. They consequently split their star-forming red galaxies into bright centrals with nuclear star formation and red but currently starbursting cluster galaxies. Although some of these identified sub-populations share some properties with the Red Misfits presented in this work, I see no bimodality in any Red Misfit property (e.g. dust, age, environment, morphology) to suggest that my Red Misfit population should be divided into two or more populations.

Spatially-resolved information about Red Misfits would help immensely in investigating the trends I have seen in integrated data and in interpreting the role of Red Misfits in galaxy evolution. Red Misfits are among the targets of ongoing multiplexed integral field spectroscopy surveys such as the Sydney-

AAO Multi-object Integral Field Spectrograph survey (SAMI; Croom et al., 2012) and the Mapping Nearby Galaxies at Apache Point Observatory survey (MaNGA; Bundy et al., 2015). The spatially-resolved spectra provided by these surveys will allow us to not only explore the spatial variation of star formation, dust extinction and stellar ages and metallicities within Red Misfits, but also to confirm that the 'AGN' emission of Red Misfits is genuine nuclear emission and not extended LINER-type emission (see Section 2.3.5 and Section 3.2). Red Misfits will also be found in the upcoming Hector survey (Bland-Hawthorn, 2015), whose high-resolution 2D stellar and gas kinematics observations will allow us to probe how Red Misfits build their bulgy-disk morphology and to possibly identify their progenitor populations.

To more fully understand the nature of Red Misfits this optical study could be complemented with observations at longer wavelength. Sub-mm observations from e.g. ALMA or JCMT could be used to measure the molecular gas mass in these galaxies and their gas depletion times. These sub-mm observations could also help constrain the dust mass of Red Misfits relative to Blue Actives and Red Passives. HI measurements at 21cm from e.g. the ALFALFA survey (Giovanelli et al., 2005) could constrain the reservoir of neutral gas available to Red Misfits.

This thesis has explored in detail red, actively star-forming galaxies, a population previously dismissed by many as highly-inclined spirals. In addition to showing that this population persists when the reddening effects of inclination are corrected for, the properties of Red Misfits that I uncover reveal them to be an exciting population worth studying. This work highlights the value of studying interesting outlier galaxy populations. Large data sets on the horizon provided by surveys pushing observations to wider angles, higher redshifts and fainter magnitudes such as the Dark Energy Survey (Flaugher et al., 2015) and the Large Synoptic Survey Telescope (Ivezic et al., 2008) will only facilitate the study of these interesting outlier populations in the future.

Bibliography

Abell, G. O., Corwin, Jr., H. G., & Olowin, R. P. 1989, ApJS, 70, 1

Baldry, I. K., Glazebrook, K., Brinkmann, J., Ivezić, Ž., Lupton, R. H., Nichol, R. C., & Szalay, A. S. 2004, ApJ, 600, 681

Balogh, M., Eke, V., Miller, C., Lewis, I., Bower, R., Couch, W., Nichol, R., Bland-Hawthorn, J., Baldry, I. K., Baugh, C., Bridges, T., Cannon, R., Cole, S., Colless, M., Collins, C., Cross, N., Dalton, G., Propris, R. D., Driver, S. P., Efstathiou, G., Ellis, R. S., Frenk, C. S., Glazebrook, K., Gomez, P., Gray, A., Hawkins, E., Jackson, C., Lahav, O., Lumsden, S., Maddox, S., Madgwick, D., Norberg, P., Peacock, J. A., Percival, W., Peterson, B. A., Sutherland, W., & Taylor, K. 2004a, MNRAS, 348, 1355

Balogh, M. L., Baldry, I. K., Nichol, R., Miller, C., Bower, R., & Glazebrook, K. 2004b, ApJ, 615, L101

Bland-Hawthorn, J. 2015, in IAU Symposium, Vol. 309, Galaxies in 3D across the Universe, ed. B. L. Ziegler, F. Combes, H. Dannerbauer, & M. Verdugo, 21–28

Blanton, M. R., Brinkmann, J., Csabai, I., Doi, M., Eisenstein, D., Fukugita, M., Gunn, J. E., Hogg, D. W., & Schlegel, D. J. 2003, AJ, 125, 2348

Brand, K., Moustakas, J., Armus, L., Assef, R. J., Brown, M. J. I., Cool, R. R., Desai, V., Dey, A., Floc'h, E. L., Jannuzi, B. T., Kochanek, C. S., Melbourne, J., Papovich, C. J., & Soifer, B. T. 2009, ApJ, 693, 340

Brinchmann, J., Charlot, S., White, S. D. M., Tremonti, C., Kauffmann, G., Heckman, T., & Brinkmann, J. 2004, MNRAS, 351, 1151

Bundy, K., Bershady, M. A., Law, D. R., Yan, R., Drory, N., MacDonald, N., Wake, D. A., Cherinka, B., Sánchez-Gallego, J. R., Weijmans, A.-M., Thomas, D., Tremonti, C., Masters, K., Coccato, L., Diamond-Stanic, A. M., Aragón-Salamanca, A., Avila-Reese, V., Badenes, C., Falcón-Barroso, J., Belfiore, F., Bizyaev, D., Blanc, G. A., Bland-Hawthorn, J., Blanton, M. R., Brownstein, J. R., Byler, N., Cappellari, M., Conroy, C., Dutton, A. A., Emsellem, E., Etherington, J., Frinchaboy, P. M., Fu, H., Gunn, J. E., Harding, P., Johnston, E. J., Kauffmann, G., Kinemuchi, K., Klaene, M. A., Knapen, J. H., Leauthaud, A., Li, C., Lin, L., Maiolino, R., Malanushenko, V., Malanushenko, E., Mao, S., Maraston, C., McDermid, R. M., Merrifield, M. R., Nichol, R. C., Oravetz, D., Pan, K., Parejko, J. K., Sanchez, S. F., Schlegel, D., Simmons, A., Steele, O., Steinmetz, M., Thanjavur, K., Thompson, B. A., Tinker, J. L., van den Bosch, R. C. E., Westfall, K. B., Wilkinson, D., Wright, S., Xiao, T., & Zhang, K. 2015, ApJ, 798, 7

Cardamone, C., Schawinski, K., Sarzi, M., Bamford, S. P., Bennert, N., Urry, C. M., Lintott, C., Keel, W. C., Parejko, J., Nichol, R. C., Thomas, D., Andreescu, D., Murray, P., Raddick, M. J., Slosar, A., Szalay, A., & Vandenberg, J. 2009, MNRAS, 399, 1191

Coia, D., McBreen, B., Metcalfe, L., Biviano, A., Altieri, B., Ott, S., Fort, B., Kneib, J.-P., Mellier, Y., Miville-Deschênes, M.-A., O'Halloran, B., & Sanchez-Fernandez, C. 2005, A&A, 431, 433

Croom, S. M., Lawrence, J. S., Bland-Hawthorn, J., Bryant, J. J., Fogarty, L., Richards, S., Goodwin, M., Farrell, T., Miziarski, S., Heald, R., Jones, D. H., Lee, S., Colless, M., Brough, S., Hopkins, A. M., Bauer, A. E., Birchall, M. N., Ellis, S., Horton, A., Leon-Saval, S., Lewis, G., López-Sánchez, Á. R., Min, S.-S., Trinh, C., & Trowland, H. 2012, MNRAS, 421, 872

Crossett, J. P., Pimbblet, K. A., Stott, J. P., & Jones, D. H. 2014, MNRAS, 437, 2521

Davoodi, P., Pozzi, F., Oliver, S., Polletta, M., Afonso-Luis, A., Farrah, D., Hatziminaoglou, E., Rodighiero, G., Berta, S., Waddington, I., Lonsdale, C., Rowan-Robinson, M., Shupe, D. L., Evans, T., Fang, F., Smith, H. E., & Surace, J. 2006, MNRAS, 371, 1113

Demarco, R., Rosati, P., Lidman, C., Homeier, N. L., Scannapieco, E., Benítez, N., Mainieri, V., Nonino, M., Girardi, M., Stanford, S. A., Tozzi, P., Borgani, S., Silk, J., Squires, G., & Broadhurst, T. J. 2005, A&A, 432, 381

Flaugher, B., Diehl, H. T., Honscheid, K., Abbott, T. M. C., Alvarez, O., Angstadt, R., Annis, J. T., Antonik, M., Ballester, O., Beaufore, L., Bernstein, G. M., Bernstein, R. A., Bigelow, B., Bonati, M., Boprie, D., Brooks, D., Buckley-Geer, E. J., Campa, J., Cardiel-Sas, L., Castander, F. J., Castilla, J., Cease, H., Cela-Ruiz, J. M., Chappa, S., Chi, E., Cooper, C., da Costa, L. N., Dede, E., Derylo, G., DePoy, D. L., de Vicente, J., Doel, P., Drlica-Wagner, A., Eiting, J., Elliott, A. E., Emes, J., Estrada, J., Fausti Neto, A., Finley, D. A., Flores, R., Frieman, J., Gerdes, D., Gladders, M. D., Gregory, B., Gutierrez, G. R., Hao, J., Holland, S. E., Holm, S., Huffman, D., Jackson, C., James, D. J., Jonas, M., Karcher, A., Karliner, I., Kent, S., Kessler, R., Kozlovsky, M., Kron, R. G., Kubik, D., Kuehn, K., Kuhlmann, S., Kuk, K., Lahav, O., Lathrop, A., Lee, J., Levi, M. E., Lewis, P., Li, T. S., Mandrichenko, I., Marshall, J. L., Martinez, G., Merritt, K. W., Miquel, R., Muñoz, F., Neilsen, E. H., Nichol, R. C., Nord, B., Ogando, R., Olsen, J., Palaio, N., Patton, K., Peoples, J., Plazas, A. A., Rauch, J., Reil, K., Rheault, J.-P., Roe, N. A., Rogers, H., Roodman, A., Sanchez, E., Scarpine, V., Schindler, R. H., Schmidt, R., Schmitt, R., Schubnell, M., Schultz, K., Schurter, P., Scott, L., Serrano, S., Shaw, T. M., Smith, R. C., Soares-Santos, M., Stefanik, A., Stuermer, W., Suchyta, E., Sypniewski, A., Tarle, G., Thaler, J., Tighe, R., Tran, C., Tucker, D., Walker, A. R., Wang, G.,

Watson, M., Weaverdyck, C., Wester, W., Woods, R., Yanny, B., & DES Collaboration. 2015, AJ, 150, 150

Franzetti, P., Scodeggio, M., Garilli, B., Vergani, D., Maccagni, D., Guzzo, L., Tresse, L., Ilbert, O., Lamareille, F., Contini, T., Le Fèvre, O., Zamorani, G., Brinchmann, J., Charlot, S., Bottini, D., Le Brun, V., Picat, J. P., Scaramella, R., Vettolani, G., Zanichelli, A., Adami, C., Arnouts, S., Bardelli, S., Bolzonella, M., Cappi, A., Ciliegi, P., Foucaud, S., Gavignaud, I., Iovino, A., McCracken, H. J., Marano, B., Marinoni, C., Mazure, A., Meneux, B., Merighi, R., Paltani, S., Pellò, R., Pollo, A., Pozzetti, L., Radovich, M., Zucca, E., Cucciati, O., & Walcher, C. J. 2007, A&A, 465, 711

Gallazzi, A., Bell, E. F., Wolf, C., Gray, M. E., Papovich, C., Barden, M., Peng, C. Y., Meisenheimer, K., Heymans, C., van Kampen, E., Gilmour, R., Balogh, M., McIntosh, D. H., Bacon, D., Barazza, F. D., Böhm, A., Caldwell, J. A. R., Häußler, B., Jahnke, K., Jogee, S., Lane, K., Robaina, A. R., Sanchez, S. F., Taylor, A., Wisotzki, L., & Zheng, X. 2008, ApJ, 690, 1883

Giovanelli, R., Haynes, M. P., Kent, B. R., Perillat, P., Saintonge, A., Brosch, N., Catinella, B., Hoffman, G. L., Stierwalt, S., Spekkens, K., Lerner, M. S., Masters, K. L., Momjian, E., Rosenberg, J. L., Springob, C. M., Boselli, A., Charmandaris, V., Darling, J. K., Davies, J., Garcia Lambas, D., Gavazzi, G., Giovanardi, C., Hardy, E., Hunt, L. K., Iovino, A., Karachentsev, I. D., Karachentseva, V. E., Koopmann, R. A., Marinoni, C., Minchin, R., Muller, E., Putman, M., Pantoja, C., Salzer, J. J., Scodeggio, M., Skillman, E., Solanes, J. M., Valotto, C., van Driel, W., & van Zee, L. 2005, AJ, 130, 2598

Goto, T., Okamura, S., Sekiguchi, M., Bernardi, M., Brinkmann, J., Gómez, P. L., Harvanek, M., Kleinman, S. J., Krzesinski, J., Long, D., Loveday,

J., Miller, C. J., Neilsen, E. H., Newman, P. R., Nitta, A., Sheth, R. K., Snedden, S. A., & Yamauchi, C. 2003, PASJ, 55, 757

Graham, J. R. & Dey, A. 1996, ApJ, 471, 720

Haines, C. P., Gargiulo, A., & Merluzzi, P. 2008, MNRAS, 385, 1201

Hammer, F., Flores, H., Lilly, S. J., Crampton, D., Le Fèvre, O., Rola, C., Mallen-Ornelas, G., Schade, D., & Tresse, L. 1997, ApJ, 481, 49

Homeier, N. L., Demarco, R., Rosati, P., Postman, M., Blakeslee, J. P., Bouwens, R. J., Bradley, L. D., Ford, H. C., Goto, T., Gronwall, C., Holden, B., Jee, M. J., Martel, A. R., Mei, S., Menanteau, F., Zirm, A., Clampin, M., Hartig, G. F., Illingworth, G. D., Ardila, D. R., Bartko, F., Benítez, N., Broadhurst, T. J., Brown, R. A., Burrows, C. J., Cheng, E. S., Cross, N. J. G., Feldman, P. D., Franx, M., Golimowski, D. A., Infante, L., Kimble, R. A., Krist, J. E., Lesser, M. P., Meurer, G. R., Miley, G. K., Motta, V., Sirianni, M., Sparks, W. B., Tran, H. D., Tsvetanov, Z. I., White, R. L., & Zheng, W. 2005, ApJ, 621, 651

Ivezic, Z., Tyson, J. A., Abel, B., Acosta, E., Allsman, R., AlSayyad, Y., Anderson, S. F., Andrew, J., Angel, R., Angeli, G., Ansari, R., Antilogus, P., Arndt, K. T., Astier, P., Aubourg, E., Axelrod, T., Bard, D. J., Barr, J. D., Barrau, A., Bartlett, J. G., Bauman, B. J., Beaumont, S., Becker, A. C., Becla, J., Beldica, C., Bellavia, S., Blanc, G., Blandford, R. D., Bloom, J. S., Bogart, J., Borne, K., Bosch, J. F., Boutigny, D., Brandt, W. N., Brown, M. E., Bullock, J. S., Burchat, P., Burke, D. L., Cagnoli, G., Calabrese, D., Chandrasekharan, S., Chesley, S., Cheu, E. C., Chiang, J., Claver, C. F., Connolly, A. J., Cook, K. H., Cooray, A., Covey, K. R., Cribbs, C., Cui, W., Cutri, R., Daubard, G., Daues, G., Delgado, F., Digel, S., Doherty, P., Dubois, R., Dubois-Felsmann, G. P., Durech, J., Eracleous, M., Ferguson, H., Frank, J., Freemon, M., Gangler, E., Gawiser, E., Geary, J. C., Gee,

P., Geha, M., Gibson, R. R., Gilmore, D. K., Glanzman, T., Goodenow, I., Gressler, W. J., Gris, P., Guyonnet, A., Hascall, P. A., Haupt, J., Hernandez, F., Hogan, C., Huang, D., Huffer, M. E., Innes, W. R., Jacoby, S. H., Jain, B., Jee, J., Jernigan, J. G., Jevremovic, D., Johns, K., Jones, R. L., Juramy-Gilles, C., Juric, M., Kahn, S. M., Kalirai, J. S., Kallivayalil, N., Kalmbach, B., Kantor, J. P., Kasliwal, M. M., Kessler, R., Kirkby, D., Knox, L., Kotov, I., Krabbendam, V. L., Krughoff, S., Kubanek, P., Kuczewski, J., Kulkarni, S., Lambert, R., Le Guillou, L., Levine, D., Liang, M., Lim, K., Lintott, C., Lupton, R. H., Mahabal, A., Marshall, P., Marshall, S., May, M., McKercher, R., Migliore, M., Miller, M., Mills, D. J., Monet, D. G., Moniez, M., Neill, D. R., Nief, J., Nomerotski, A., Nordby, M., O'Connor, P., Oliver, J., Olivier, S. S., Olsen, K., Ortiz, S., Owen, R. E., Pain, R., Peterson, J. R., Petry, C. E., Pierfederici, F., Pietrowicz, S., Pike, R., Pinto, P. A., Plante, R., Plate, S., Price, P. A., Prouza, M., Radeka, V., Rajagopal, J., Rasmussen, A., Regnault, N., Ridgway, S. T., Ritz, S., Rosing, W., Roucelle, C., Rumore, M. R., Russo, S., Saha, A., Sassolas, B., Schalk, T. L., Schindler, R. H., Schneider, D. P., Schumacher, G., Sebag, J., Sembroski, G. H., Seppala, L. G., Shipsey, I., Silvestri, N., Smith, J. A., Smith, R. C., Strauss, M. A., Stubbs, C. W., Sweeney, D., Szalay, A., Takacs, P., Thaler, J. J., Van Berg, R., Vanden Berk, D., Vetter, K., Virieux, F., Xin, B., Walkowicz, L., Walter, C. W., Wang, D. L., Warner, M., Willman, B., Wittman, D., Wolff, S. C., Wood-Vasey, W. M., Yoachim, P., Zhan, H., & for the LSST Collaboration. 2008, ArXiv e-prints

Kauffmann, G., Heckman, T. M., White, D. M. S., Charlot, S., Tremonti, C., Brinchmann, J., Bruzual, G., Peng, E. W., Seibert, M., Bernardi, M., Blanton, M., Brinkmann, J., Castander, F., Csábai, I., Fukugita, M., Ivezic, Z., Munn, J. A., Nichol, R. C., Padmanabhan, N., Thakar, A. R., Weinberg, D. H., & York, D. 2003, MNRAS, 341, 33

Koyama, Y., Kodama, T., Nakata, F., Shimasaku, K., & Okamura, S. 2011, ApJ, 734, 66

Koyama, Y., Kodama, T., Shimasaku, K., Hayashi, M., Okamura, S., Tanaka, I., & Tokoku, C. 2010, MNRAS, 403, 1611

Koyama, Y., Kodama, T., Shimasaku, K., Okamura, S., Tanaka, M., Lee, H. M., Im, M., Matsuhara, H., Takagi, T., Wada, T., & Oyabu, S. 2008, MNRAS, 391, 1758

Lane, K. P., Gray, M. E., Aragon-Salamanca, A., Wolf, C., & Meisenheimer, K. 2007, MNRAS, 378, 716

Mahajan, S. & Raychaudhury, S. 2009, MNRAS, 400, 687

Masters, K. L., Mosleh, M., Romer, A. K., Nichol, R. C., Bamford, S. P., Schawinski, K., Lintott, C. J., Andreescu, D., Campbell, H. C., Crowcroft, B., Doyle, I., Edmondson, E. M., Murray, P., Raddick, M. J., Slosar, A., Szalay, A. S., & Vandenberg, J. 2010, MNRAS, 405, 783

Popesso, P., Biviano, A., Romaniello, M., & Böhringer, H. 2007, A&A, 461, 411

Saintonge, A., Tran, K.-V. H., & Holden, B. P. 2008, ApJ, 685, L113

Schawinski, K., Lintott, C., Thomas, D., Sarzi, M., Andreescu, D., Bamford, S. P., Kaviraj, S., Khochfar, S., Land, K., Murray, P., Nichol, R. C., Raddick, M. J., Slosar, A., Szalay, A., Vandenberg, J., & Yi, S. K. 2009, MNRAS, 396, 818

Strateva, I., Ivezić, Ž., Knapp, G. R., Narayanan, V. K., Strauss, M. A., Gunn, J. E., Lupton, R. H., Schlegel, D., Bahcall, N. A., Brinkmann, J., Brunner, R. J., Budavári, T., Csabai, I., Castander, F. J., Doi, M., Fukugita, M., Győry, Z., Hamabe, M., Hennessy, G., Ichikawa, T., Kunszt, P. Z., Lamb,

D. Q., McKay, T. A., Okamura, S., Racusin, J., Sekiguchi, M., Schneider, D. P., Shimasaku, K., & York, D. 2001, AJ, 122, 1861

Tojeiro, R., Masters, K. L., Richards, J., Percival, W. J., Bamford, S. P., Maraston, C., Nichol, R. C., Skibba, R., & Thomas, D. 2013, MNRAS, 432, 359

Verdugo, M., Ziegler, B. L., & Gerken, B. 2008, A&A, 486, 9

Weinmann, S. M., van den Bosch, F. C., Yang, X., & Mo, H. J. 2006, MNRAS, 366, 2

Wolf, C., Aragón-Salamanca, A., Balogh, M., Barden, M., Bell, E. F., Gray, M. E., Peng, C. Y., Bacon, D., Barazza, F. D., Böhm, A., Caldwell, J. A. R., Gallazzi, A., Häußler, B., Heymans, C., Jahnke, K., Jogee, S., van Kampen, E., Lane, K., McIntosh, D. H., Meisenheimer, K., Papovich, C., Sánchez, S. F., Taylor, A., Wisotzki, L., & Zheng, X. 2009, MNRAS, 393, 1302

Wolf, C., Gray, M. E., & Meisenheimer, K. 2005, Astronomy and Astrophysics, 443, 435

Zhu, G., Blanton, M. R., Burles, S. M., Coil, A. L., Cool, R. J., Eisenstein, D. J., Moustakas, J., Wong, K. C., & Aird, J. 2011, ApJ, 726, 110

This page intentionally left blank.